Galileo for Science (G4S) a new experiment in General Relativity with Galileo-FOC satellites: state of the art and perspectives

25 Maggio 2021

David Lucchesi

On behalf of the G4S_2.0 Project

Istituto di Astrofisica e Planetologia Spaziali (IAPS) – Istituto Nazionale di Astrofisica (INAF)
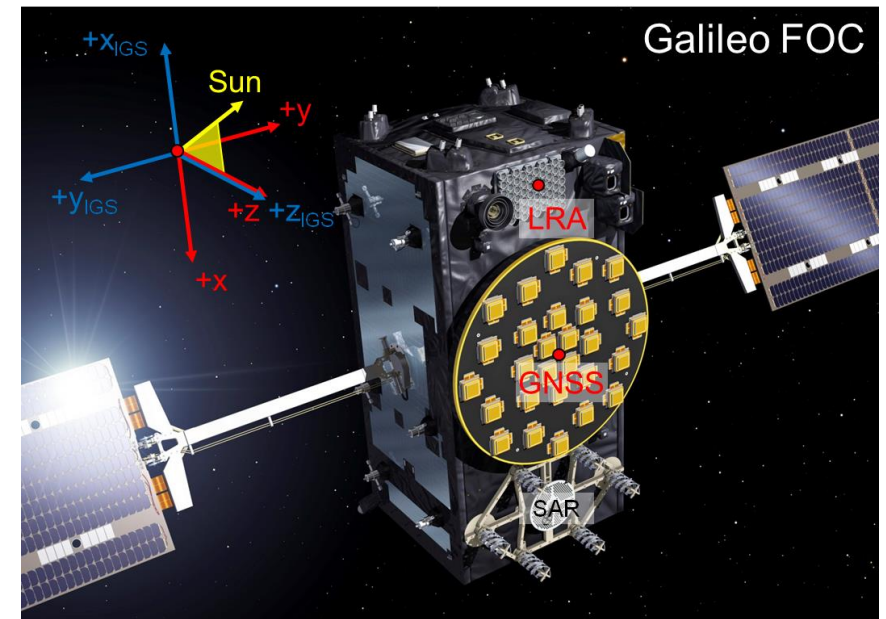
Via Fosso del Cavaliere n. 100, 00133 Tor Vergata – Roma

david.lucchesi@inaf.it

Sommario

(image credit: ESA)

Il progetto G4S_2.0

Galileo for Science (**G4S_2.0**) è stato presentato ed è risultato vincitore del "Bando interno per la valutazione e la selezione di progetti di ricerca e sviluppo **ASI**, afferenti al fondo indiviso assegnato dal **MIUR**, da selezionare con criteri di premialità" (CI-COT-2018-085)

G4S_2.0 si propone di effettuare una serie di misure di fisica della gravitazione per mezzo dei satelliti **GSAT0201** e **GSAT0202**, appartenenti alla costellazione **Galileo FOC** (**Full Operational Capability**), sfruttando sia l'eccentricità delle loro orbite sia l'accuratezza degli orologi atomici di bordo
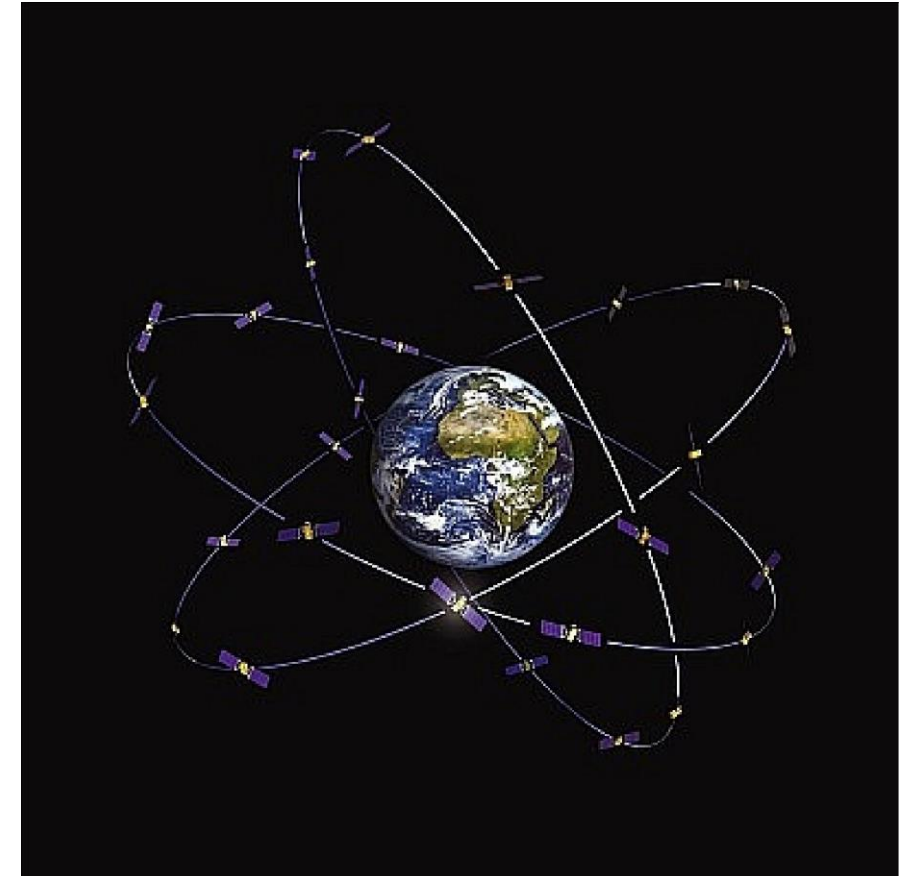
The Galileo constellation of 30 spacecraft
(image credit: ESA)

Il progetto G4S_2.0

Three research centers are involved in this project

- Center for Space Geodesy (**ASI-CGS**) in Matera
- Istituto di Astrofisica e Planetologia Spaziali (**IAPS/INAF**) in Roma and **OATO/INAF** in Torino
- Politecnico (**POLITO**) in Torino

High level goals of the project

1. A new measurement of the **Gravitational Redshift**
2. A measurement of the **General Relativity precessions** on the orbits of the satellites
3. Constraints on **Dark Matter**
4. Realize (in a reverse use) a pure **Relativistic Positioning System**
5. Detection of **Gravitational Waves** with the **GALILEO** system

Il progetto G4S_2.0

Three research centers are involved in this project

- Center for Space Geodesy (**ASI-CGS**) in Matera
- Istituto di Astrofisica e Planetologia Spaziali (**IAPS/INAF**) in Roma and **OATO/INAF** in Torino
- Politecnico (**POLITO**) in Torino

Other fundamental goals of the project

1. To develop new and more accurate models for the **Non-Gravitational Perturbations**
2. To develop a new **Accelerometer concept** for next generation of Galileo

Il progetto G4S_2.0

ASI ha firmato questa mattina 25 Maggio 2021

Tavolo Negoziale

Il Tavolo Negoziale fra **ASI** e **INAF**, per la definizione dell'Accordo Attuativo di **Galileo for Science_2.0**, si è tenuto lo scorso 8 Aprile in teleconferenza alla presenza del Coordinatore **ASI** del progetto, Dottor Francesco Vespe

Riunione iniziale del progetto

La Riunione Iniziale del progetto sarà fissata dopo la firma dell'Accordo Attuativo da parte del Direttore Generale di **ASI**, Dottor Fabrizio Tosone, e del Direttore Generale di **INAF**, Dottor Gaetano Telesio

Durata del progetto

La durata nominale del progetto è di tre anni

Il Team scientifico di INAF e la WBS

Il Team scientifico di IAPS-INAF

1. AdR-1
2. AdR-2
3. Simone Benedetti (Tecnico TD)
4. Diana Martella (Tecnologo TD)
5. Emiliano Fiorenza (Tecnico)
6. Carlo Lefevre (Tecnologo)
7. David Lucchesi (Primo Ricercatore)
8. Marco Lucente (Ricercatore TD)
9. Carmelo Magnafico (Tecnologo)
10. Roberto Peron (Ricercatore)
11. Francesco Santoli (Primo Tecnologo)
12. Feliciana Sapio (Dottoranda)
13. Angelo Tartaglia (Professore in quiescenza: OATO-INAF)
14. Massimo Visco (Ricercatore)
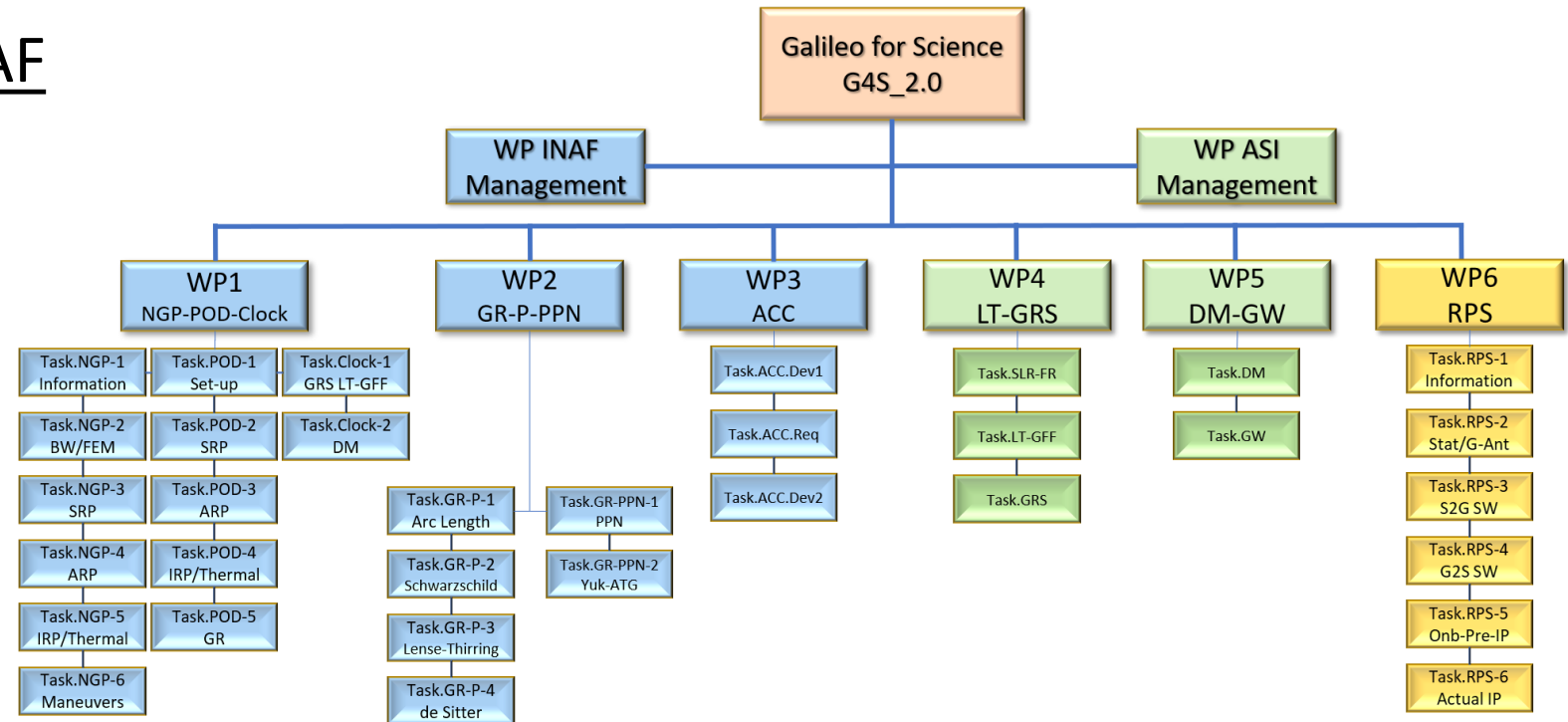
FTE complessive: 11.1

In **G4S_2.0** è coinvolto tutto il **Gruppo Gravitazionale** dello **IAPS-INAF**

Il Team scientifico di INAF e la WBS

15. Team Summary

15. Personale INAF coinvolto

Numero di partecipanti INAF al progetto: 10

Struttura	Nfte	N0	TI 21	TI 22	TI 23	TD 21	TD 22	TD 23	Nex	Extra
IAPS ROMA	9	1	1.20	1.85	1.80	0.00	1.00	1.00	1	0.10
Totali	9	1	**1.20**	**1.85**	**1.80**	**0.00**	**1.00**	**1.00**	1	**0.10**

16. Personale Associato INAF coinvolto

Numero di partecipanti Associati INAF: 4

#	Struttura	TI 2021	TI 2022	TI 2023	TD 2021	TD 2022	TD 2023	Extra
1	OATO/INAF, Associato INAF presso l'Osservatorio di Torino	0	0	0	0.00	0.00	0.00	1.00
2	IAPS	0	0	0	0.50	0.50	0.50	0.00
	Totali	**0.00**	**0.00**	**0.00**	**0.50**	**0.50**	**0.50**	**1.00**

FTE complessive: 11.1

FTE medie/anno: 3.7

Il Team scientifico di INAF e la WBS

Personale coinvolto nel WP0: Management

1. **Diana Martella**

**Personale coinvolto nel WP1: POD.NGP.Clocks**

1. AdR-1
2. AdR-2
3. Carlo Lefevre
4. **David Lucchesi**
5. Marco Lucente
6. Carmelo Magnafico
7. Roberto Peron
8. Feliciana Sapio
9. Angelo Tartaglia
10. Massimo Visco

Personale coinvolto nel WP2: GR-P-PPN

1. **David Lucchesi**
2. Marco Lucente
3. Carmelo Magnafico
4. Roberto Peron
5. Feliciana Sapio
6. Angelo Tartaglia
7. Massimo Visco

Personale coinvolto nel WP3: ACC.Dev1.Req.Dev2

1. Simone Benedetti
2. **Emiliano Fiorenza**
3. Carlo Lefevre
4. David Lucchesi
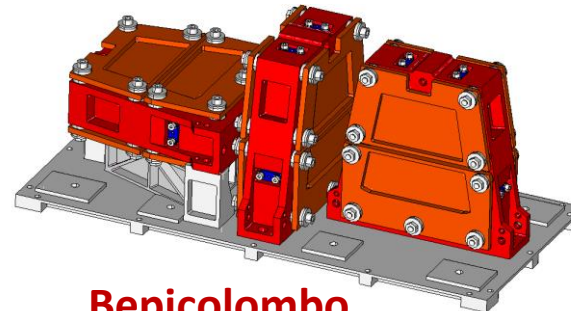5. Marco Lucente
6. Francesco Santoli
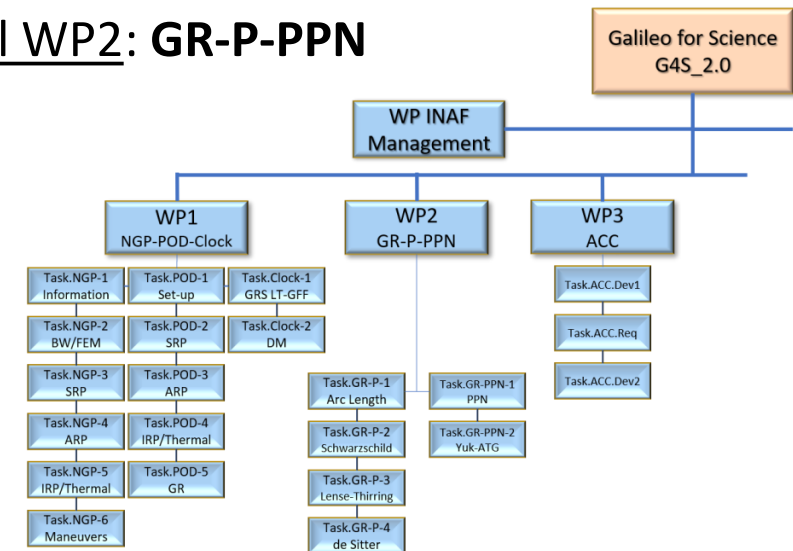
Il contesto scientifico e tecnologico

Il **Gruppo Gravitazionale** dello **IAPS-INAF** vanta una lunga esperienza in alcuni dei settori chiave necessari allo sviluppo del progetto **G4S_2.0** e al raggiungimento dei suoi obiettivi.

In particolare:

- Nello sviluppo di modelli perturbativi delle orbite di satelliti artificiali per forze:
  - non-gravitazionali
  - gravitazionali
- Nella determinazione orbitale di precisione per misure di fisica fondamentale con dati di inseguimento laser (LAGEOS, LAGEOS II, LARES)
- Analisi dati (siamo un Centro di Analisi Associato dell'**ILRS**)
- Sviluppo di accelerometri di elevata sensibilità per la misura di piccoli spostamenti:
  - Misure di accelerazioni non-gravitazionali
  - Misure geofisiche
  - Misure di fisica fondamentale

LAGEOS: courtesy of NASA

Photo by Franco Ambrico (courtesy G. Bianco, ASI-CGS)

ISA   Bepicolombo
HAA   JUICE

Il contesto scientifico e tecnologico

L'importanza per **ESA** e per la **CE** degli aspetti scientifici e tecnologici dei satelliti **GNSS** per la navigazione è ben illustrato nel documento (29 Gennaio 2019):

H2020-ESA-038

GNSS Evolutions Experimental Payloads and Science

Activities – Call for Ideas

Statement of Work

GNSS scientific prospects can benefit a large variety of fields including, for example:

- **Fundamental Physics**
- **Earth and Atmospheric Sciences**
- **Astronomy**
- **Time Metrology**

(image credit: ESA)

Currently the most important scientific applications fall into the following fields:

1. **Geodesy and Geodynamics**
   1. Orbits and clocks
   2. Station coordinates (ITRF)
   3. EOP parameters
   4. Geocenter
   5. Precise Positioning Techniques (PPT)
   6. Rigid Plate Motions
   7. Plate Boundary Deformation and Earthquake Cycle
2. **Atmosphere Monitoring**
   1. Neutral atmosphere
   2. Radio occultation measurements
   3. Ionosphere
3. **Reflectometry**
4. **Time and Frequency Transfer**
5. **Fundamental Physics**
   1. Gravitational Redshift measurement (GREAT)

Il contesto scientifico e tecnologico

L'importanza per **ESA** e per la **CE** degli aspetti scientifici e tecnologici dei satelliti **GNSS** per la navigazione è ben illustrato nel documento (29 Gennaio 2019):

Galileo in particular offers some particular features of special relevance for scientific experimentation, namely:

1. Galileo satellites include highly stable atomic clocks
2. New signals, robust modulation schemes with lower noise (e.g. E5-AltBOC)
3. More signals in three frequencies (E1-E5-E6) for multi-frequency applications
4. Laser Retro Reflectors present on all Galileo satellites
5. Mass and Centre-of-Mass provision to the International Laser Ranging Service (ILRS)
6. Absolute calibration of Galileo satellite antennas
7. Accurate attitude law of Galileo satellites during eclipse
8. Stable Galileo orbits without manoeuvres
9. Specific characteristics of the Galileo satellites' revolution period (avoiding Earth rotation resonances)
10. Radiation monitors in a number of satellites
11. Two Galileo satellites placed in eccentric orbit, observing larger differences in Earth's gravity field
12. Galileo disseminates Galileo System Time (GST) together with Coordinated Universal Time (UTC) information from the combination of several of the most accurate realisations of UTC in Europe
13. Availability of precise Differential Code Biases for Galileo
14. Compatibility/interoperability with other GNSS systems allowing multi-constellation experiments
15. Availability of Satellite Metadata information for scientific usage

Il contesto scientifico e tecnologico

L'importanza per **ESA** e per la **CE** degli aspetti scientifici e tecnologici dei satelliti **GNSS** per la navigazione è ben illustrato nel documento (29 Gennaio 2019):

Galileo is approaching its completion towards Full Operational Capability. Additionally, a formal process involving all relevant stakeholders has been established for the definition of the evolution of the Galileo and the new features to be incorporated into the next generation of the system (Galileo Second Generation – G2G).

Activities in support of the definition of possible G2G scenarios have been put in place through Horizon 2020 R&D Framework Programme including System/Segment engineering activities as well the associated technological pre-developments – some of which had been initiated under the ESA EGEP Programme - to improve the current system and to enable the implementation of the potential new features.

As part of the H2020 programme objectives, fostering the scientific utilization of Galileo that may result in evolutions of Galileo are considered. In addition, a number of candidate experimental hosted non-navigation payloads have been identified, in coordination with ESA's Galileo Science Advisory Committee (GSAC) [RD 3], that could be hosted in future satellites, which would require consolidation of requirements, proposed experimental/operational concept and payload initial prototyping.

A call for ideas, focused on key topics, allows to gather feedback from the scientists to designers and integrators of the next generation navigation satellites with a view to maximize the scientific value of the exploitation of the European GNSS signals and data.

1. **Category 1: Experimental Payloads**
2. **Category 2: On-Board Atomic Clocks**
3. **Category 3: European GNSS Scientific Studies**

Il contesto scientifico e tecnologico

L'importanza per **ESA** e per la **CE** degli aspetti scientifici e tecnologici dei satelliti **GNSS** per la navigazione è ben illustrato nel documento (29 Gennaio 2019):

1. Category 1: Experimental Payloads

This category covers the prototyping of experimental hosted non-navigation payloads for future Galileo satellites, including:

1. Optical payloads for ranging and communications (including QKD experiments)
2. Space Environment & Space Weather instruments
3. Advanced Laser Retro-Reflector
4. VLBI Transmitter
5. <u>Accelerometer</u>
6. Remote Sensing instruments supporting tropospheric or ionospheric models
7. ...

Such payloads shall provide scientific or technical benefit possibly also to third parties, while at the same time, they shall provide an added value to the Galileo system:

- Operations
- Performance
- Monitoring and Control
- ...

IAPS-INAF
TAS-I

Accelerometry for **G**alileo **E**nhancements and **S**cience (**AGES**)

Il contesto scientifico e tecnologico

L'importanza per **ESA** e per la **CE** degli aspetti scientifici e tecnologici dei satelliti **GNSS** per la navigazione è ben illustrato nel documento (29 Gennaio 2019):

2. Category 2: On-Board Atomic Clocks

This category includes short studies on future on-board atomic clocks technologies for Galileo, that may improve performance, robustness and/or independence of the supply chain. The studies include technology maturity assessment and development plan.

The overall objectives of this category of activities are:

1. to assess the suitability of alternative on-board clock technologies for future batches of Galileo satellites
2. to define the required design and development plan up to flight model, with a target flight model availability date between 2023 and 2026.

With the goal to identify the alternative technology meeting the G2G on-board clock requirements with the lower development risk (technical, industrial, programmatic)

Alternative on-board clock technologies primarily mean all technologies that differ from Passive Hydrogen Maser (PHM) and Rubidium Atomic Frequency Standard (RAFS) or their on-going evolutions. Performance, robustness and reliability are critical aspects for new technologies. Independence in the industrial supply chain will also be considered as a criteria for the identification of the most promising alternative candidate. Examples of alternative technologies are (but not limited to):

- Optically-pumped Cs beam
- Laser pumped Vapour cell
- Hg ions trap
- cold atoms

Il contesto scientifico e tecnologico

L'importanza per **ESA** e per la **CE** degli aspetti scientifici e tecnologici dei satelliti **GNSS** per la navigazione è ben illustrato nel documento (29 Gennaio 2019):
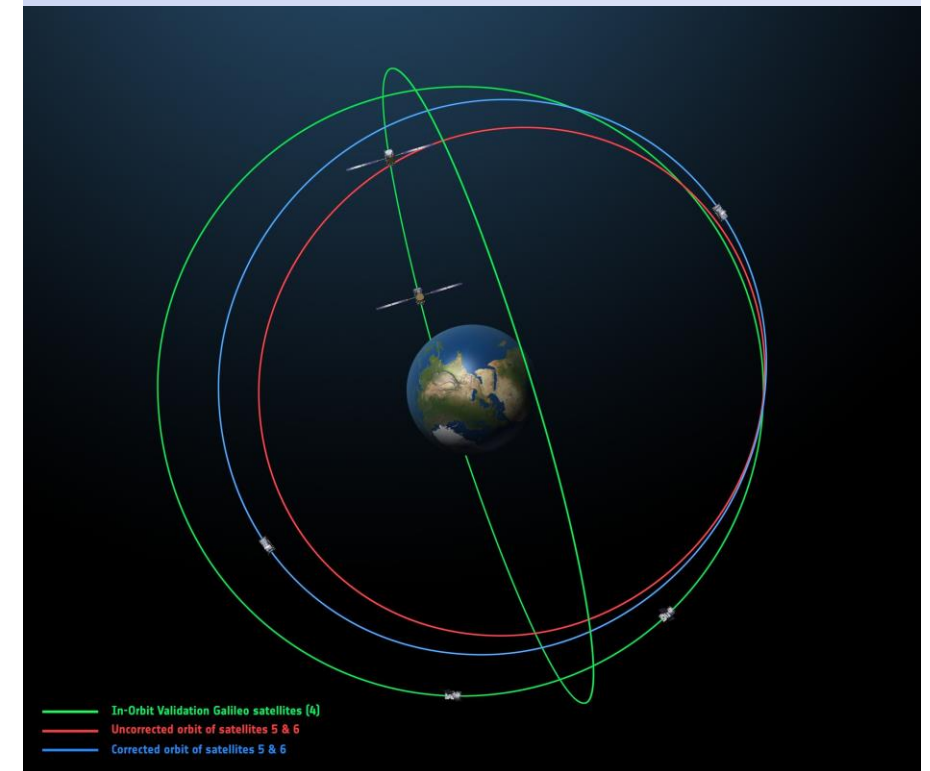
3. **Category 3: European GNSS Scientific Studies**

This category includes innovative scientific studies exploiting differentiators of Galileo (and/or EGNOS) – with particular attention, but not limited to the following topics:

1. Fundamental Physics with Galileo
2. Scientific usage of Galileo signals (AltBOC, triple-frequency, potentially future signals), for Earth and Atmospheric Sciences, Metrology, etc...
3. Scientific studies of innovative nature (with respect to previous ones), exploiting unique features from Galileo and/or EGNOS (with respect to other GNSS or RNSS)

This may consider enhancements of scientific models and algorithms with respect to state-of-art

Eccentric orbits

In-Orbit Validation Galileo satellites (4)
Uncorrected orbit of satellites 5 & 6
Corrected orbit of satellites 5 & 6

Il contesto scientifico e tecnologico

Il progetto Franco/Tedesco **GREAT**:

Gravitational Redshift: past and recent measurements

- **G**ravity **P**robe **A** (**GPA**), 1976-1980: $|\alpha| = (1 \pm 2) \times 10^{-4}$ $|\alpha| \leq 7 \times 10^{-5}$

  R.F.C. Vessot, M.W. Levine, Gen. Rel. Grav., 10, 3, 181-204 (1979)
  R.F.C. Vessot, et al., Phys. Rev. Letter, 45, 2081 (1980)

- **G**alileo gravitational **R**edshift **E**xperiment with eccentric s**AT**ellites (**GREAT**), 2018

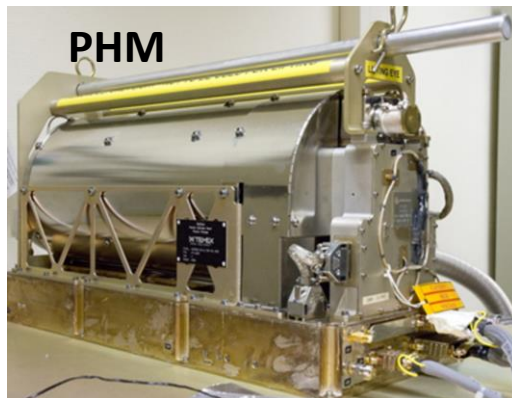 - **SYRTE**: $\alpha = (0.19 \pm 2.48) \times 10^{-5}$ P. Delva, et al., Phys. Rev. Letter, 121, 231101 (2018)
  - **ZARM**: $\alpha = (4.5 \pm 3.1) \times 10^{-5}$ S. Herrmann, et al., Phys. Rev. Lett. , 121, 231102 (2018)

PHM

Systematics:

- Temperature effects
- Earth's magnetic field
- Orbit/clock solution
- Onground clocks

RAFS

PHM (Passive Hydrogen Maser): <4.5 x 10^{-14} at 30000 s
RAFS (Rubidium Atomic Frequency Standard): <5.1 x 10^{-14} at 10000 s

Il contesto scientifico e tecnologico

Il progetto Franco/Tedesco **GREAT**:

GREAT, il progetto congiunto fra **SYRTE** e **ZARM**, è stato finanziato da **ESA** e si è sviluppato su un intervallo di tempo di circa 4 anni avendo come unico obiettivo la misura del **Redshift Gravitazionale**

Inoltre, i due gruppi di ricerca si sono concentrati principalmente nella <u>analisi dei dati degli orologi</u> e nello <u>studio degli errori sistematici</u>

La determinazione orbitale di precisione (**POD**) delle orbite dei satelliti, di fondamentale importanza per la misura, è stata portata a termine da **ESA** con il s/w **NAPEOS**

Il contesto scientifico e tecnologico

Il progetto Franco/Tedesco **GREAT**:

Editors' Suggestion   Featured in Physics

Gravitational Redshift Test Using Eccentric *Galileo* Satellites

P. Delva,[1,*] N. Puchades,[2,1] E. Schönemann,[3] F. Dilssner,[3] C. Courde,[4] S. Bertone,[5] F. Gonzalez,[6] A. Hees,[1] Ch. Le Poncin-Lafitte,[1] F. Meynadier,[1] R. Prieto-Cerdeira,[6] B. Sohet,[1] J. Ventura-Traveset,[7] and P. Wolf[1]

[1] *SYRTE, Observatoire de Paris, Université PSL, CNRS, Sorbonne Université, LNE, 61 avenue de l'Observatoire 75014 Paris, France*
[2] *Departamento de Astronomia y Astrofisica, Edificio de Investigación Jerónimo Muñoz, C/ Dr. Moliner, 50, 46100 Burjassot (Valencia), Spain*
[3] *European Space Operations Center, ESA/ESOC, 64293 Darmstadt, Germany*
[4] *UMR Geoazur, Université de Nice, Observatoire de la Côte d'Azur, 250 rue A. Einstein, F-06560 Valbonne, France*
[5] *Astronomical Institute, University of Bern, Sidlerstrasse 5 CH-3012 Bern, Switzerland*
[6] *European Space and Technology Centre, ESA/ESTEC, 2200 AG Noordwijk, Netherlands*
[7] *European Space and Astronomy Center, ESA/ESAC, 28692 Villanueva de la Cañada, Spain*

SYRTE + ESA

ZARM + ESA

Editors' Suggestion   Featured in Physics

Test of the Gravitational Redshift with *Galileo* Satellites in an Eccentric Orbit

Sven Herrmann,[1,*] Felix Finke,[1] Martin Lülf,[2] Olga Kichakova,[1] Dirk Puetzfeld,[1] Daniela Knickmann,[3] Meike List,[1] Benny Rievers,[1] Gabriele Giorgi,[4] Christoph Günther,[2,4] Hansjörg Dittus,[5] Roberto Prieto-Cerdeira,[6] Florian Dilssner,[7] Francisco Gonzalez,[6] Erik Schönemann,[7] Javier Ventura-Traveset,[8] and Claus Lämmerzahl[1]

[1] *University of Bremen, ZARM Center of Applied Space Technology and Microgravity, Bremen 28359, Germany*
[2] *Technical University Munich, Munich 80333, Germany*
[3] *OHB System AG, Bremen 28359, Germany*
[4] *Deutsches Zentrum für Luft- und Raumfahrt, Oberpfaffenhofen-Wessling 82234, Germany*
[5] *Deutsches Zentrum für Luft- und Raumfahrt, Köln 51147, Germany*
[6] *European Space and Technology Centre, ESA ESTEC, AZ Noordwijk 2201, Netherlands*
[7] *European Space Operations Centre, ESA ESOC, Darmstadt 64293, Germany*
[8] *European Space and Astronomy Centre, ESA ESAC, Villanueva de la Cañada, Madrid 28692, Spain*

Second-generation Galileo contract awarded to Thales

April 19, 2021 - By Tracy Cozzens

Illustration: Thales Alenia Space

Project will boost the positioning performance and real-time operability of the Galileo system.

The European Space Agency (ESA) has selected Thales Alenia Space to support the implementation and experimentation of the navigation algorithms that will be used in the Galileo Second Generation program. Under the contract, Thales will develop the Advanced Orbit Determination and Time Synchronisation (ODTS) Algorithms Test Platform (A-OATP).

Thales Alenia Space, a joint venture between Thales (67%) and Leonardo (33%), is the prime contractor for Galileo First Generation's Ground Mission Segment,.

ESA granted the contract on behalf of the European Commission in the Horizon 2020 Satellite Navigation Program (HSNAV).

In a previous contract, Thales Alenia Space was chosen to provide six satellites and initiate the B2 phase of development and implementation of its ground segment for the Galileo Second Generation constellation.

Using its long-standing legacy regarding navigation algorithms in addition to an innovative approach, Thales Alenia Space will develop and test a new Advanced ODTS solution. The new orbitography algorithms will allow a significant improvement in positioning performance and real-time operability of the Galileo system. It will exploit the accuracy of the GNSS orbit and clock estimation, with a solution optimized for the real-time generation of Galileo navigation messages, and take full advantage of the evolution of satellites and ground stations considered in the Galileo Second Generation.

With this new contract, Thales Alenia Space applies on a deep experience concerning orbitography algorithms as well as knowledge of the Galileo system to strengthen its position as a major actor for the development of the new generation of this satellite system, the company stated in a press release.

Risultati e prospettive

Attività preliminari

Visti i molteplici obiettivi del progetto e l'elevato grado di difficoltà che alberga in ciascuno di essi al fine del suo raggiungimento, sono state preliminarmente intraprese un certo numero di attività focalizzate sullo sviluppo di nuovi modelli per le forze non-conservative:

1. **Modello 3D** del satellite per future analisi agli elementi finiti tramite Ray-Tracing
2. **Modello Box-Wing** del satellite e determinazione delle accelerazioni prodotte da alcune perturbazioni Non-Gravitazionali
3. Attività preliminari al **Ray-Tracing**

Alcuni risultati sono già stati presentati in contesti internazionali:
- 3th IEEE International Workshop on Metrology for Aerospace 2016
- **6th International Colloquium on Scientific and Fundamental aspects of GNSS 2017**
- 5th IEEE International Workshop on Metrology for Aerospace 2018
- COSPAR 2018
- EGU 2019
- **7th International Colloquium on Scientific and Fundamental aspects of GNSS 2019**
- **COSPAR 2021**
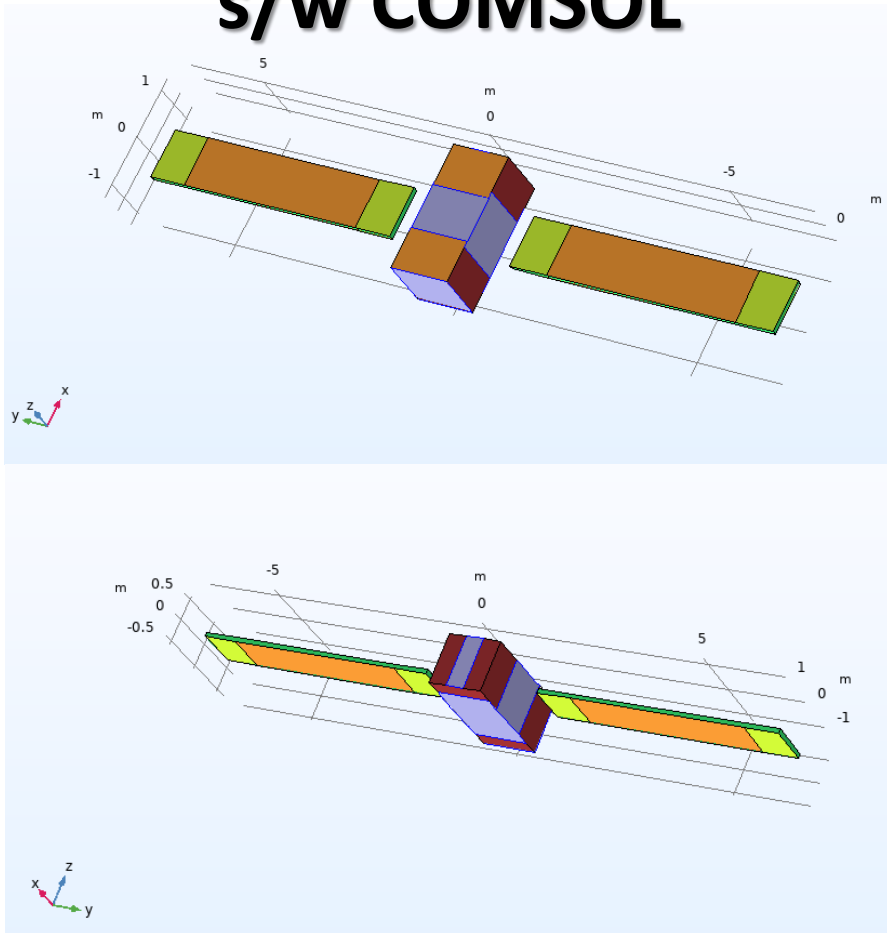- **EGU2021**

Risultati e prospettive

Attività preliminari: Modello 3D
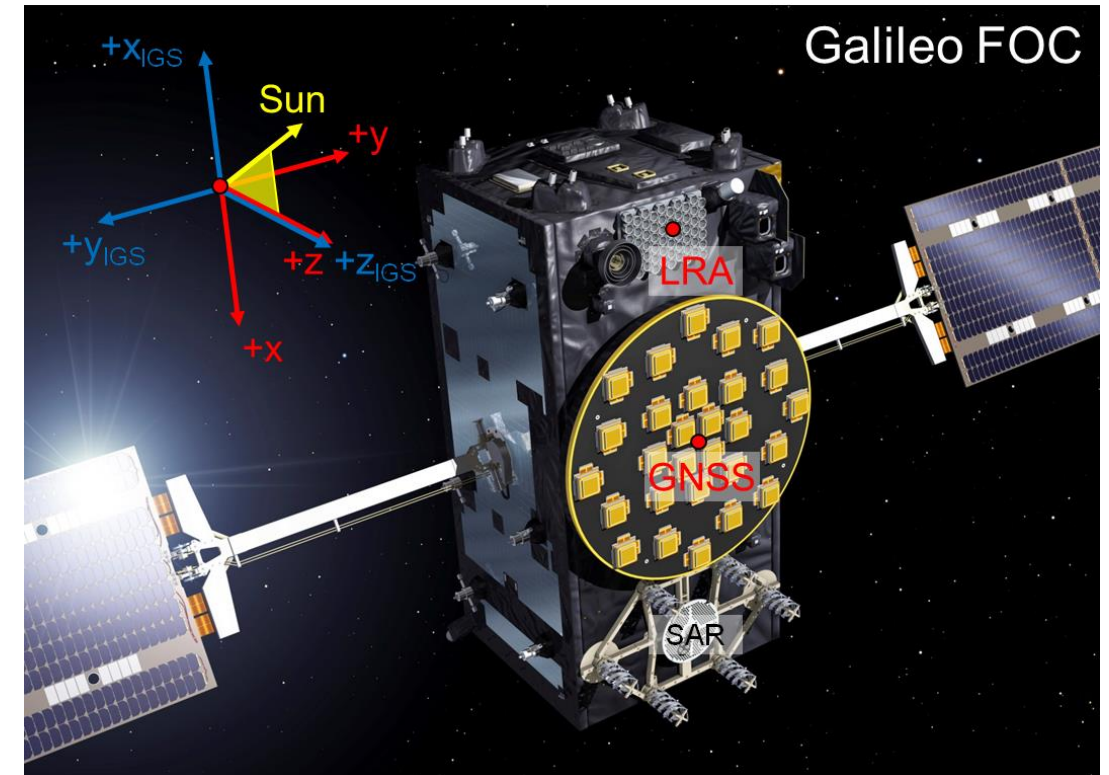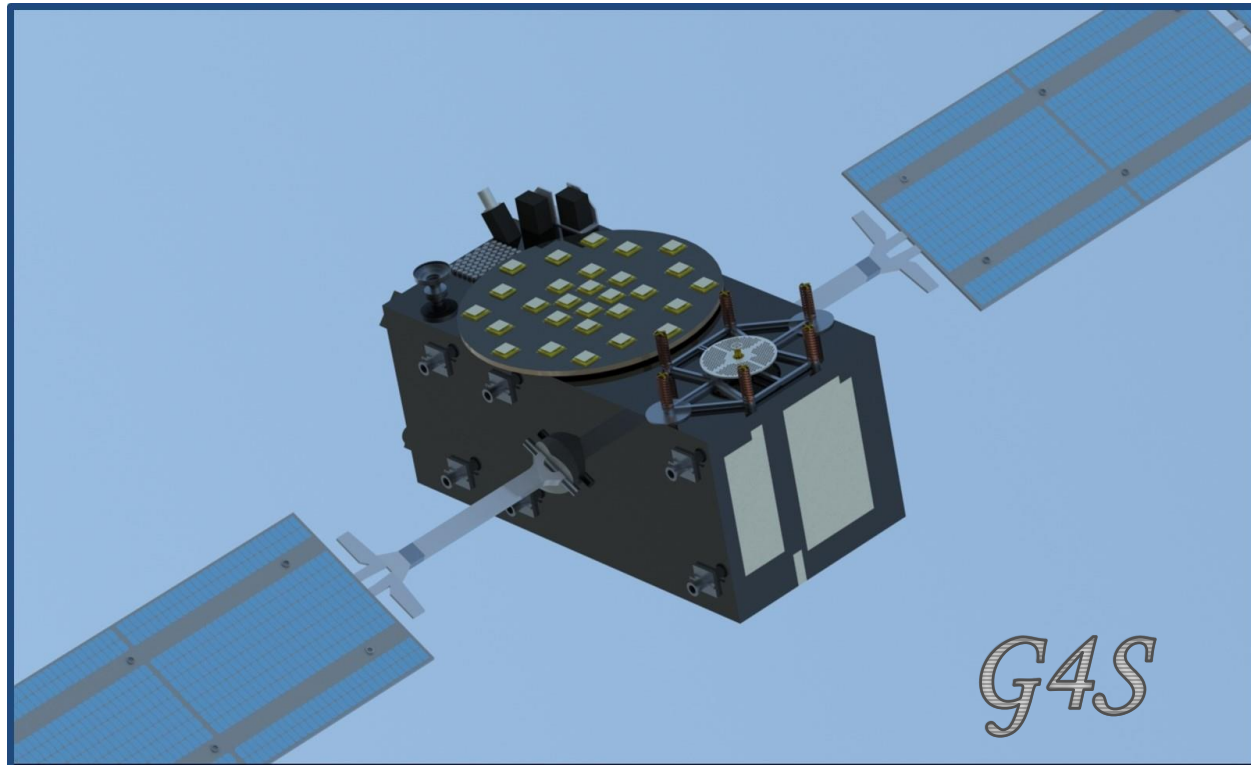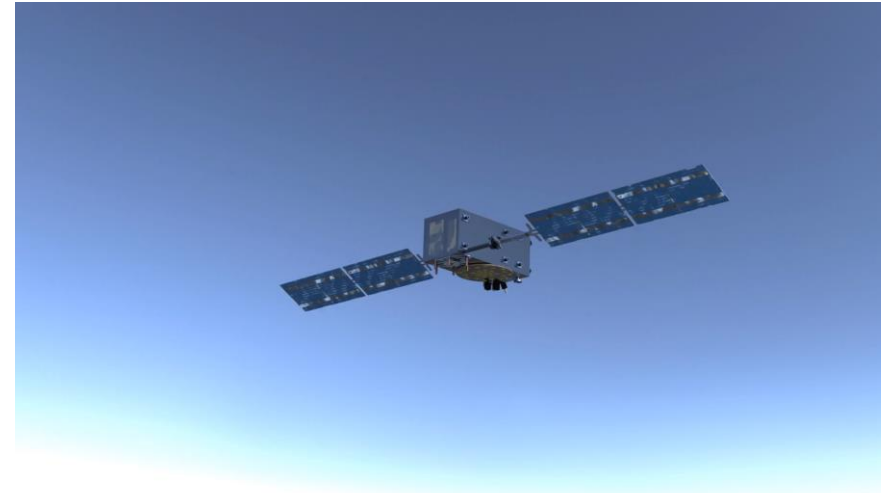
Risultati e prospettive

Attività preliminari: Modello Box-Wing

s/w COMSOL

Surface		Material	Area $[m^2]$	$\alpha[-]$	$\rho[-]$	$\delta[-]$
Box	+X	A	0.440	0.93	0.00	0.07
		C	0.880	0.08	0.73	0.19
	-X	A	1.320	0.93	0.00	0.07
	+Y	A	1.129	0.93	0.00	0.07
		C	1.654	0.08	0.73	0.19
	-Y	A	1.244	0.93	0.00	0.07
		C	1.539	0.08	0.73	0.19
	+Z	A	1.053	0.93	0.00	0.07
		B	1.969	0.57	0.22	0.21
	-Z	A	2.077	0.93	0.00	0.07
		C	0.959	0.08	0.73	0.19
Wing	+SA	E	3.880	0.92	0.08	0.00
		D	1.530	0.90	0.10	0.00
	-SA	E	3.880	0.92	0.08	0.00
		D	1.530	0.90	0.10	0.00

Risultati e prospettive

Attività preliminari: Modello Box-Wing

$$a_\odot \simeq 1 \cdot 10^{-7} \; m/s^2$$

The direct **SRP** depends on:

1. the solar flux $\Phi_\odot$
2. the distance of the Earth-satellite system from the Sun
3. the satellite attitude and its shape/geometry
4. the physical properties (optical, thermal,...) of the various surfaces (constituents) and their time degradation

$\hat{S}_\odot$ $\hat{n}$

$\cos\beta = \hat{n} \cdot \hat{S}_\odot$

dA
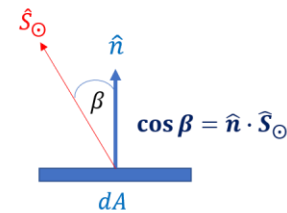
The resulting elementary acceleration on a surface element

$$\alpha + \rho + \delta = 1$$

$$d\vec{a} = -\frac{\Phi_\odot}{mc}\left[(1-\rho)\hat{S}_\odot + 2\left(\frac{\delta}{3} + \rho\cos\beta\right)\hat{n}\right]dA|\cos\beta|$$

$$d\vec{a} = d\vec{a}_\alpha + d\vec{a}_\rho + d\vec{a}_\delta$$

A. Milani, A.M. Nobili, P. Farinella. Adam Hilger, Bristol (1987)

Simplifying assumptions:

a) the absorbed light is not-re-emitted
b) for a given direction, the intensity of diffused light is proportional to the cosine of the angle with the unit vector $\hat{n}$ (**Lambert's law**, i.e. spherical diffusion lobe)
c) the reflection is perfectly specular
d) dA behaves like a linear combination of a black body, a perfect mirror and a Lambert diffuser

$$d\vec{a}_\alpha = -\frac{\Phi_\odot}{mc}\alpha \, dA \, |\cos\beta| \, \hat{S}_\odot$$

$$d\vec{a}_\rho = -\frac{\Phi_\odot}{mc}2\rho\cos\beta \, dA \, |\cos\beta|\hat{n}$$

$$d\vec{a}_\delta = -\frac{\Phi_\odot}{mc}\delta \, dA \, |\cos\beta|\hat{S}_\odot - \frac{\Phi_\odot}{mc}\frac{2}{3}\delta dA \, |\cos\beta|\hat{n}$$

- We need to improve the modeling of the **NGPs** down to an acceleration level $\leq 10^{-10}$ m/s²

- On the basis of our experience with **LAGEOS** satellites, the main challenge is represented by the knowledge of the temperature distribution of the S/C and the development of a reliable model for the thermal perturbations

- We need almost all the physical information characterizing the S/C materials:

  ❑ The characteristics provided in the **FOC** metadata are not enough for a **FEM**

$$\Delta a_\odot \simeq 1 \cdot 10^{-10} \; m/s^2$$

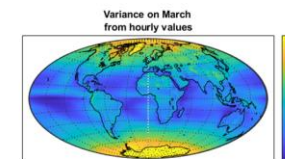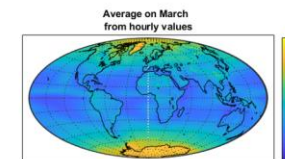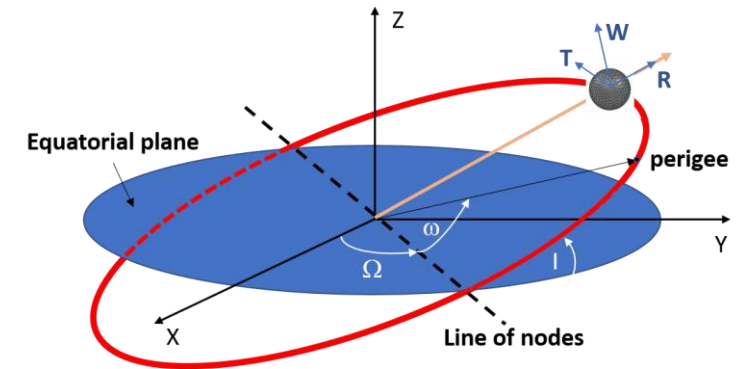# Risultati e prospettive

Attività preliminari: Modello Box-Wing

A 1-year simulation with the S-BW model
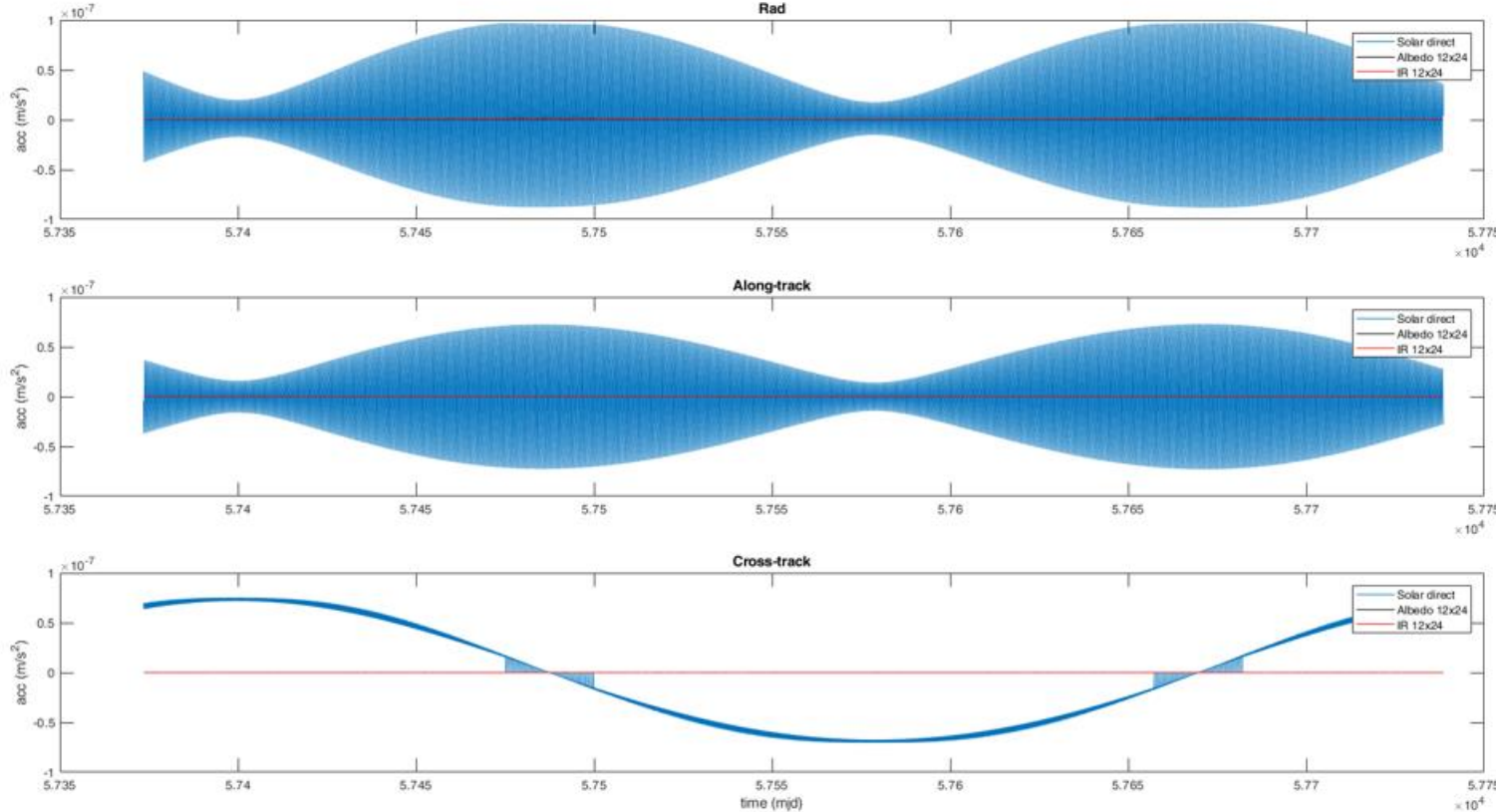
Galileo FOC E08

1. **Direct Solar Radiation Pressure**
2. **Earth's albedo**
3. **Earth's infrared radiation**

$$\vec{a} = R\hat{r} + T\hat{t} + W\hat{w}$$

- **CERES (Clouds and Earth's Radiant Energy System)** measures in three bands solar-reflected and Earth-emitted radiation from the top of the atmosphere to the Earth's surface

- Using data from **CERES** we can calculate different averages (hourly, monthly, etc.) of Earth's Albedo and Infrared radiation

- https://ceres.larc.nasa.gov/data/
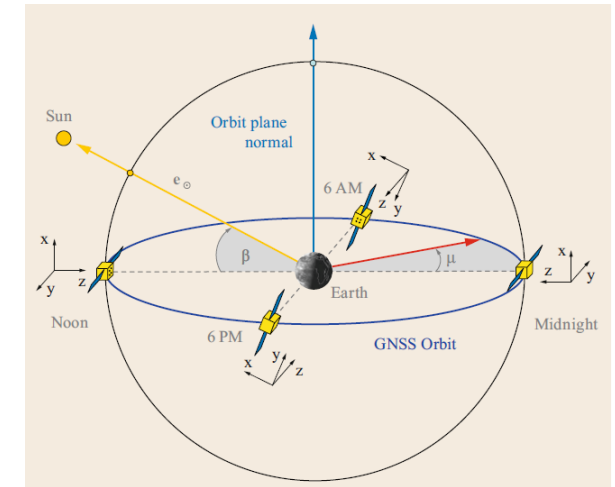
Risultati e prospettive

Attività preliminari: Modello Box-Wing
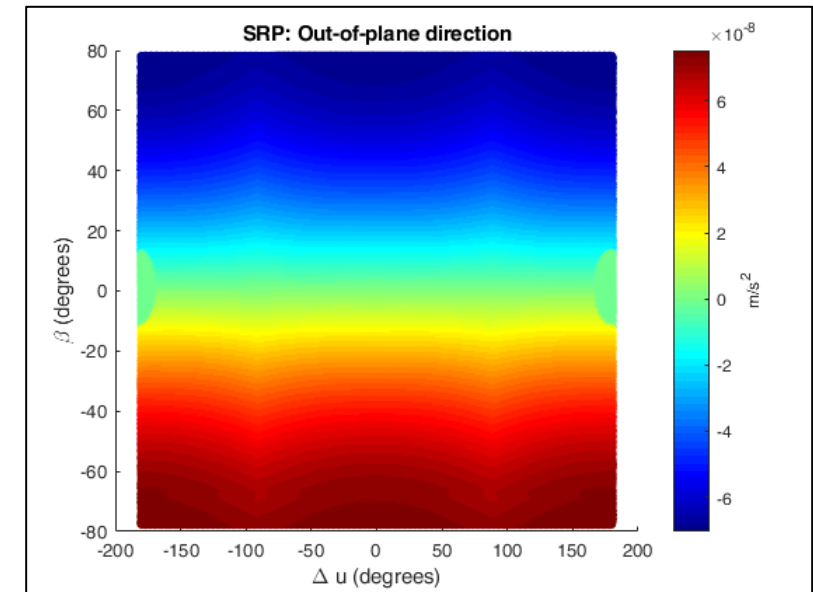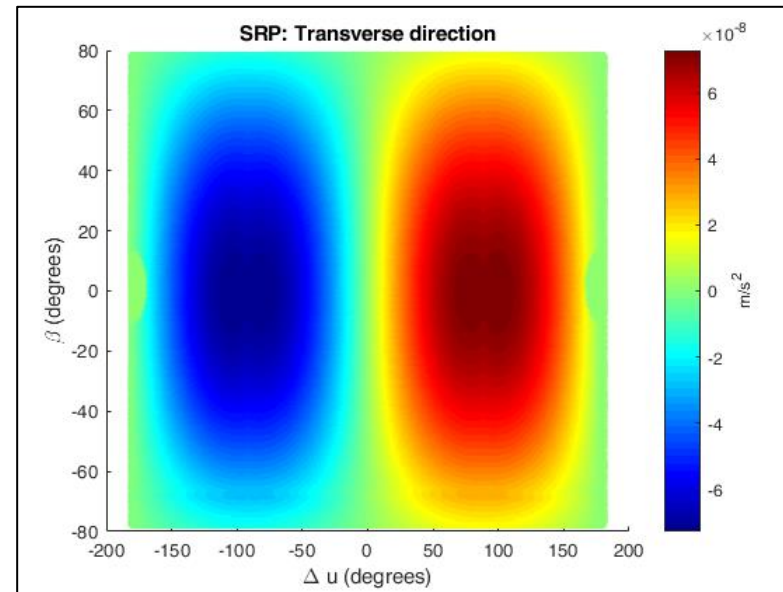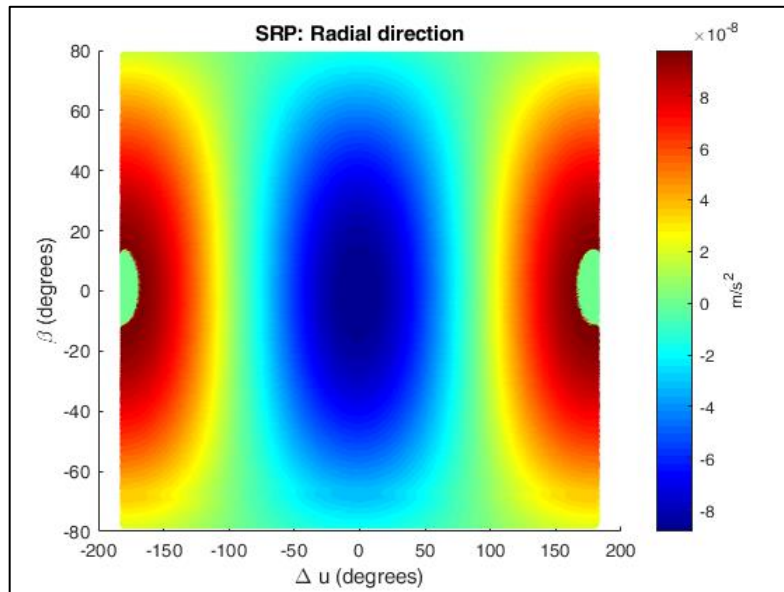
Solar Radiation Pressure acceleration

$$R = R(\beta, \Delta u)$$
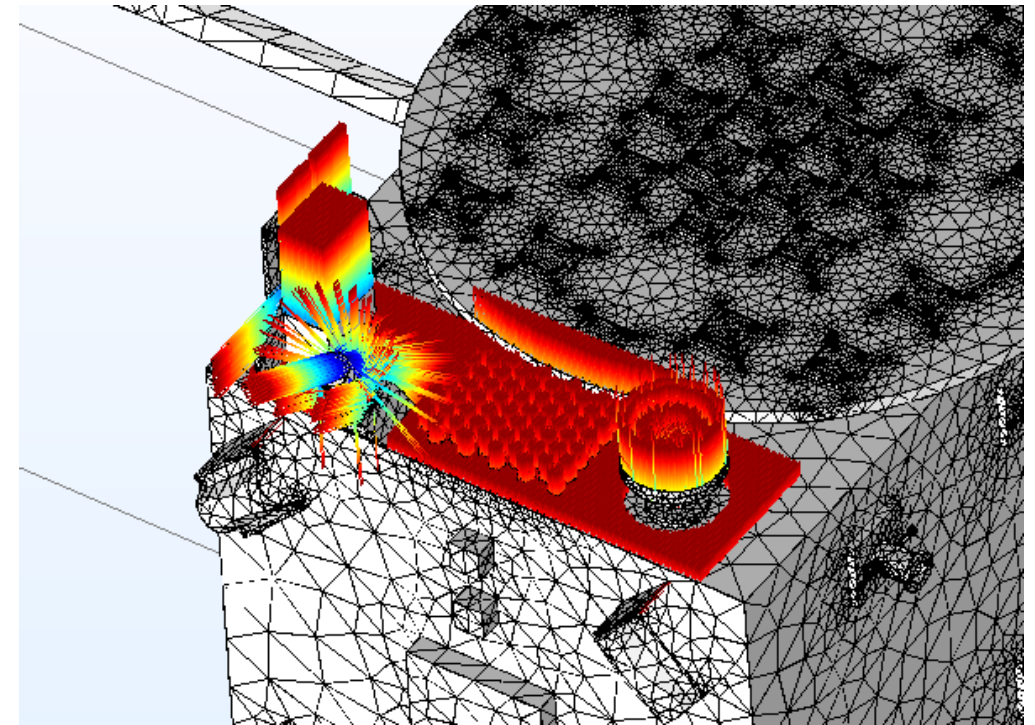$$T = T(\beta, \Delta u)$$
$$W = T(\beta, \Delta u)$$

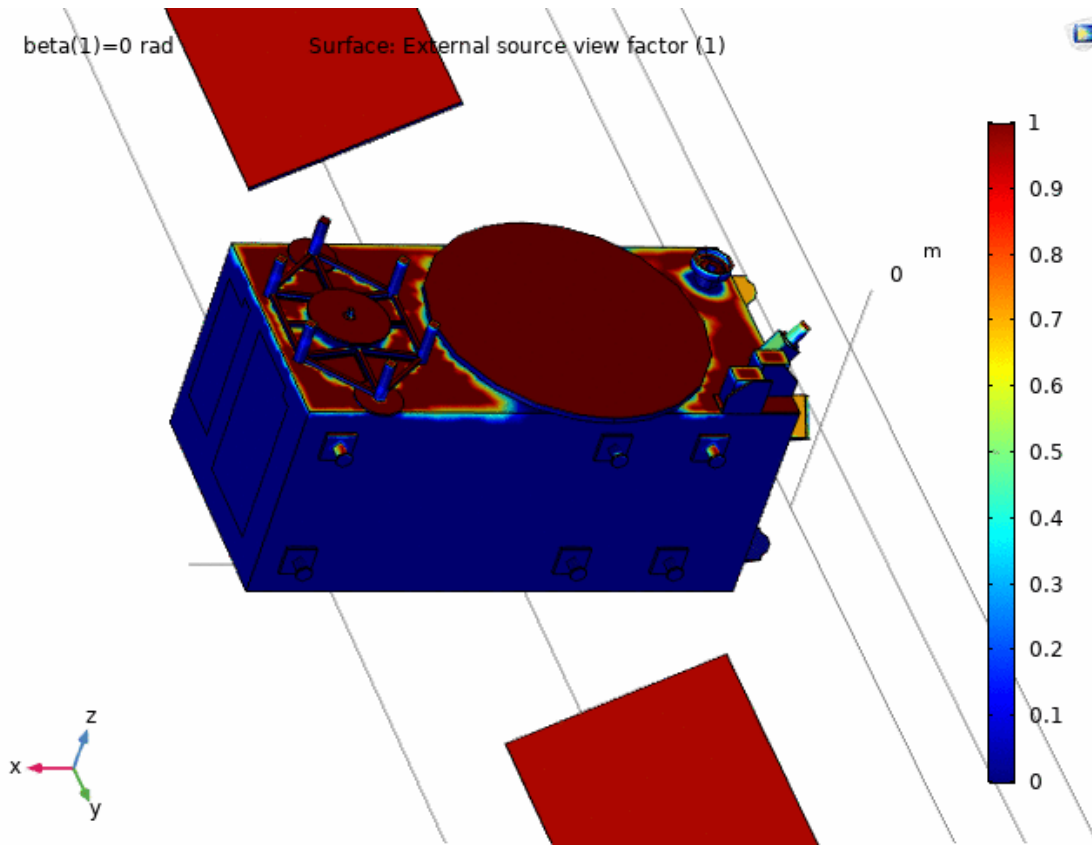**Galileo FOC E08**

Risultati e prospettive

Attività preliminari: verso il Ray-Tracing

s/w COMSOL

Risultati e prospettive

Prospettive: **Gravitational Redshift**

Special Relativity (**SR**) and **GR** are responsible of frequency shifts of the onboard clocks that can be carefully measured by exploiting both the precise onboard **H-maser clocks** and the **high eccentricity** of the orbits

- among these effects the **Gravitational Redshift** plays a special role, since it represents a test of the **Local Position Invariance** (**LPI**)

Indeed, **LPI** is one of the ingredients of **Einstein Equivalence Principle** (**EEP**) which is at the basis of Einstein's **GR** and of all metric theories of gravitation:

1. **Universality of Free Fall (UFF)**
2. **Local Lorentz Invariance (LLI)**
3. **Local Position Invariance (LPI)**

G4S_2.0 approach (orbit models + systematics):
- FEM for the satellite
- SLR data: NP and FR
- Gravity Field Free (GFF) technique
- Galileo constellation

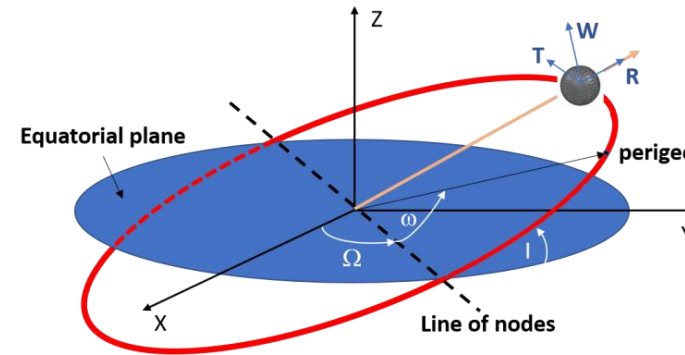$$y = \frac{\Delta v}{v} = \frac{GM_{\oplus}}{c^2}\left(\frac{1}{R_{\oplus}} - \frac{\mathbf{1}}{\mathbf{r}}\right)$$

$$y_{\alpha} = -(1+\alpha)\frac{GM_{\oplus}}{rc^2}$$

$\alpha = 0$ in GR

Goal
$|\alpha| \leq 2 \times 10^{-5}$

Risultati e prospettive

Equatorial plane, perigee, Line of nodes

Prospettive: **Relativistic precessions**

1. **Schwarzschild** or Einstein precession (gravitoelectric field)

2. **Lense-Thirrig** (**LT**) precession (gravitomagnetic field)

3. **Geodetic precession** (Coriolis-like acceleration)

$$\dot{\omega}^{Ein} = \frac{3\left(GM_\oplus\right)^{3/2}}{c^2\, a^{5/2}(1-e^2)} \qquad \dot{\omega}^{LT} = \frac{-6\, GJ_\oplus}{c^2\, a^3\left(1-e^2\right)^{3/2}}\, cos\, i \qquad \dot{\Omega}^{LT} = \frac{2\, GJ_\oplus}{c^2\, a^3\left(1-e^2\right)^{3/2}}$$

$$\dot{\Omega}^{dS} = \frac{3}{2}\frac{GM_\oplus}{c^2\, R_{\oplus\odot}^3}\left|(V_\oplus - V_\odot)\times R_{\oplus\odot}\right| cos\, \varepsilon_\odot$$

The measurements of the relativistic precessions are much more challenging in the case of the Galileo satellites

- In particular in the case of the **LT** effect (the **GR** precession is more than a factor of 10 smaller than the **LAGEOS** one)
- However, the measurement of **Schwarzschild** precession is favorable, particularly if **LAGEOS II** is also considered
- Consequently, also the constraints in **Yukawa-like** interactions are promising

Rate (mas/yr)	GSAT-201/202	GSAT-203
1 mas = 1 milli arc sec		
$\Delta\dot{\omega}_E$	+ 428.88	+ 362.74
$\Delta\dot{\omega}_{LT}$	− 5.21	− 3.67
$\Delta\dot{\Omega}_{LT}$	+ 2.69	+ 2.18
$\Delta\dot{\Omega}_{dS}$	+ 17.60	+ 17.60

Rate (mas/yr)	LAGEOS II	LAGEOS
1 mas = 1 milli arc sec		
$\Delta\dot{\omega}_E$	+ 3351.95	+ 3278.77
$\Delta\dot{\omega}_{LT}$	− 57.00	+ 32.00
$\Delta\dot{\Omega}_{LT}$	+ 31.50	+ 30.67
$\Delta\dot{\Omega}_{dS}$	+ 17.60	+ 17.60

G4S
Galileo for Science

Risultati e prospettive

Prospettive: **Constraints on dark matter (DM)**

- **DM** could arise from very light quantum fields that form macroscopic objects or clumps

- These may produce **topological defects** (**TD**), as **domain walls**, that could be responsible of glitches and transients in **GNSS** clocks time measurements related to transient variations of fundamental constants

- Roberts et al. (2017) have found no evidence for the existence of **domain walls** after an analysis of about 16 years of **GPS** data at the sensitivity level of the onboard atomic clocks

- These limits can be further improved exploiting the higher performance of the atomic clocks of the **Galileo** constellation

**B.M. Roberts et al., Nature Communications 8, 1195 (2017)**

Risultati e prospettive

Prospettive: **Relativistic Positioning System (RPS)**

- The idea is to use a **RPS** based on emitters fixed to the surface of the Earth to provide an accurate orbit determination of the two S/C

- This represents a fully **RPS** based on the complete exploit of **SR** and **GR** and on the concept of space-time

- In the case of **GNSS** satellites the positioning is "traditional" and the relativistic effects are introduced as perturbations, i.e., as corrections to a Newtonian formulation

- The counting of the pulses for a set of different emitters whose positions on the Earth and periods are assumed to be known, is used to provide **null emission** (or light) **coordinates** for the receiver on a satellite

- The measurement of the **proper time intervals** between successive arrivals of the signals from the various emitters is used to give the final localization of the receiver, within an accuracy controlled by the precision of the onboard clock

Risultati e prospettive
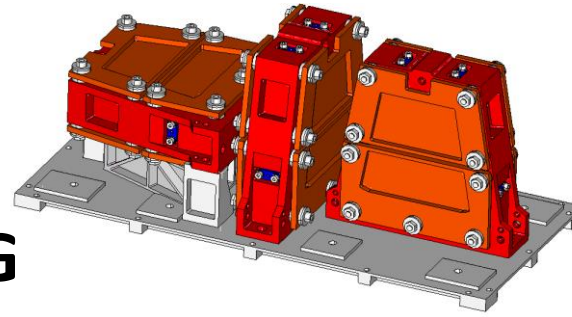
Prospettive: **Accelerometro per i G2G**

Tasks ACC.Dev1:

- To study technical solutions to overcome the limitations of the current INAF-IAPS accelerometers, intrinsic to their functioning concept, related to measurements bias and long-term stability
- To identify possible sensors arrangements to disentangle among accelerations due to linear and rotational S/C body motion

Tasks ACC.Req:

- To identify possible scientific goals and define related required measurement performance
- To study suitable instrument configurations and identify performance-critical elements

Tasks ACC.Dev2:

- To study technical solutions of performance-critical elements, in order to reach the needed performance

Risultati e prospettive

Prospettive: **Accelerometro per i G2G**
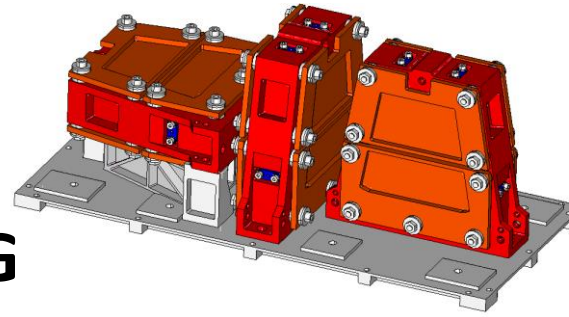
Non-Gravitational Perturbation		Amplitude [m/s²]	Models accuracy [m/s²]	
Far from eclipses			10%	5%
SRP + Albedo + IR radiation	R	1.616×10⁻⁸ @f_orb	1.62×10⁻⁹	8×10⁻¹⁰
	T	1.442×10⁻⁸ @f_orb	1.44×10⁻⁹	7×10⁻¹⁰
	W	1.04×10⁻⁹ @2f_orb	1.0×10⁻¹⁰	5×10⁻¹¹
	D	1.20×10⁻⁹ @2f_orb	1.2×10⁻¹⁰	5×10⁻¹¹
	B	1.64×10⁻⁹ @f_orb	1.6×10⁻¹⁰	1×10⁻¹⁰
	Xb	4.2×10⁻¹⁰ @2f_orb	4×10⁻¹¹	2×10⁻¹¹
	Yb	2×10⁻¹² @f_orb	2×10⁻¹³	1×10⁻¹³
During eclipses			10%	5%
SRP + Albedo + IR radiation	R	7.867×10⁻⁸ @f_orb	7.87×10⁻⁹	3.9×10⁻⁹
	T	7.597×10⁻⁸ @f_orb	7.60×10⁻⁹	3.8×10⁻⁹
	W	6.1×10⁻¹⁰ @f_orb	6×10⁻¹¹	3×10⁻¹¹
	D	1.162×10⁻⁸ @4f_orb	1.16×10⁻⁹	6×10⁻¹⁰
	B	4.866×10⁻⁸ @f_orb	4.87×10⁻⁹	2.4×10⁻⁹
	Xb	3.078×10⁻⁸ @2f_orb	3.08×10⁻⁹	1.5×10⁻⁹
	Yb	4×10⁻¹¹ @19f_orb	4×10⁻¹²	2×10⁻¹²

Lo scopo finale è quello di sviluppare un nuovo concetto di accelerometro che possa misurare le accelerazioni non-gravitazionali ad un livello di accelerazione $\approx 1 \times 10^{-10}\ m/s^2$ e che possa fornire misure utili in tutte quelle condizioni in cui i modelli non sono comunque adeguati:
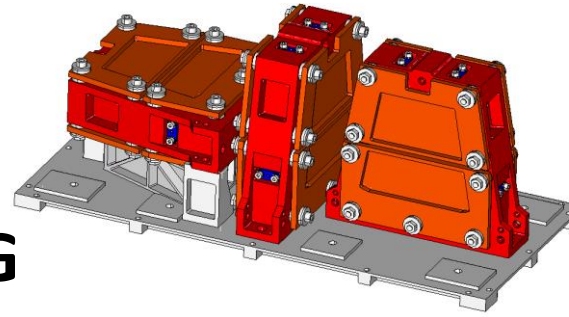
- Fase di penombra (effetti atmosferici …)
- Eclissi
- Manovre

$$a(f) \leq 2 \times 10^{-9}\ \frac{m/s^2}{\sqrt{Hz}}$$

$$f_{orb} \cong 1.973 \times 10^{-5} Hz$$

$$[1 \times 10^{-5} \div 1 \times 10^{-3}]Hz$$

Risultati e prospettive

Prospettive: **Accelerometro per i G2G**

Advantages from an on-board accelerometer: <u>as a platform instrument</u>

1. COM movements due to fuel sloshing and mass variation
2. Mass variation
3. Satellite attitude knowledge in general and, especially, during the eclipses and the penumbra transitions
4. Solar panel wings normal modes and their variation
5. Manoeuvres and orbit recovery after manoeuvres
6. In band micro-vibration level monitoring
7. High frequency out-of-band monitoring once converted to low frequency in the measurement band
8. New POD concept

$$\ddot{\vec{x}} = \nabla U(\vec{x}) + \vec{a}_{ngp}$$ **Eq. of motion for the S/C CoM**

$$\ddot{\vec{x}} + \ddot{\vec{y}} = \nabla U(\vec{x} + \vec{y}) - \vec{a}_{acc}$$ **Eq. of motion of the ACC reference point (Vertex)**
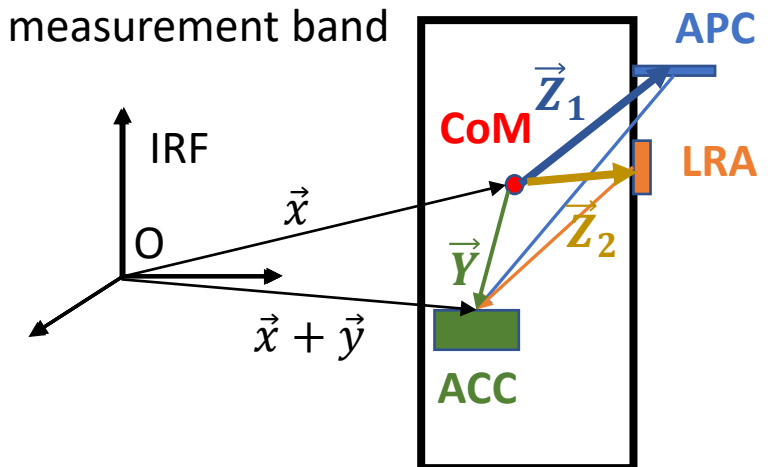
Risultati e prospettive

Prospettive: **Accelerometro per i G2G**
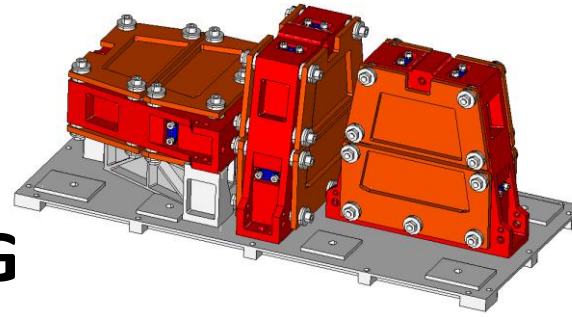
Advantages from an on-board accelerometer: <u>as a scientific payload</u>

1. POD improvements (direct products):
   - Precise orbits
   - Clock solutions
   - Broadcast ephemeris

2. POD improvements (indirect products)
   - Calibration of NGP models
   - Calibration of empirical models
   - IGS products in the field of space geodesy and geophysics
     - Terrestrial reference frame
     - Geocentre coordinates
     - Earth orientation and rotation parameters
   - IGS products in the field of atmospheric physics
     - Tropospheric zenith path delay
     - Radio occultation
     - Meteorology
     - Climate changes
   - Fundamental physics measurements

Programmazione

Cronoprogramma
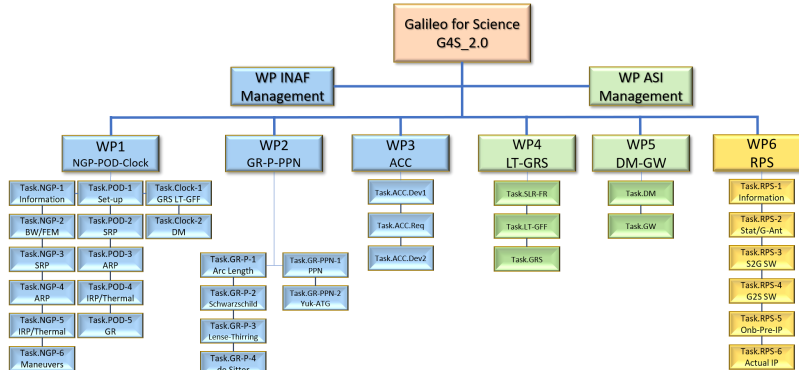
		Primo Anno												Secondo Anno												Terzo Anno									
		1	2	3	4	5	6	7	8	9	10	11	12	13	14	15	16	17	18	19	20	21	22	23	24	25	26	27	28	29	30	31	32	33	34	35	36
WP1	1		NGP-2				NGP-3				NGP-4				NGP-5		NGP-6																				
							POD-1			POD-2			POD-3			POD-4																					
														POD-5																						
													Clock-1																							
																		Clock-2																		
WP2																		P-1		P-2			P-3			P-4			PPN-1			PPN-2				
WP3							ACC.Dev1												ACC.Req							ACC.Dev2									
		1	2	3	4	5	6	7	8	9	10	11	12	13	14	15	16	17	18	19	20	21	22	23	24	25	26	27	28	29	30	31	32	33	34	35	36
WP4			SLR-FR				LT-GFF																													
					GRS																															
WP5								DM																												
											GW																									
		1	2	3	4	5	6	7	8	9	10	11	12	13	14	15	16	17	18	19	20	21	22	23	24	25	26	27	28	29	30	31	32	33	34	35	36
WP6		RPS-1		RPS-2			RPS-3							RPS-4							RPS-5				RPS-6					RPS-7						

Programmazione

Riunioni di avanzamento e prodotti

Le attività del progetto saranno cadenzate (verso **ASI**) da
- Tre riunioni di avanzamento
- Una riunione finale

Per ogni riunione sono stati programmati alcuni prodotti da produrre
- Progress reports e presentazioni
- Reports e Note tecniche

Si produrrà inoltre molto s/w di diversa tipologia

Evento	Descrizione	Tempistica
TN	Tavolo Negoziale	
RI – KOM	Riunione iniziale di avvio lavori	T0
RA1	1a Riunione di Avanzamento	T0 + 7 mesi
RA2	2a Riunione di Avanzamento	T0 + 19 mesi
RA3	3a Riunione di Avanzamento	T0 + 31 mesi
RF	Riunione Finale	T0 + 36 mesi

PROGETTO G4S_2.0

ALLEGATO 1: ELENCO DOCUMENTAZIONE

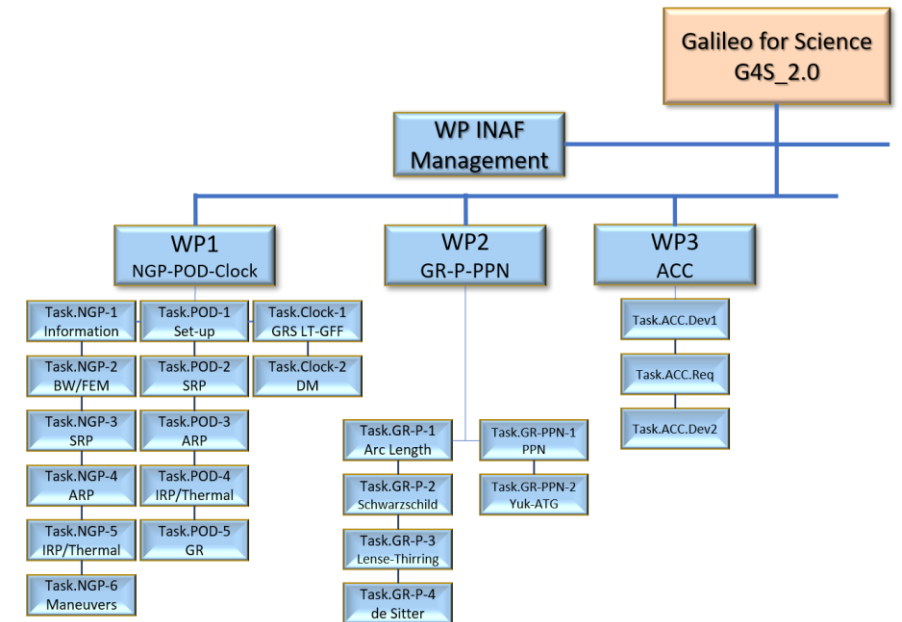| CODICE	TITOLO	RESP	EVENTO DI CONSEGNA	RIF
DEL 001	Progress Report Presentazione#1 attività RA1	ASI/EP	Riunione di avanzamento #1	N/A
DEL 002	Progress Report Presentazione#2 attività RA2	ASI/EP	Riunione di avanzamento #2	N/A
	Report WP4(SLR-FR)	ASI		
	Report WP1(NGP-POD) Nota tecnica WP1(BW/FEM) Nota tecnica WP3(ACC.Dev1)	INAF		
	Report Task.RPS-1-2-3	POLITO		
DEL 003	Progress Report Presentazione#3 attività RA3	ASI/EP	Riunione di avanzamento #3	N/A
	Report WP4(Finale)	ASI		
	Report WP1(Finale) Report WP2(GR-P) Nota tecnica WP3(ACC.Req)	INAF		
	Report Task.RPS-4-5-6	POLITO		
DEL 004	Rapporto Finale Presentazione#4 fine attività	ASI/EP	RF	N/A
	Report WP5(Finale)	ASI		
	Report WP2(Finale); Nota tecnica WP3(ACC.Dev2)	INAF		
	Report Task.RPS-7	POLITO		

Programmazione

Riunioni interne allo IAPS-INAF

Abbiamo svolto tre riunioni del **Gruppo Gravitazionale (WP1)**:

1. Determinazione Orbitale #1:   5 Maggio 2021
2. Modelli Forze Non-Gravitazionali #1:   11 Maggio 2021
3. Determinazione Orbitale #2:   21 Maggio 2021

A breve terremo la prima riunione sulle attività di Laboratorio per **l'Accelerometro (WP3):**

4.   Accelerometro #1:   ? Giugno 2021

Fondi

Finanziamento del progetto

Sulla base dell'analisi svolta il costo complessivo dell'accordo è di € 1.034.960,43 con la seguente ripartizione fra gli enti partecipanti descritta in tabella:

Istituto	Finanziamento Premiale	Co-finanziamento
ASI/CGS	40.000,00	130.246,52
INAF	460.000,00	275.035,47
POLITO	80.000,00	49.678,45
Totali	580.000,00	454.960,44

Lo IAPS/INAF infatti si avvarrà della collaborazione del Politecnico di Torino come altro ente partecipante.

INAF co-finanzia il progetto per il 60%

- Il progetto è finanziato da **ASI** per 580 k€
- **INAF** riceverà tre tranches da 180 k€ alle RA per un totale di 540 k€
  - ❑ 460 k€ @**IAPS-INAF**
  - ❑ 80 k€ @**POLITO**

Evento	Descrizione	Tempistica
TN	Tavolo Negoziale	
RI – KOM	Riunione iniziale di avvio lavori	T0
RA1	1a Riunione di Avanzamento	T0 + 7 mesi
RA2	2a Riunione di Avanzamento	T0 + 19 mesi
RA3	3a Riunione di Avanzamento	T0 + 31 mesi
RF	Riunione Finale	T0 + 36 mesi

180 k€ (RA1)
180 k€ (RA2)
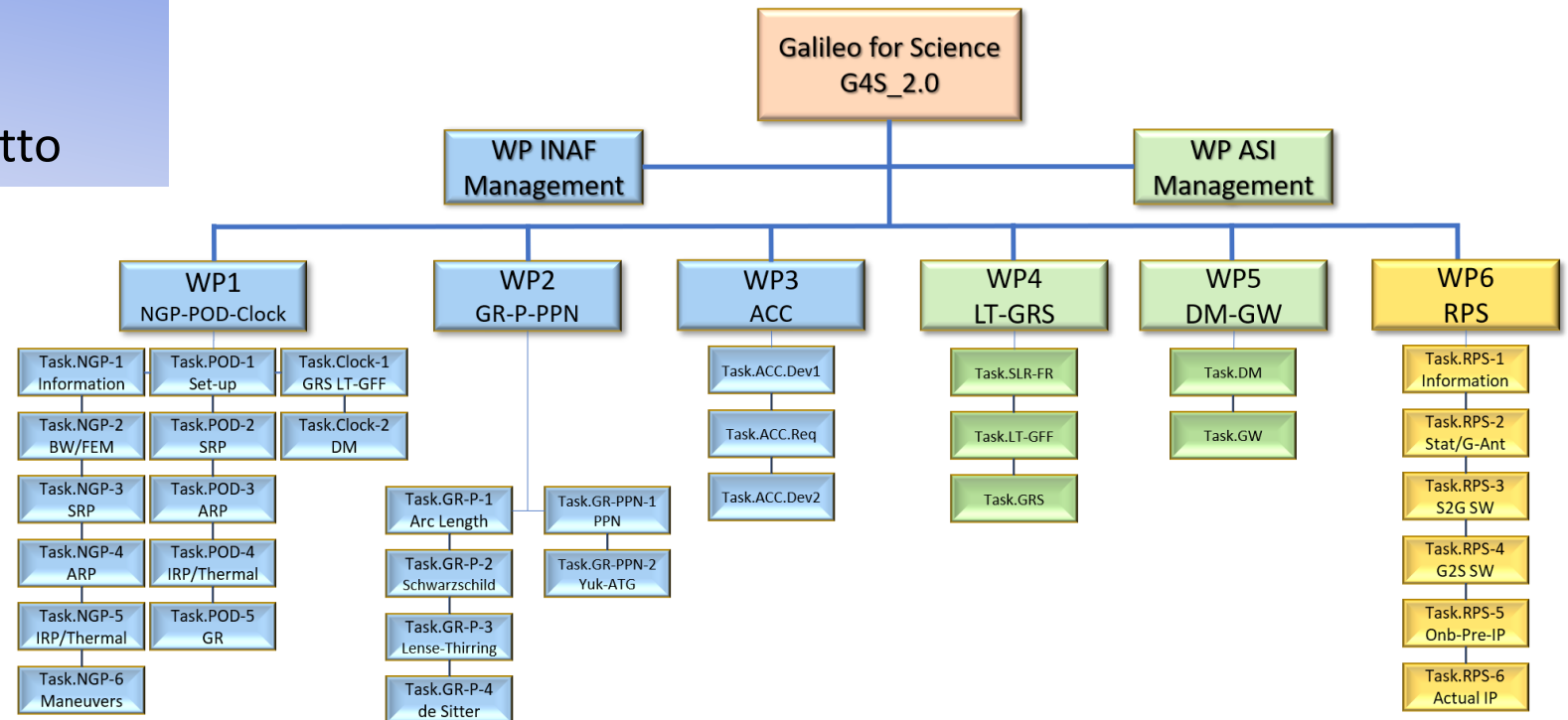**180 k€** (RA3)

80 k€ → **POLITO**

Fondi a sostegno

21. Totale fondi a disposizione (dato aggregato, k€)

Certi 2021	Certi 2022	Certi 2023	Presunti 21	Presunti 22	Presunti 23
0.0	0.0	0.0	180.0	180.0	180.0

Leadership

INAF ha la Leadership del progetto

- 79% del finanziamento del progetto
- 82% delle attività del progetto
- 60% del co-finanziamento del progetto

Criticità

Si evidenziano le seguenti principali criticità

1. Umane
   - Legate al personale impegnato su diversi fronti
   - Competenze da acquisire
     - POD in generale (i Galileo sono «nuovi» satelliti per noi)
     - POD con il Bernese (nuovo s/w): AdR-1 (non banale)
     - Orologi atomici: AdR-2 (meno problematico)

2. Tecniche (informazioni mancanti da ESA per i modelli da sviluppare e la POD)
   - Caratteristiche fisiche delle superfici dei satelliti e degli elementi che le compongono
   - Campagna dedicata di tracking laser (SLR)
   - Orologi e Stazioni

3. Difficoltà delle misure

4. Gruppi concorrenti in UE e non solo

5. Gruppo di ricerca piccolo (posizione a tempo indeterminato)

Conclusioni

Gli obiettivi principali del progetto **G4S_2.0** sono stati presentati, contestualizzando le misure dal punto di vista scientifico e delineando l'organizzazione programmatica delle diverse attività

Un aspetto importante da sottolineare ulteriormente riguarda una delle attività del progetto, la **determinazione orbitale di precisione** (**POD**) delle orbite dei satelliti

Quella della **POD** è una peculiarità, in ambito **INAF**, del solo **Gruppo Gravitazionale** dello **IAPS** e che non ha mai goduto di un finanziamento diretto da parte di **INAF**

Queste competenze, che risulteranno ulteriormente estese e rafforzate al termine del progetto, se strategicamente sostenute da **INAF** consentirebbero:

1. **POD** per missioni in orbita terrestre e interplanetaria per
    *   Misure di fisica della gravitazione (RG vs. altre teorie) in campo terrestre, lunare e nel sistema solare in generale
    *   Misure di gravimetria, stato rotazionale e struttura interna dei corpi del sistema solare in piena sinergia con l'attività di laboratorio del **Gruppo Gravitazionale** e con lo sviluppo di sensori dedicati: accelerometri, gradiometri, …
2. Ricadute scientifiche e tecnologiche significative
3. Maggiore e più ampia possibilità di collaborazione con altri Gruppi di ricerca in questo settore

Un piccolo (ma continuativo) finanziamento di **INAF** ci consentirebbe di poter affrontare sfide future, partecipando a nuovi progetti con conseguente crescita del **Gruppo Gravitazionale**

Grazie per l'attenzione

Back-up Slides

Misura Lense-Thirring

Results of the LARASE experiment

universe — MDPI

Article

A 1% Measurement of the Gravitomagnetic Field of the Earth with Laser-Tracked Satellites

David Lucchesi [1,2,3,*], Massimo Visco [1,3], Roberto Peron [1,3], Massimo Bassan [3,4], Giuseppe Pucacco [3,4], Carmen Pardini [2], Luciano Anselmo [2] and Carmelo Magnafico [1,3]

[1]   Istituto di Astrofisica e Planetologia Spaziali (IAPS)—Istituto Nazionale di Astrofisica (INAF), Via Fosso del Cavaliere 100, Tor Vergata, 00133 Roma, Italy; massimo.visco@inaf.it (M.V.); roberto.peron@inaf.it (R.P.); carmelo.magnafico@inaf.it (C.M.)

[2]   Istituto di Scienza e Tecnologia dell'Informazione (ISTI)—Consiglio Nazionale delle Ricerche, Via G. Moruzzi 1, 56124 Pisa, Italy; carmen.pardini@isti.cnr.it (C.P.); luciano.anselmo@isti.cnr.it (L.A.)

[3]   Istituto Nazionale di Fisica Nucleare, Sezione di Roma Tor Vergata, Via della Ricerca Scientifica 1, 00133 Roma, Italy; massimo.bassan@roma2.infn.it (M.B.); giuseppe.pucacco@roma2.infn.it (G.P.)

[4]   Dipartimento di Fisica, Università di Roma Tor Vergata, Via della Ricerca Scientifica 1, 00133 Roma, Italy

[*]   Correspondence: david.lucchesi@inaf.it
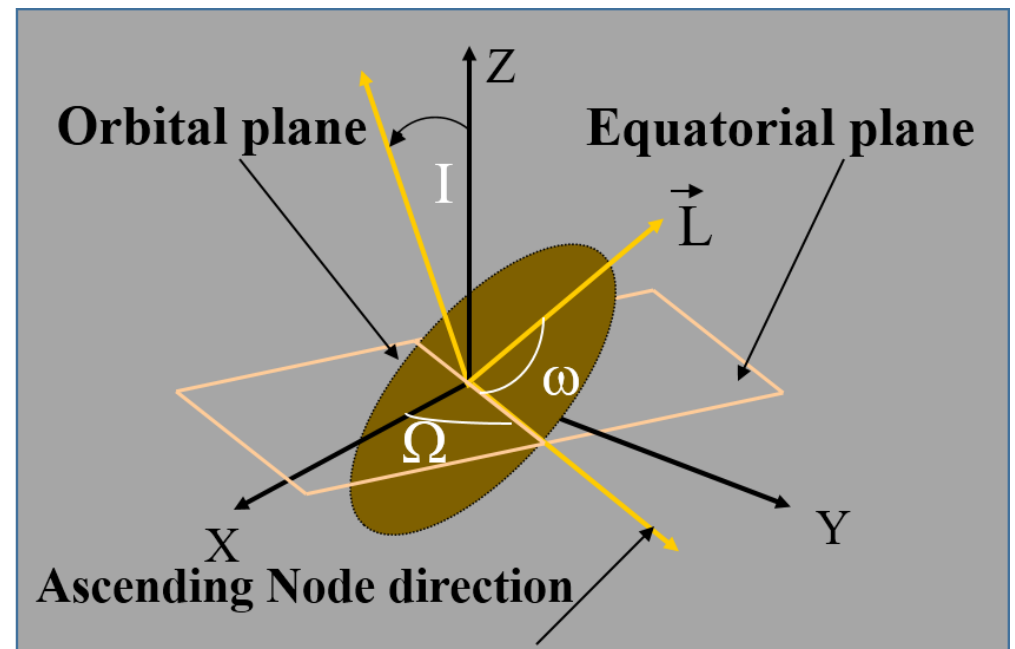
Results of the LARASE experiment

The **Lense-Thirring** effect consists of a precession of the orbit of a satellite around a primary produced by its rotation, i.e. by its angular momentum (mass-currents)

This precession produces a secular effect in two orbital elements:

- the right ascension of the ascending node
- the argument of pericenter

$$\left|\frac{d\Omega}{dt}\right|_{sec} = \frac{2G}{c^2 a^3} \frac{J_\oplus}{(1-e^2)^{3/2}}$$

$$\left|\frac{d\omega}{dt}\right|_{sec} = -\frac{6G}{c^2 a^3} \frac{J_\oplus}{(1-e^2)^{3/2}} \cos i$$

Results of the LARASE experiment

On the **Lense-Thirring** effect and the importance of an accurate measurement of the **Gravitomagnetic Field**

$$\vec{\dot{\Omega}}_{GM} = -\frac{1}{2c}\vec{B}_{GM} = \frac{G}{c^2 r^3}\left[3(\vec{S}\cdot\hat{r})\hat{r} - \vec{S}\right]$$

An accurate and reliable measurement of the gravitomagnetic field of the Earth is not only important *per se*, as a further and robust test of the **GR** predictions in the **WFSM** limit. There are at least three main issues that, for their importance, require a much more precise and accurate measurement of gravitomagnetism, even in weak-field conditions:

- Intrinsic gravitomagnetism

- Strong fields and compact objects

- Mach's Principle
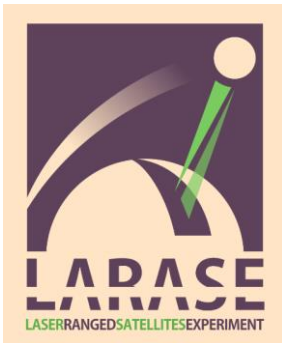
Results of the LARASE experiment

Gravity Probe B (GPB)

GPB, after 40 years of effort and $ 700 million satellite project, was launched on April 19, 2004 from Vandenberg Air Force Base (CA/USA) with a Delta II rocket
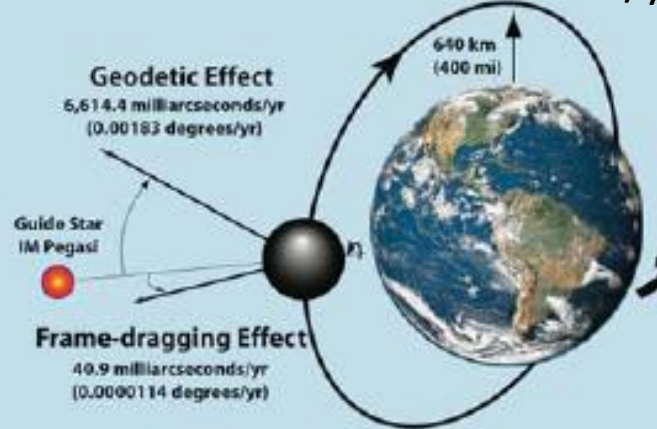

Photos: (Left) Russ Underwood, Lockheed Martin Corporation; (Right) Boeing Corporation

http://einstein.stanford.edu   PI Prof. Francis Everitt

The two primary goals of GPB were:

1. The measurement of the frame–dragging effect with an accuracy of about **0.3%**;

2. The measurement of the de Sitter effect with an accuracy of about **0.002%**;

For 18 months of nominal duration

The readout error was ≤ 0.016 mas/yr

Geodetic Effect
6,614.4 milliarcseconds/yr
(0.00183 degrees/yr)

Guide Star
IM Pegasi

640 km
(400 mi)

Frame-dragging Effect
40.9 milliarcseconds/yr
(0.0000114 degrees/yr)

$$\vec{\dot{\Omega}}_{rel.} = \frac{3}{2}\frac{M_\oplus}{r^2}(\hat{r} \times \vec{v}) + \frac{-\vec{J}_\oplus + 3\hat{r}(\vec{J}_\oplus \bullet \hat{r})}{r^3}$$

de Sitter	Lense–Thirring
6,614.4 mas/yr	40.9 mas/yr
$\approx 2 \cdot 10^{-5}$	$\approx 3 \cdot 10^{-3}$

Comparable with the CASSINI measurement (2002) of γ ($\delta\gamma \cong 2 \cdot 10^{-5}$, Bertotti et al. 2003, Letters to Nature).

Results of the LARASE experiment

Selected for a Viewpoint in *Physics*

PHYSICAL REVIEW LETTERS

week ending
3 JUNE 2011

Gravity Probe B: Final Results of a Space Experiment to Test General Relativity

C. W. F. Everitt,[1,*] D. B. DeBra,[1] B. W. Parkinson,[1] J. P. Turneaure,[1] J. W. Conklin,[1] M. I. Heifetz,[1] G. M. Keiser,[1] A. S. Silbergleit,[1] T. Holmes,[1] J. Kolodziejczak,[2] M. Al-Meshari,[3] J. C. Mester,[1] B. Muhlfelder,[1] V. G. Solomonik,[1] K. Stahl,[1] P. W. Worden, Jr.,[1] W. Bencze,[1] S. Buchman,[1] B. Clarke,[1] A. Al-Jadaan,[3] H. Al-Jibreen,[3] J. Li,[1] J. A. Lipa,[1] J. M. Lockhart,[1] B. Al-Suwaidan,[3] M. Taber,[1] and S. Wang[1]

[1]HEPL, Stanford University, Stanford, California 94305-4085, USA
[2]George C. Marshall Space Flight Center, Huntsville, Alabama 35808, USA
[3]King Abdulaziz City for Science and Technology, Riyadh, Saudi Arabia
(Received 1 April 2011; published 31 May 2011)

Gravity Probe B, launched 20 April 2004, is a space experiment testing two fundamental predictions of Einstein's theory of general relativity (GR), the geodetic and frame-dragging effects, by means of cryogenic gyroscopes in Earth orbit. Data collection started 28 August 2004 and ended 14 August 2005. Analysis of the data from all four gyroscopes results in a geodetic drift rate of -6601.8 ± 18.3 mas/yr and a frame-dragging drift rate of -37.2 ± 7.2 mas/yr, to be compared with the GR predictions of -6606.1 mas/yr and -39.2 mas/yr, respectively ("mas" is milliarcsecond; 1 mas = 4.848×10^{-9} rad).

Measurement of de Sitter precession 0.3%

Measurement of Gravitomagnetism 19%

... both measures are far from the initial objectives ...

Results of the LARASE experiment

$$\left|\frac{d\Omega}{dt}\right|_{sec} = \frac{2G}{c^2 a^3}\frac{J_\oplus}{(1-e^2)^{3/2}}$$

$$\left|\frac{d\omega}{dt}\right|_{sec} = -\frac{6G}{c^2 a^3}\frac{J_\oplus}{(1-e^2)^{3/2}}\cos i$$

The **Lense-Thirring** precession is very small compared to classical orbit precessions due to deviations from the spherical symmetry for the Earth's mass distribution, or with the same relativistic **Schwarzschild** precession produced by the mass of the primary (≈ 3350 mas/yr for **LAGEOS**)

TABLE I. Mean orbital elements of LAGEOS, LAGEOS II and LARES.

Element	Unit	Simbol	LAGEOS	LAGEOS II	LARES
semi-major axis	[km]	a	12 270.00	12 162.07	7 820.31
eccentricity		e	0.004433	0.013798	0.001196
inclination	[deg]	i	109.84	52.66	69.49

$$V(r,\varphi,\lambda) = -\frac{GM_\oplus}{r}\left[1 + \sum_{\ell=2}^{\infty}\sum_{m=0}^{\ell}\left(\frac{R_\oplus}{r}\right)^\ell P_{\ell m}(\sin\varphi)(C_{\ell m}\cos m\lambda + S_{\ell m}\sin m\lambda)\right]$$

$$\langle\dot{\Omega}_{class}\rangle_{sec} = -\frac{3}{2}n\left(\frac{R_\oplus}{a}\right)^2\frac{\cos i}{(1-e^2)^2}\{-\sqrt{5}\bar{C}_{2,0}\} + \cdots$$

TABLE II. Rate in milli-arc-sec per year (mas/yr) for the secular Lense-Thirring precession on the right ascension of the ascending node and on the argument of pericenter of LAGEOS, LAGEOS II and LARES satellites.

Rate in the element	LAGEOS	LAGEOS II	LARES
$\dot{\Omega}_{L\text{-}T}$	30.67	31.50	118.48
$\dot{\omega}_{L\text{-}T}$	31.23	−57.31	−334.68

$$\begin{cases} G & \cong 6.670 \cdot 10^{-8} cm^3 s^{-2} g^{-1} \\ J_\oplus & \cong 5.861 \cdot 10^{40} cm^2 g s^{-1} \\ c & \cong 2.99792458 \cdot 10^{10}\ cm/s \end{cases}$$

$$\dot{\Omega}^{Obser}_{Lageos} \approx +126\ deg/yr \qquad \dot{\Omega}^{Obser}_{LageosII} \approx -231\ deg/yr$$

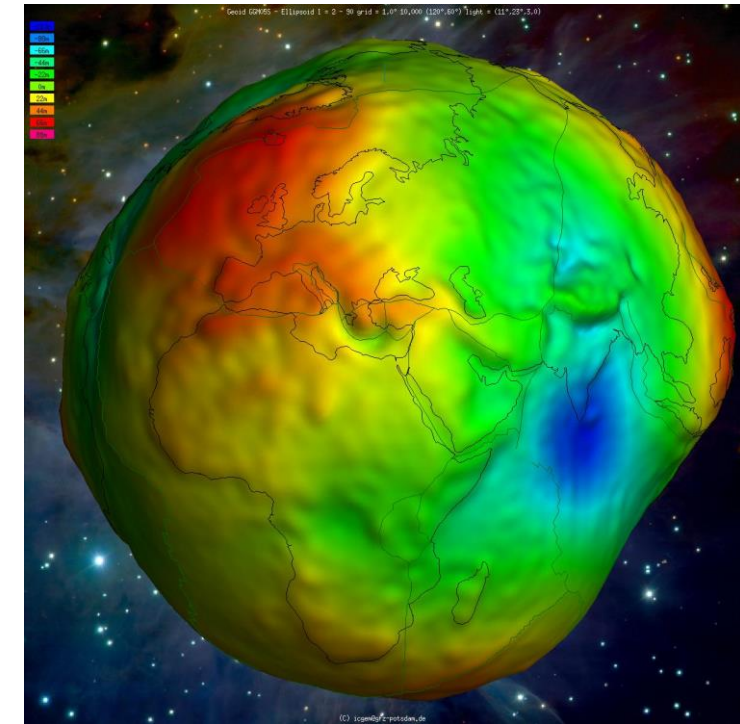$$\dot{\Omega}^{Obser}_{Lares} \approx -624\ deg/yr$$

30 mas ≅ 1.8 m in 1-year

Results of the LARASE experiment

Therefore, the correct modelling of the even zonal harmonics ($\ell = \text{even}$, $m = 0$) represents the main challenge in this kind of measurements, since they have the same signature of the relativistic effect but much larger amplitudes

2,0   4,0   6,0

$$\langle \dot{\Omega}_{class} \rangle_{sec} = -\frac{3}{2} n \left(\frac{R_{\oplus}}{a} \right)^2 \frac{\cos i}{(1-e^2)^2} \{-\sqrt{5}\,\bar{C}_{2,0}\} + \cdots$$

Results of the LARASE experiment

By solving a linear system of three equations in three unknowns, we can solve for the relativistic precession while reducing the impact in the measurement of the non perfect knowledge of the Earth's gravitational field:

$$\begin{cases} \dot{\Omega}_2^{L1}\delta\bar{C}_{2,0} + \dot{\Omega}_4^{L1}\delta\bar{C}_{4,0} + \dot{\Omega}_{LT}^{L1}\mu + \cdots = \delta\dot{\Omega}_{res}^{L1} \\ \dot{\Omega}_2^{L2}\delta\bar{C}_{2,0} + \dot{\Omega}_4^{L2}\delta\bar{C}_{4,0} + \dot{\Omega}_{LT}^{L2}\mu + \cdots = \delta\dot{\Omega}_{res}^{L2} \\ \dot{\Omega}_2^{LR}\delta\bar{C}_{2,0} + \dot{\Omega}_4^{LR}\delta\bar{C}_{4,0} + \dot{\Omega}_{LT}^{LR}\mu + \cdots = \delta\dot{\Omega}_{res}^{LR} \end{cases}$$

$$\dot{\Omega}_{GR}^{comb} = 50.17 \ mas/yr$$

$$\mu = \frac{\dot{\Omega}^{comb}}{\dot{\Omega}_{GR}^{comb}} = \begin{cases} 1 & \quad \bullet \quad \text{In General Relativity} \\ 0 & \quad \bullet \quad \text{In Newtonian physics} \end{cases}$$

$$k_1 \cong 0.345$$
$$k_2 \cong 0.073$$

$$\dot{\Omega}^{comb} = \delta\dot{\Omega}_{res}^{L1} + k_1\delta\dot{\Omega}_{res}^{L2} + k_2\delta\dot{\Omega}_{res}^{LR}$$

- LT effect observable

- k_1 and k_2 are such that to cancel the unmodelled effects/errors of two even zonal harmonics (order $m=0$) of the Earth's gravitational field: quadrupole and octupole coefficients

$$\langle\delta\dot{\Omega}_{class}\rangle_{sec} = -\frac{3}{2}n\left(\frac{R_\oplus}{a}\right)^2\frac{\cos i}{(1-e^2)^2}\{-\sqrt{5}\delta\bar{C}_{2,0}\} + \cdots$$

Results of the LARASE experiment

By solving a linear system of three equations in three unknowns, we can solve for the relativistic precession while reducing the impact in the measurement of the non perfect knowledge of the Earth's gravitational field:

$$\begin{cases} \dot{\Omega}_2^{L1}\delta\bar{C}_{2,0} + \dot{\Omega}_4^{L1}\delta\bar{C}_{4,0} + \boxed{\dot{\Omega}_{LT}^{L1}\mu} + \cdots = \boxed{\delta\dot{\Omega}_{res}^{L1}} \\ \dot{\Omega}_2^{L2}\delta\bar{C}_{2,0} + \dot{\Omega}_4^{L2}\delta\bar{C}_{4,0} + \boxed{\dot{\Omega}_{LT}^{L2}\mu} + \cdots = \boxed{\delta\dot{\Omega}_{res}^{L2}} \\ \dot{\Omega}_2^{LR}\delta\bar{C}_{2,0} + \dot{\Omega}_4^{LR}\delta\bar{C}_{4,0} + \boxed{\dot{\Omega}_{LT}^{LR}\mu} + \cdots = \boxed{\delta\dot{\Omega}_{res}^{LR}} \end{cases}$$

$$\dot{\Omega}_{GR}^{comb} = 50.17\ mas/yr$$

$$\mu = \frac{\dot{\Omega}^{comb}}{\dot{\Omega}_{GR}^{comb}} = \begin{cases} 1 & \text{In General Relativity} \\ 0 & \text{In Newtonian physics} \end{cases}$$

$$k_1 \cong 0.345$$
$$k_2 \cong 0.073$$

1. Ciufolini, I.; Lucchesi, D.; Vespe, F.; Mandiello, A. Measurement of dragging of inertial frames and gravitomagnetic field using laser-ranged satellites. *Nuovo Cim*. A, 109, 575–590, 1996
2. Ciufolini, I. On a new method to measure the gravitomagnetic field using two orbiting satellites. *Nuovo Cim*. A, 109, 1709–1720, 1996
3. Lucchesi, D.M.; Balmino, G. The LAGEOS satellites orbital residuals determination and the Lense Thirring effect measurement. *Plan. Space Sci.*, 54, 581–593, 2006

Results of the LARASE experiment

Results for µ from the linear system
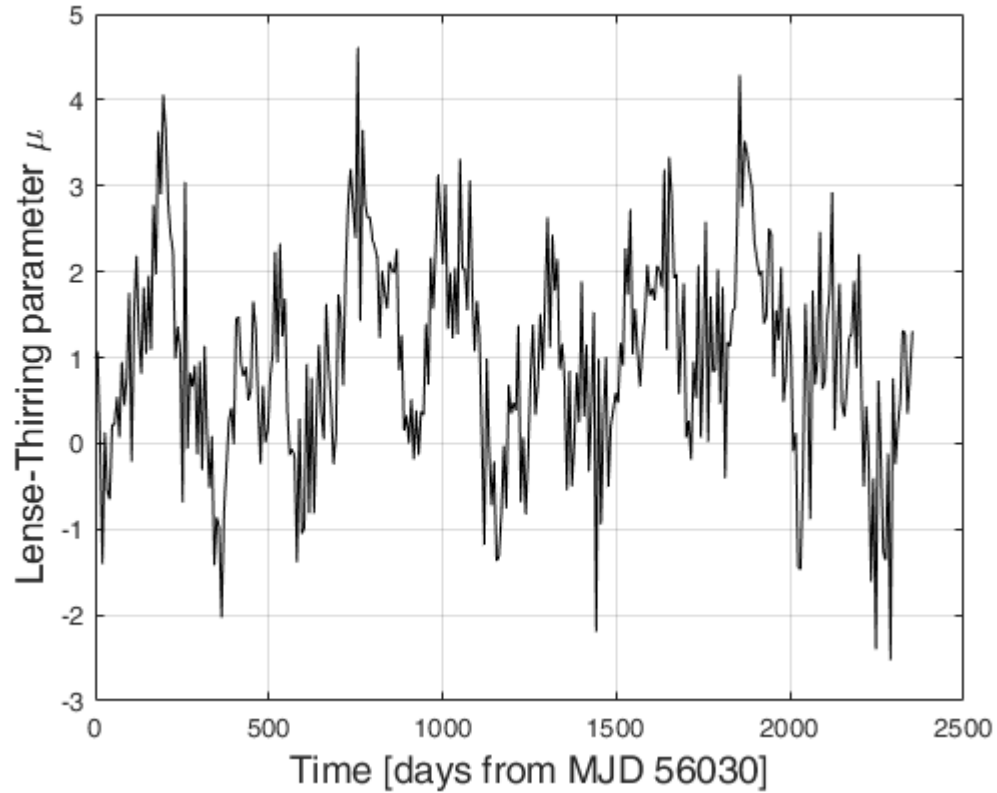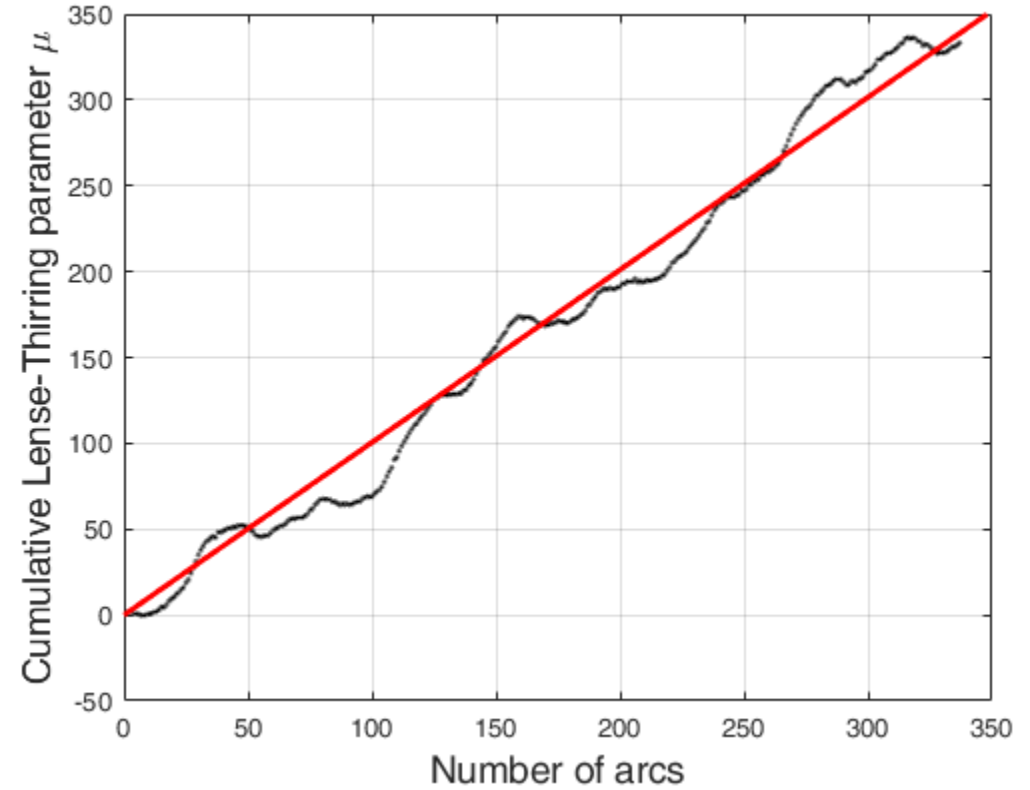
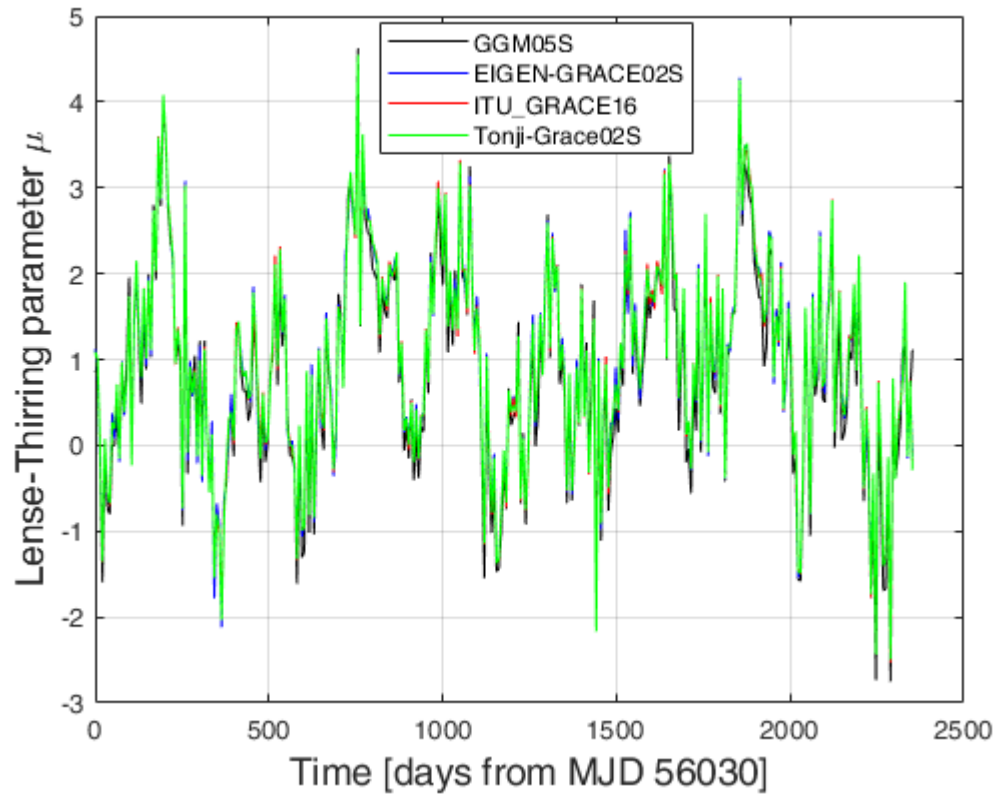Cumulative sum for µ

Gussian-like distribution

$K \cong +3.097 \quad S \cong -8.4 \times 10^{-3}$
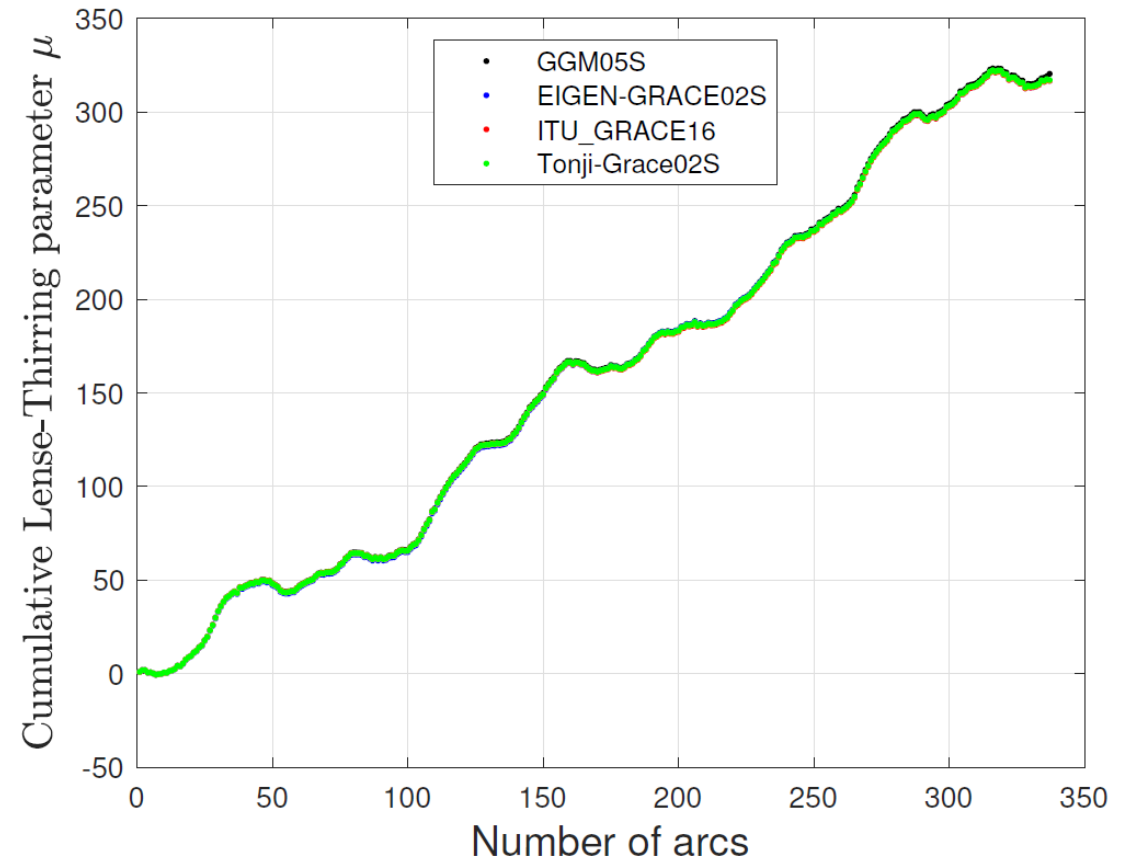
GGM05S model

Results of the LARASE experiment
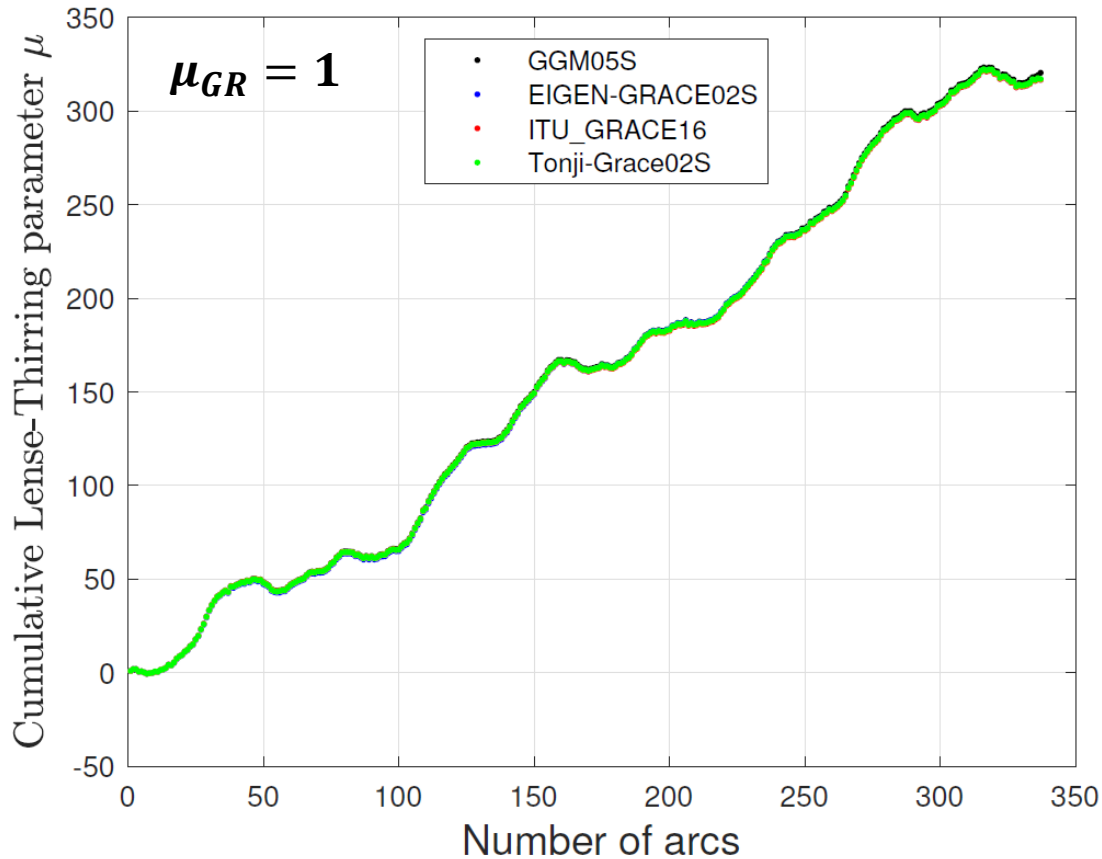
Results for μ from the linear system

Cumulative sum for μ

Results of the LARASE experiment

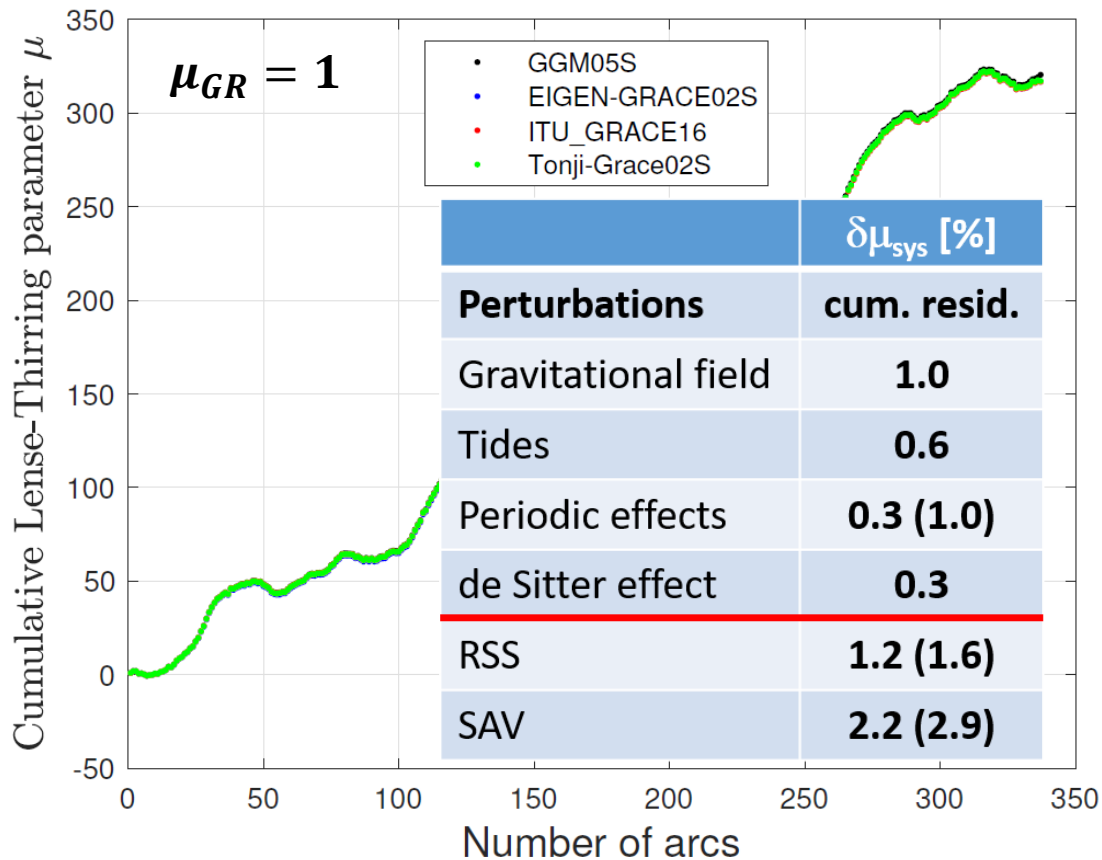Lense-Thirring effect measurement: frame dragging

Errors @ 95% CL

Model	$\mu \pm \delta\mu$	$\mu - 1$
GGM05S	1.0053 ± 0.0074	$+0.0053$
EIGEN-GRACE02S	1.0002 ± 0.0074	$+0.0002$
ITU_GRACE16	0.9996 ± 0.0074	-0.0004
Tonji-Grace02s	1.0008 ± 0.0074	$+0.0008$

$$\boxed{\mu_{meas} - 1 = 1.5 \times 10^{-3} \pm 7.4 \times 10^{-3}}$$

Results of the LARASE experiment

Lense-Thirring effect measurement: frame dragging

$\mu_{GR} = 1$

Legend:
- GGM05S
- EIGEN-GRACE02S
- ITU_GRACE16
- Tonji-Grace02S

	$\delta\mu_{sys}$ [%]
Perturbations	cum. resid.
Gravitational field	1.0
Tides	0.6
Periodic effects	0.3 (1.0)
de Sitter effect	0.3
RSS	1.2 (1.6)
SAV	2.2 (2.9)

Errors @ 95% CL

Model	$\mu \pm \delta\mu$	$\mu - 1$
GGM05S	1.0053 ± 0.0074	$+0.0053$
EIGEN-GRACE02S	1.0002 ± 0.0074	$+0.0002$
ITU_GRACE16	0.9996 ± 0.0074	-0.0004
Tonji-Grace02s	1.0008 ± 0.0074	$+0.0008$

$$\mu_{meas} - 1 = 1.5 \times 10^{-3} \pm 7.4 \times 10^{-3} \pm 16 \times 10^{-3}$$

Estimation of the systematic errors

Results of the LARASE experiment

Measurement of LAGEOS II argument of pericenter GR precession

Results of the LARASE experiment

LAGEOS II pericenter general relativistic precession (1993–2005): Error budget and constraints in gravitational physics

David M. Lucchesi[*]

*Istituto di Astrofisica e Planetologia Spaziali, Istituto Nazionale di Astrofisica, (IAPS/INAF),
Via del Fosso del Cavaliere 100, 00133 Roma, Italy,
Istituto di Scienza e Tecnologia dell'Informazione, Consiglio Nazionale delle Ricerche, (ISTI/CNR),
Via G. Moruzzi 1, 56124 Pisa, Italy, and
Istituto Nazionale di Fisica Nucleare (INFN), Sezione di Pisa, Largo B. Pontecorvo 3, 56127 Pisa, Italy*

Roberto Peron

*Istituto di Astrofisica e Planetologia Spaziali, Istituto Nazionale di Astrofisica, (IAPS/INAF), Via del Fosso
del Cavaliere 100, 00133 Roma, Italy and
Istituto Nazionale di Fisica Nucleare (INFN), Sezione di Roma Tor Vergata,
Via della Ricerca Scientifica 1, 00133 Roma, Italy*
(Received 16 April 2013; published 7 April 2014)

The aim of this paper is to extend, clarify, and deepen the results of our previous work [D. M. Lucchesi and R. Peron, Phys. Rev. Lett. **105**, 231103 (2010)], related to the precise measurement of LAGEOS (LAser GEOdynamics Satellite) II pericenter shift. A 13-year time span of LAGEOS satellites' laser tracking data has been considered, obtaining a very precise orbit and correspondingly residuals time series from which to extract the relevant signals. A thorough description is provided of the data analysis strategy and the dynamical models employed, along with a detailed discussion of the known sources of error in the experiment, both statistical and systematic. From this analysis, a confirmation of the predictions of Einstein's general relativity, as well as strong bounds on alternative theories of gravitation, clearly emerge. In particular, taking conservatively into account the stricter error bound due to systematic effects, general relativity has been confirmed in the Earth's field at the 98% level (meaning the measurement of a suitable combination of β and γ PPN parameters in weak-field conditions). This bound has been used to constrain possible deviations from the inverse-square law parameterized by a Yukawa-like new long range interaction with strength $|\alpha| \lesssim 1 \times 10^{-10}$ at a characteristic range $\lambda \simeq 1$ Earth radius, a possible nonsymmetric gravitation theory with the interaction parameter $\mathcal{C}_{\oplus \text{LAGEOS II}} \lesssim (9 \times 10^{-2} \text{ km})^4$, and a possible spacetime torsion with a characteristic parameter combination $|2t_2 + t_3| \lesssim 7 \times 10^{-2}$. Conversely, if we consider the results obtained from our best fit of the LAGEOS II orbit, the constraints in fundamental physics improve by at least 2 orders of magnitude.

1. Measurement of **LAGEOS II** argument of pericenter **GR** precession

This represents the extension and completion of a previous work published on *Phys. Rev. Lett.* in 2010

Results of the LARASE experiment

Accurate Measurement in the Field of the Earth of the General-Relativistic Precession of the LAGEOS II Pericenter and New Constraints on Non-Newtonian Gravity

David M. Lucchesi[1,2] and Roberto Peron[1]

[1]*Istituto di Fisica dello Spazio Interplanetario, Istituto Nazionale di Astrofisica, IFSI/INAF,
Via del Fosso del Cavaliere 100, 00133 Roma, Italy*
[2]*Istituto di Scienza e Tecnologie dell'Informazione, Consiglio Nazionale delle Ricerche, ISTI/CNR,
Via G. Moruzzi 1, 56124 Pisa, Italy*
(Received 18 July 2010; published 29 November 2010)

The pericenter shift of a binary system represents a suitable observable to test for possible deviations from the Newtonian inverse-square law in favor of new weak interactions between macroscopic objects. We analyzed 13 years of tracking data of the LAGEOS satellites with GEODYN II software but with no models for general relativity. From the fit of LAGEOS II pericenter residuals we have been able to obtain a 99.8% agreement with the predictions of Einstein's theory. This result may be considered as a 99.8% measurement in the field of the Earth of the combination of the γ and β parameters of general relativity, and it may be used to constrain possible deviations from the inverse-square law in favor of new weak interactions parametrized by a Yukawa-like potential with strength α and range λ. We obtained $|\alpha| \lesssim 1 \times 10^{-11}$, a huge improvement at a range of about 1 Earth radius.

Viewpoint

Via satellite

David Rubincam
Planetary Geodynamics Laboratory NASA Goddard Space Flight Center, Greenbelt, MD 20771, USA
Published November 29, 2010

More than a decade's worth of data collected from the LAGEOS II satellite is offering a new way to test general relativity.

Subject Areas: **Gravitation**

Results of the LARASE experiment

The expected GR precession vs. classical precession:

$$\langle\dot{\omega}_{Schw}\rangle_{sec} = \frac{3}{c^2 a^{5/2}} \frac{GM_\oplus^{3/2}}{(1-e^2)}$$

$$\langle\dot{\omega}_{LT}\rangle_{sec} = -\frac{6G}{c^2 a^3} \frac{J_\oplus}{(1-e^2)^{3/2}} \cos i$$

$$U = -\frac{GM_\oplus}{r} \sum_{\ell=0}^{\infty} \sum_{m=0}^{\ell} \left(\frac{R_\oplus}{r}\right)^\ell P_{\ell m}(\sin\varphi)\left(C_{\ell m}\cos m\lambda + S_{\ell m}\sin m\lambda\right),$$

$$\langle\dot{\omega}_{class}\rangle_{sec} = \frac{3}{2}n\left(\frac{R_\oplus}{a}\right)^2 \frac{1}{(1-e^2)^2}\left\{\cos i + \left(1 - \frac{3}{2}\sin^2 i\right)\right\}\left[-\sqrt{5}\bar{C}_{20}\right] + \cdots$$

PHYSICAL REVIEW D **89**, 082002 (2014)

TABLE I. Rate (mas/yr) and orbital shift (over 14 days) of the different types of secular relativistic precession on the arguments of pericenter of LAGEOS II and LAGEOS, and their sum (1 mas/yr = 1 milli-arc second per year).

	Precession	Rate (mas/yr)	Shift (m)
LAGEOS II	$\Delta\dot{\omega}^{Schw}$	3351.95	7.61
	$\Delta\dot{\omega}^{LT}$	−57.00	-1.29×10^{-1}
	Total	3294.95	7.48
LAGEOS	$\Delta\dot{\omega}^{Schw}$	3278.77	7.44
	$\Delta\dot{\omega}^{LT}$	32.00	0.72×10^{-1}
	Total	3310.77	7.51

$$\langle\dot{\omega}_{class}\rangle_{sec} = \begin{cases} -2.8 \times 10^8 \; mas/yr & LAGEOS \\ 5.7 \times 10^8 \; mas/yr & LAGEOS\ II \end{cases}$$

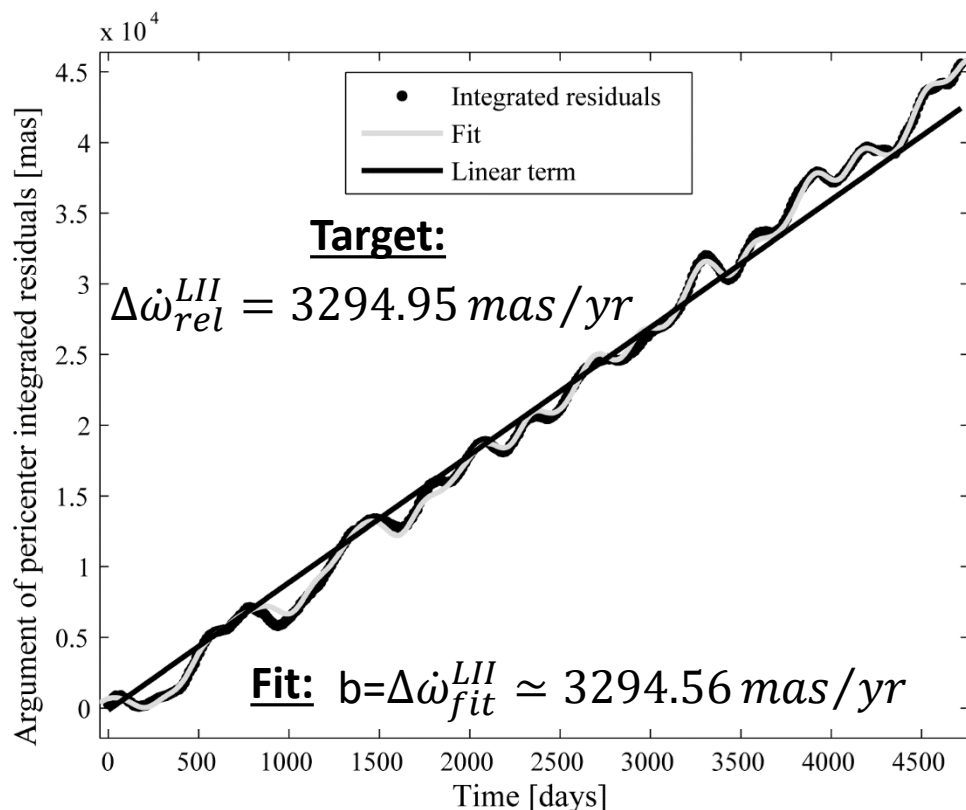$$\dot{\omega}_{GR} \cong 3300 \; mas/yr$$ **The GR precession is about 5 orders of magnitude smaller!**
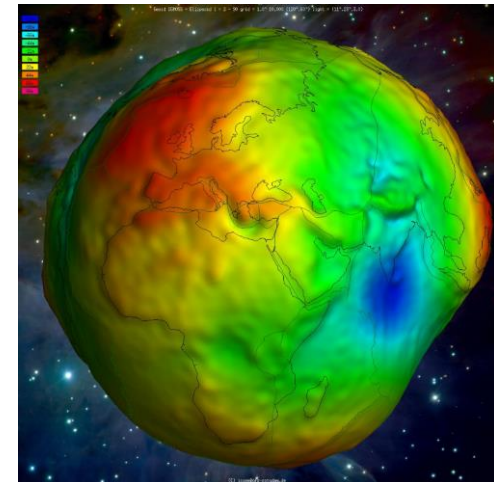
Results of the LARASE experiment

Fit to the pericenter residuals:

$$\Delta\omega^{FIT} = a + b \cdot t + c\left(t - t_0\right)^2 + \sum_{i=1}^{n} D_i \sin\left(\frac{2 \cdot \pi}{P_i} \cdot t + \Phi_i\right)$$

We obtained b $\cong$ 3294.6 mas/yr, very close to the prediction of **GR**

The discrepancy is just **0.01%**

From a sensitivity analysis, with constraints on some of the parameters that enter into the least squares fit, we obtained an upper bound of **0.2%**

$$\Delta\dot{\omega} = \Delta\dot{\omega}_{GP} + \Delta\dot{\omega}_{NGP} + \varepsilon \cdot \Delta\dot{\omega}_{GR}$$

$$\varepsilon = 1 - (0.12 \pm 2.10) \cdot 10^{-3} \pm 2.5 \cdot 10^{-2}$$

Results of the LARASE experiment

The overall error budget

TABLE XVII. Error budget of the LAGEOS II pericenter general relativity shift. Top: summary of the errors from the data reduction and the *a posteriori* best fit (see Sections VI and VII). Middle: summary of the systematic errors from the gravitational perturbations (see Section VIII). Bottom: summary of the systematic errors from the nongravitational perturbations (see Section IX).

Statistical errors		
Residuals	Mean	Standard deviation
Range	9.67 cm	3.88 cm
Pericenter	4.57 mas	1.87 mas
Adjusted $\mathcal{R}_a^2$	0.998	
Reduced χ_ν^2 test	0.14	

$$\epsilon_\omega^{\mathrm{sta}} - 1 = (-0.12 \pm 2.10) \times 10^{-3}$$

Systematic errors: gravitational perturbations		
Error source	Error value (% $\Delta\dot{\omega}_{\mathrm{II}}^{\mathrm{rel}}$)	Total not correlated (% $\Delta\dot{\omega}_{\mathrm{II}}^{\mathrm{rel}}$)
Even zonal harmonics	2.45	
Odd zonal harmonics	4.10×10^{-2}	
Tides (solid + ocean)	2.48×10^{-2}	2.46
Secular trends ($\ell = $ even)	3.30×10^{-2}	
Seasonal-like effects	0.24	

Systematic errors: nongravitational perturbations		
Error source	Error value (% $\Delta\dot{\omega}_{\mathrm{II}}^{\mathrm{rel}}$)	Total not correlated (% $\Delta\dot{\omega}_{\mathrm{II}}^{\mathrm{rel}}$)
Direct solar radiation	0.50	
Earth's albedo	0.39	
Thermal thrusts	0.09	0.64
Drag (neutral + charged)	negligible	
Total not correlated		2.54

$$\epsilon_\omega^{\mathrm{sys}} - 1 = \pm 2.54 \times 10^{-2}$$

Results of the LARASE experiment

The overall error budget

TABLE XVII.   Error budget of the LAGEOS II pericenter general relativity shift. Top: summary of the errors from the data reduction and the *a posteriori* best fit (see Sections VI and VII). Middle: summary of the systematic errors from the gravitational perturbations (see Section VIII). Bottom: summary of the systematic errors from the nongravitational perturbations (see Section IX).

Statistical errors		
Residuals	Mean	Standard deviation
Range	9.67 cm	3.88 cm
Pericenter	4.57 mas	1.87 mas
Adjusted $\mathcal{R}_a^2$	0.998	
Reduced χ_ν^2 test	0.14	
	$\epsilon_\omega^{\text{sta}} - 1 = (-0.12 \pm 2.10) \times 10^{-3}$	

Systematic errors: gravitational perturbations		
Error source	Error value (% $\Delta\dot\omega_{\text{II}}^{\text{rel}}$)	Total not correlated (% $\Delta\dot\omega_{\text{II}}^{\text{rel}}$)
Even zonal harmonics	2.45	
Odd zonal harmonics	4.10×10^{-2}	
Tides (solid + ocean)	2.48×10^{-2}	2.46
Secular trends ($\ell = $ even)	3.30×10^{-2}	
Seasonal-like effects	0.24	

Systematic errors: nongravitational perturbations		
Error source	Error value (% $\Delta\dot\omega_{\text{II}}^{\text{rel}}$)	Total not correlated (% $\Delta\dot\omega_{\text{II}}^{\text{rel}}$)
Direct solar radiation	0.50	
Earth's albedo	0.39	
Thermal thrusts	0.09	0.64
Drag (neutral + charged)	negligible	
Total not correlated		2.54
	$\epsilon_\omega^{\text{sys}} - 1 = \pm 2.54 \times 10^{-2}$	

Results of the LARASE experiment

Summary of the constraints obtained

TABLE XVIII. Summary of the results obtained in the present work; together with the measurement error budget, the constraints on fundamental physics are listed and compared with the literature.

Parameter	Values and uncertainties (this study)	Uncertainties (literature)	Remarks
$\epsilon_\omega - 1$	$-1.2 \times 10^{-4} \pm 2.10 \times 10^{-3} \pm 2.54 \times 10^{-2}$	$\cdots$	Error budget of the perigee precession measurement in the field of the Earth
$\frac{\|2+2\gamma-\beta\|}{3} - 1$	$-1.2 \times 10^{-4} \pm 2.10 \times 10^{-3} \pm 2.54 \times 10^{-2}$	$\pm(1.0 \times 10^{-3}) \pm (2 \times 10^{-2})^{\mathrm{a}}$	Constraint on the combination of PPN parameters
$\|\alpha\|$	$\lesssim \|0.5 \pm 8.0 \pm 101\| \times 10^{-12}$	$\pm 1 \times 10^{-8 \mathrm{b}}$	Constraint on a possible (Yukawa-like) NLRI
$\mathcal{C}_{\oplus \mathrm{LAGEOSII}}$	$\leq (0.003\,\mathrm{km})^4 \pm (0.036\,\mathrm{km})^4 \pm (0.092\,\mathrm{km})^4$	$\pm(0.16\,\mathrm{km})^{4\mathrm{c}}; \pm(0.087\,\mathrm{km})^{4\mathrm{d}}$	Constraint on a possible NSGT
$\|2t_2 + t_3\|$	$\lesssim 3.5 \times 10^{-4} \pm 6.2 \times 10^{-3} \pm 7.49 \times 10^{-2}$	$3 \times 10^{-3 \mathrm{e}}$	Constraint on torsion

[a]From the preliminary estimate of the systematic errors of [166] for the perihelion precession of Mercury.
[b]From [167] with Lunar-LAGEOS GM measurements.
[c]From [5] and based on a partial estimate for the systematic errors.
[d]From [7] and based on the analysis of the systematic errors only.
[e]From [168] with no estimate for the systematic errors.

Results of the LARASE experiment

Summary of the constraints obtained

TABLE XVIII. Summary of the results obtained in the present work; together with the measurement error budget, the constraints on fundamental physics are listed and compared with the literature.

Parameter	Values and uncertainties (this study)	Uncertainties (literature)	Remarks
$\epsilon_\omega - 1$	$-1.2 \times 10^{-4} \pm 2.10 \times 10^{-3} \pm 2.54 \times 10^{-2}$	$\cdots$	Error budget of the perigee precession measurement in the field of the Earth
$\frac{|2+2\gamma-\beta|}{3} - 1$	$-1.2 \times 10^{-4} \pm 2.10 \times 10^{-3} \pm 2.54 \times 10^{-2}$	$\pm(1.0 \times 10^{-3}) \pm (2 \times 10^{-2})^a$	Constraint on the combination of PPN parameters
$|\alpha|$	$\lesssim |0.5 \pm 8.0 \pm 101| \times 10^{-12}$	$\pm 1 \times 10^{-8b}$	Constraint on a possible (Yukawa-like) NLRI
$C_{\oplus LAGEOSII}$	$\leq (0.003 \text{ km})^4 \pm (0.036 \text{ km})^4 \pm (0.092 \text{ km})^4$	$\pm(0.16 \text{ km})^{4c}; \pm(0.087 \text{ km})^{4d}$	Constraint on a possible NSGT
$|2t_2 + t_3|$	$\lesssim 3.5 \times 10^{-4} \pm 6.2 \times 10^{-3} \pm 7.49 \times 10^{-2}$	3×10^{-3e}	Constraint on torsion

[a] From the preliminary estimate of the systematic errors of [166] for the perihelion precession of Mercury.
[b] From [167] with Lunar-LAGEOS GM measurements.
[c] From [5] and based on a partial estimate for the systematic errors.
[d] From [7] and based on the analysis of the systematic errors only.
[e] From [168] with no estimate for the systematic errors.

[166] I.I. Shapiro, in General Relativity and Gravitation, 1989, edited by N. Ashby, D. F. Bartlett, and W. Wyss (Cambridge University Press, Cambridge, 1990), p. 313.

Combination of PPN Parameters

$$\langle \dot{\omega}_{Schw} \rangle_{sec} = \left(\frac{2 + 2\gamma - \beta}{3} \right) \frac{3}{c^2 a^{5/2}} \frac{GM_\oplus^{3/2}}{(1 - e^2)}$$

$$\frac{|2 + 2\gamma - \beta|}{3} - 1 = -1.2 \cdot 10^{-4} \pm 2.10 \cdot 10^{-3} \pm 2.5 \cdot 10^{-2}$$

This result can be compared with the measurement by Shapiro and collaborators of Mercury's perihelion advance, determined by the radar ranging technique based on the measurement of the echo delay between the Earth and Mercury in the period between 1966 and 1990

Results of the LARASE experiment

Summary of the constraints obtained

TABLE XVIII. Summary of the results obtained in the present work; together with the measurement error budget, the constraints on fundamental physics are listed and compared with the literature.

Parameter	Values and uncertainties (this study)	Uncertainties (literature)	Remarks
$\epsilon_\omega - 1$	$-1.2 \times 10^{-4} \pm 2.10 \times 10^{-3} \pm 2.54 \times 10^{-2}$	...	Error budget of the perigee precession measurement in the field of the Earth
$\frac{\|2+2\gamma-\beta\|}{3} - 1$	$-1.2 \times 10^{-4} \pm 2.10 \times 10^{-3} \pm 2.54 \times 10^{-2}$	$\pm(1.0 \times 10^{-3}) \pm (2 \times 10^{-2})^a$	Constraint on the combination of PPN parameters
$\|\alpha\|$	$\lesssim \|0.5 \pm 8.0 \pm 101\| \times 10^{-12}$	$\pm 1 \times 10^{-8b}$	Constraint on a possible (Yukawa-like) NLRI
$C_{\oplus LAGEOSII}$	$\leq (0.003 \text{ km})^4 \pm (0.036 \text{ km})^4 \pm (0.092 \text{ km})^4$	$\pm (0.16 \text{ km})^{4c}; \pm(0.087 \text{ km})^{4d}$	Constraint on a possible NSGT
$\|2t_2 + t_3\|$	$\lesssim 3.5 \times 10^{-4} \pm 6.2 \times 10^{-3} \pm 7.49 \times 10^{-2}$	3×10^{-3e}	Constraint on torsion

[a]From the preliminary estimate of the systematic errors of [166] for the perihelion precession of Mercury.
[b]From [167] with Lunar-LAGEOS GM measurements.
[c]From [5] and based on a partial estimate for the systematic errors.
[d]From [7] and based on the analysis of the systematic errors only.
[e]From [168] with no estimate for the systematic errors.

Violation of $1/r^2$ law: Yukawa-like potential

- Fujii; Fischbach; Damour

$$V(r) = -G_\infty \frac{M_1 M_2}{r}\left(1 + \alpha e^{-r/\lambda}\right)$$

$$\vec{F}(r) = -\vec{\nabla}V(r) = -G_\infty \left[1 + \alpha\left(1 + \frac{r}{\lambda}\right)e^{-r/\lambda}\right]\frac{M_1 M_2}{r^2}\hat{r}$$

$$\alpha = \frac{1}{G_\infty}\left(\frac{K_1}{M_1} \cdot \frac{K_2}{M_2}\right) \qquad \lambda = \frac{h}{\mu c}$$

As we have described, this type of parameterization, at the lowest interaction order and in the non-relativistic limit, is compatible with many metric theories of gravitation and with modern theories of physics regardless of the additional fields they consider: Scalar, Tensor and Vector fields

Results of the LARASE experiment

Violation of 1/r² law: Yukawa-like potential

$$\Re = -\frac{G_\infty M_\oplus}{a^2}\left(\frac{a}{r}\right)^2 \alpha \left(1 + \frac{r}{\lambda}\right) e^{-\frac{r}{\lambda}}$$

In order to retain the long period and secular effects we need to average Gauss equations over one cycle of a fast variable, like M or f :

GAUSS equations

$$\dot{a} = e\frac{2}{n\sqrt{1-e^2}}\Re \sin f$$

$$\dot{e} = \frac{\sqrt{1-e^2}}{na}\Re \sin f$$

$$\dot{I} = 0$$

$$\dot{\Omega} = 0$$

$$\dot{\omega} = -\frac{\sqrt{1-e^2}}{nae}\Re \cos f$$

$$\dot{M} = n + \frac{1}{na}\Re\left(\frac{\cos u}{e(1-e^2)} - \sqrt{1-e^2}\sin f \sin u + 2\frac{(1-e^2)}{(1+e\cos f)}\right)$$

$$r = \frac{a(1-e^2)}{1+e\cos f}$$

$$\cos f = -e + \frac{2(1-e)}{e}\sum_{k=1}^{\infty} J_k(ke)\cos kM$$

$$\sin f = 2\sqrt{1-e^2}\sum_{k=1}^{\infty}\frac{1}{k}J_k'(ke)\sin kM$$

$$\cos u = \frac{e+\cos f}{1+e\cos f}$$

$$\sin u = \sqrt{1-e^2}\frac{\sin f}{1+e\cos f}$$

$$dM = \left(\frac{r}{a}\right)^2 \frac{df}{\sqrt{1-e^2}}$$

$$\langle\dot{a}\rangle_{2\pi} = 0$$
$$\langle\dot{e}\rangle_{2\pi} = 0$$
$$\langle\dot{\omega}\rangle_{2\pi} \neq 0$$
$$\langle\dot{M}\rangle_{2\pi} \neq 0$$

We have secular effects only on the satellite perigee ω and mean anomaly M

n = Satellite mean motion of the unperturbed two–body problem

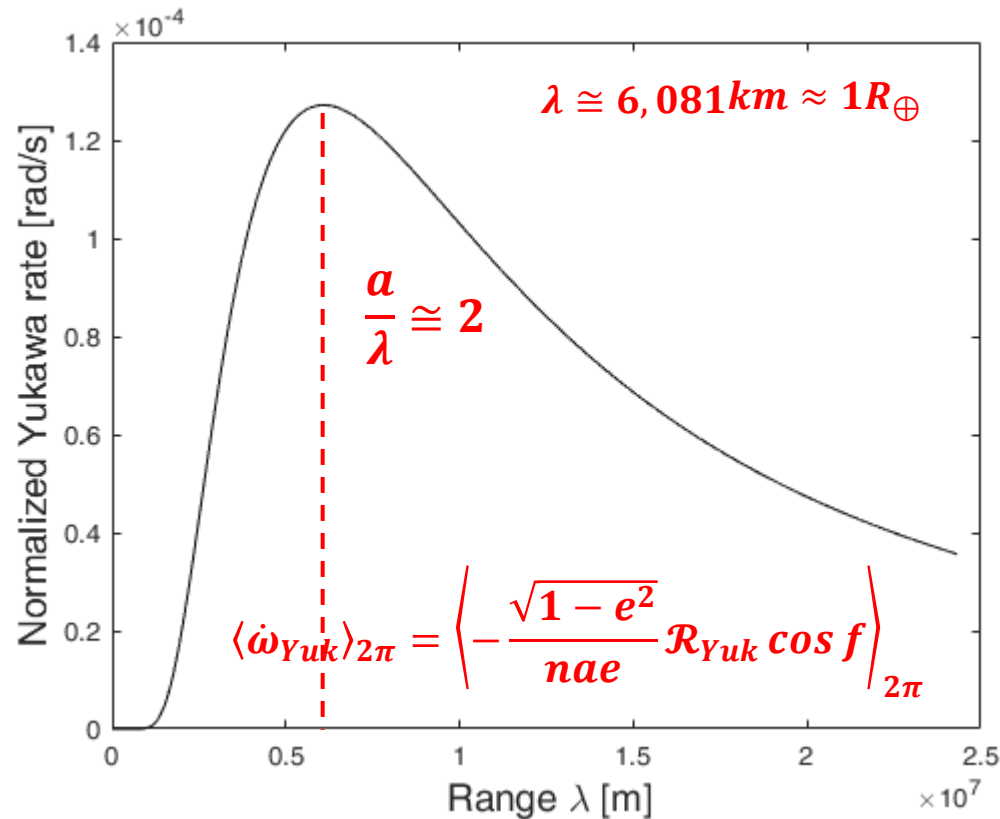$$n^2 a^3 = G_\infty(M_\oplus + m_s) \cong G_\infty M_\oplus$$

Results of the LARASE experiment

Violation of 1/r² law: Yukawa-like potential

$$\vec{\mathcal{R}}_{Yuk} = -\alpha \frac{G_\infty M_\oplus}{r^2}\left(1+\frac{r}{\lambda}\right)e^{-r/\lambda}\hat{r}$$

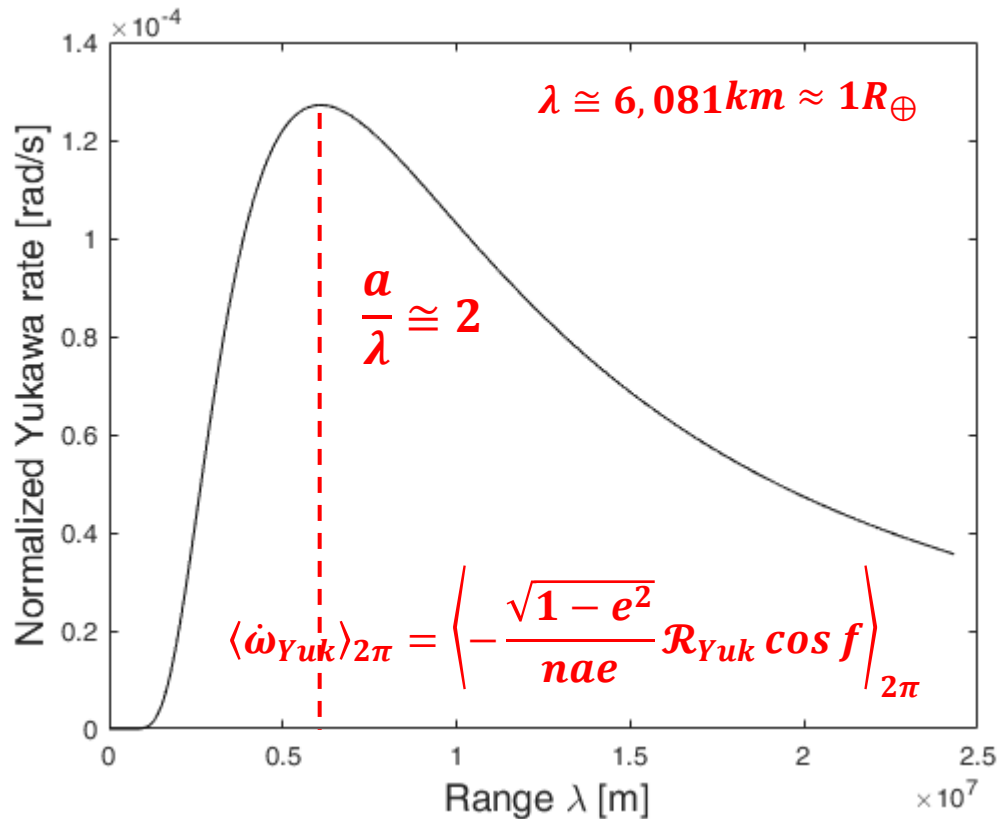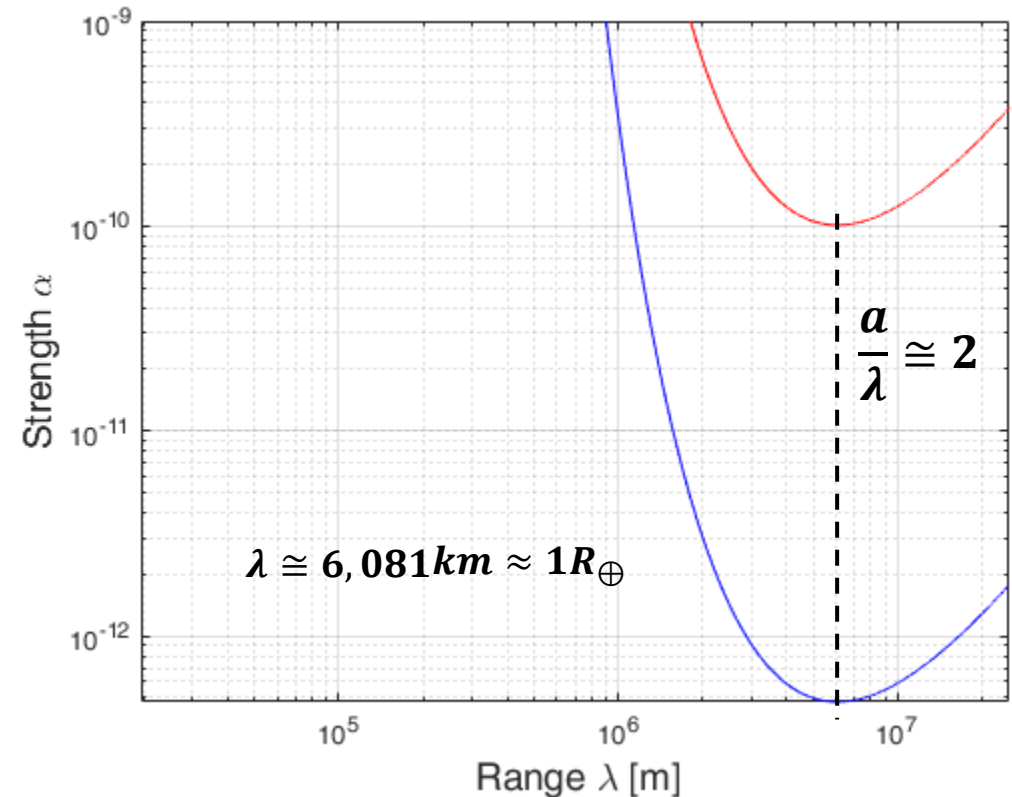$$|\alpha| \cong \left|(0.5 \pm 8)\cdot 10^{-12} \pm 101 \cdot 10^{-12}\right|$$

$\lambda \cong 6,081 km \approx 1 R_\oplus$

$\frac{a}{\lambda} \cong 2$

$$\langle\dot{\omega}_{Yuk}\rangle_{2\pi} = \left\langle -\frac{\sqrt{1-e^2}}{nae}\mathcal{R}_{Yuk}\cos f \right\rangle_{2\pi}$$

$$\left\langle\left|\frac{d\omega}{dt}\right|\right\rangle_{2\pi}^{Peak} \cong 1.27394 \cdot 10^{-4}\cdot\alpha\, rad/s$$

Results of the LARASE experiment

Violation of 1/r^2 law: Yukawa-like potential

$$\vec{\mathcal{R}}_{Yuk} = -\alpha \frac{G_\infty M_\oplus}{r^2} \left(1 + \frac{r}{\lambda}\right) e^{-r/\lambda} \hat{r}$$

$$|\alpha| \cong \left|(0.5 \pm 8) \cdot 10^{-12} \pm 101 \cdot 10^{-12}\right|$$

$\lambda \cong 6,081 km \approx 1R_\oplus$

$\frac{a}{\lambda} \cong 2$

$$\langle \dot{\omega}_{Yuk} \rangle_{2\pi} = \left\langle -\frac{\sqrt{1-e^2}}{nae} \mathcal{R}_{Yuk} \cos f \right\rangle_{2\pi}$$

$$\left\langle \frac{d\omega}{dt} \right\rangle_{2\pi}^{Peak} \cong 1.27394 \cdot 10^{-4} \cdot \alpha \, rad/s$$

Results of the LARASE experiment

Constraints on a long-range force: Yukawa like interaction

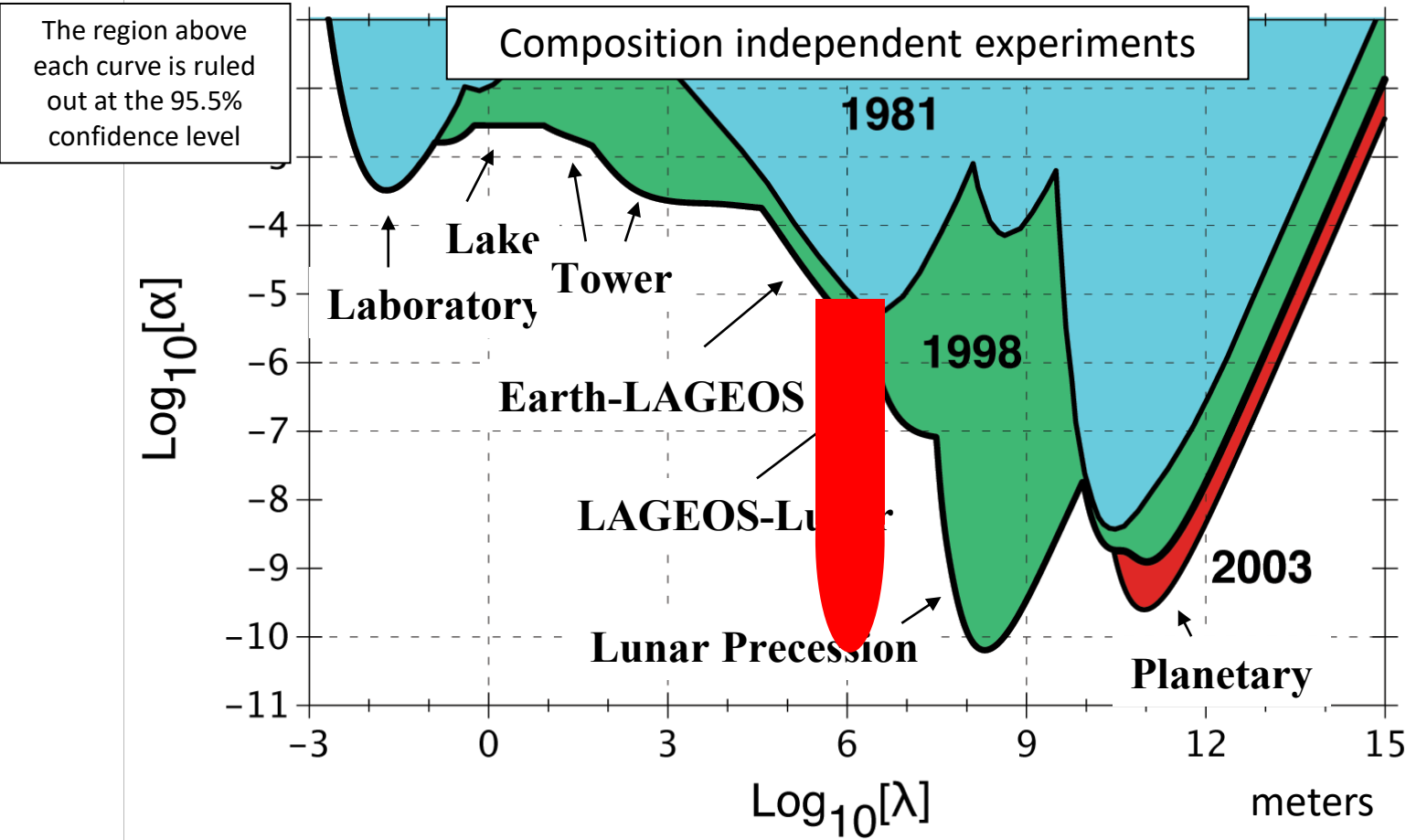$$|\alpha| \cong |(0.5 \pm 8) \cdot 10^{-12} \pm 101 \cdot 10^{-12}|$$

The region above each curve is ruled out at the 95.5% confidence level

Composition independent experiments
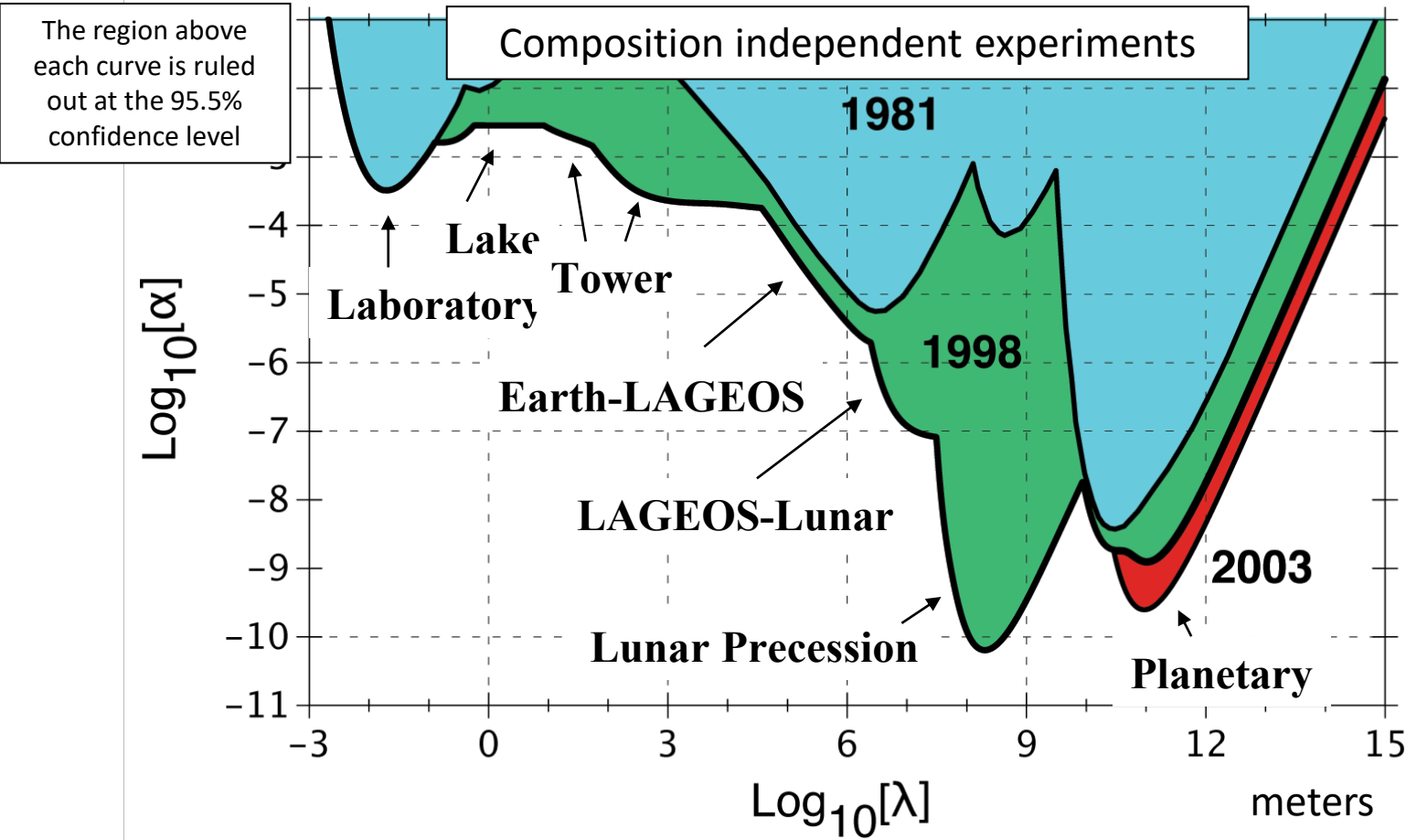
Previous limits with **LAGEOS's**:

$$|\alpha| < 10^{-5} \div 10^{-8}$$

Results of the LARASE experiment

Reference: Coy, Fischbach, Hellings, Standish, & Talmadge (2003)

Constraints on a long-range force: Yukawa like interaction

$$|\alpha| \cong |(0.5 \pm 8) \cdot 10^{-12} \pm 101 \cdot 10^{-12}|$$

The region above each curve is ruled out at the 95.5% confidence level

Composition independent experiments

1981

Lake

Tower

Laboratory

Earth-LAGEOS

1998

LAGEOS-Lunar

Lunar Precession

2003

Planetary

$Log_{10}[\alpha]$

$Log_{10}[\lambda]$

meters

Previous limits with **LAGEOS's**:

$$|\alpha| < 10^{-5} \div 10^{-8}$$

$$|\alpha| \cong 1 \cdot 10^{-10}$$

$$|\alpha| \cong 5 \cdot 10^{-13}$$

The Principle of the measurement

The counting of the pulses for a set of different emitters whose positions on the earth and periods are assumed to be known, is used to provide null emission, or light, coordinates for the receiver on a satellite
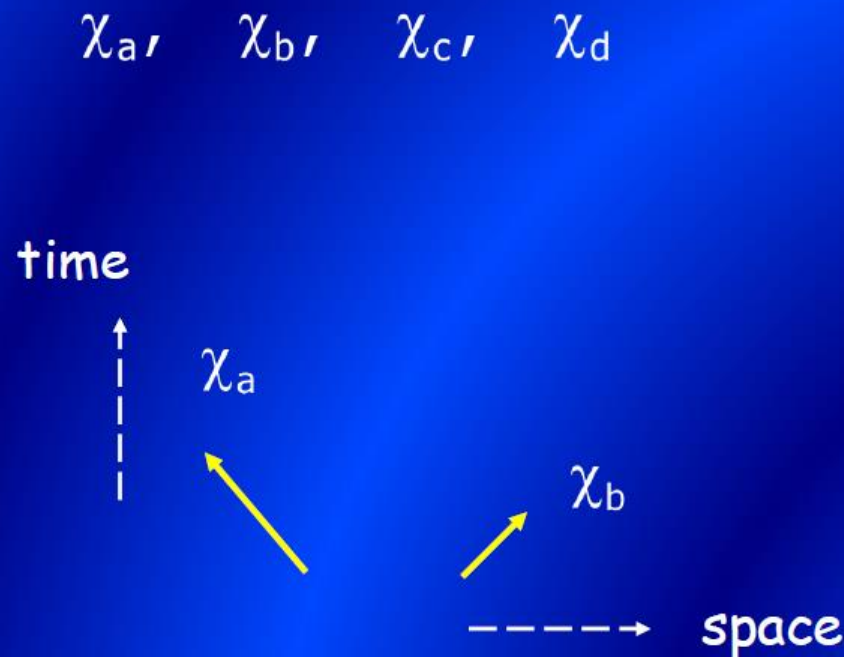
The measurement of the proper time intervals between successive arrivals of the signals from the various emitters is used to give the final localization of the receiver, within an accuracy controlled by the precision of the onboard clock
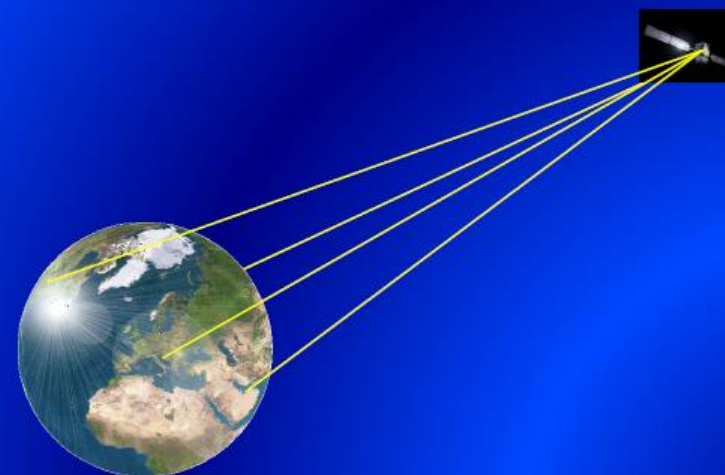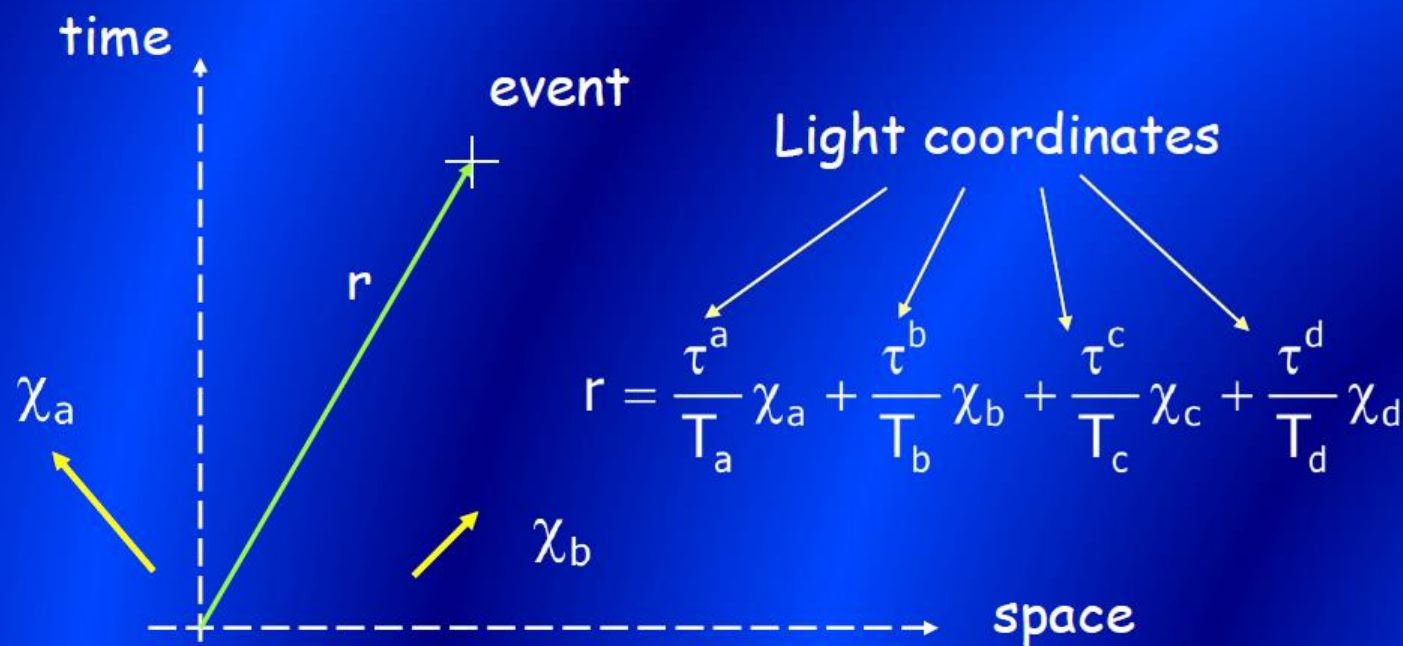
Null bases for space-time

Null vectors corresponding to the space-time directions of electromagnetic signals emitted from four independent sources comprise a null base

$$\chi_a, \quad \chi_b, \quad \chi_c, \quad \chi_d$$

time

χ_a

χ_b

space

A position in space-time in terms of null wave-vectors

time

event

Light coordinates

r

χ_a

χ_b

$$r = \frac{\tau^a}{T_a}\chi_a + \frac{\tau^b}{T_b}\chi_b + \frac{\tau^c}{T_c}\chi_c + \frac{\tau^d}{T_d}\chi_d$$

space

EGU - Vienna - 2018

Wavevectors in terms of an ordinary timelike base

Null geodesics have null tangent wave-vectors

$$\chi = cT\left(1, \cos\alpha, \cos\beta, \cos\gamma\right) = cT\left(1, \hat{n}\right)$$

Direction cosines

Period of the signal

$$\chi^2 = 0$$

Null wave fronts

Null hyperplane
(in flat space-time
and source at infinity) $\longrightarrow$

$$\varpi^{abc} = \varepsilon^{abcd}\chi_d$$

χ_d

Null hypersurface in
three dimensions
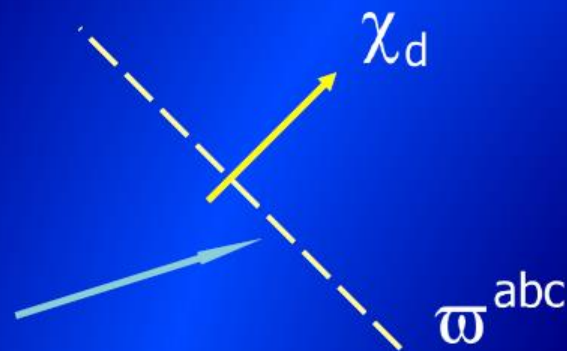
ϖ^{abc}
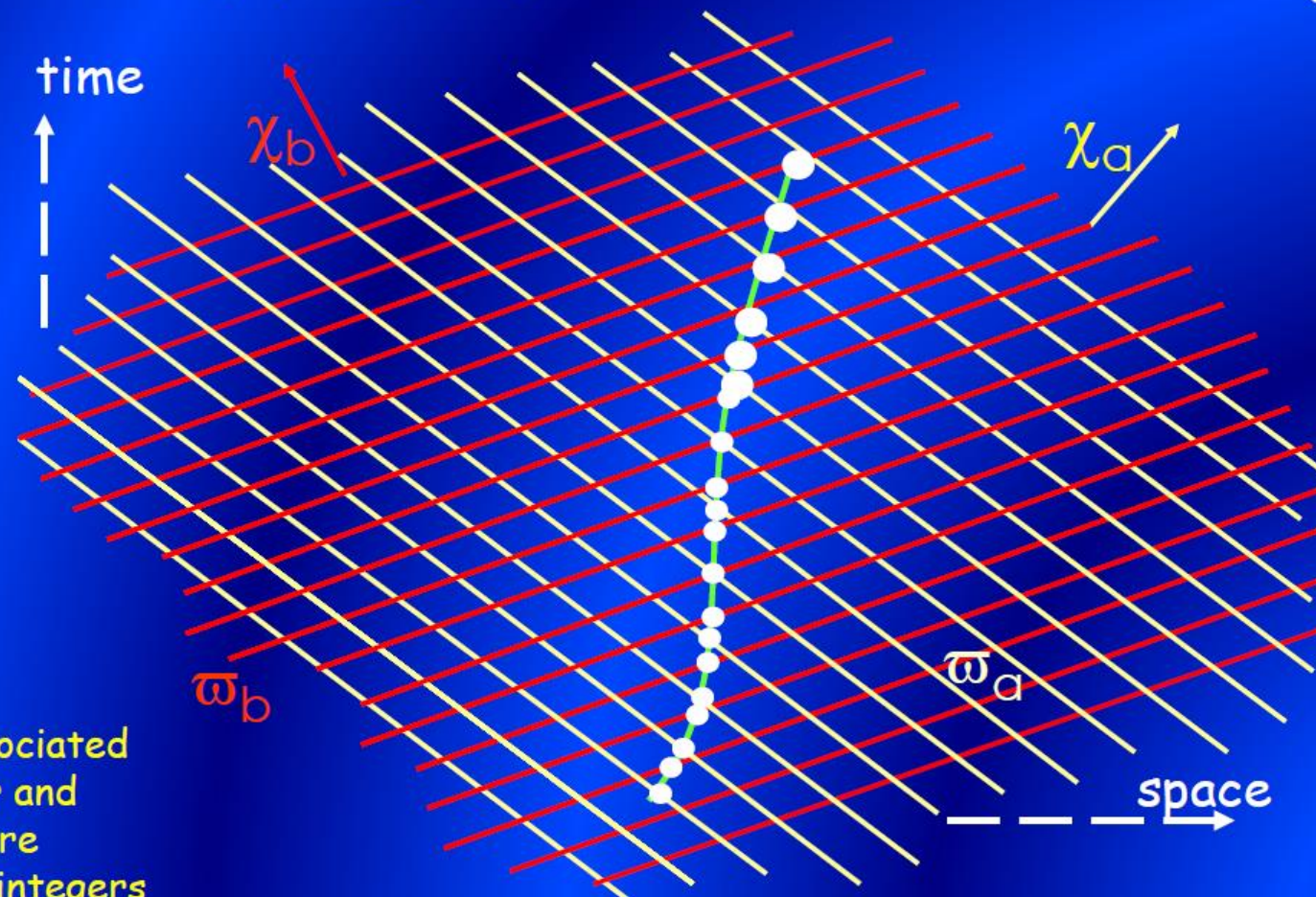
Light coordinates of an event

$$\tau_{a,b,c,d} = \left[(n + x) T \right]_{a,b,c,d}$$

integer

fractional

$$r_i = X_{ai} \chi^a \qquad\qquad X_{ai} = \frac{\tau_{ai}}{T_a} = n_{ai} + x_{ai}$$

$$r = \frac{\tau^a}{T_a} \chi_a + \frac{\tau^b}{T_b} \chi_b + \frac{\tau^c}{T_c} \chi_c + \frac{\tau^d}{T_d} \chi_d$$
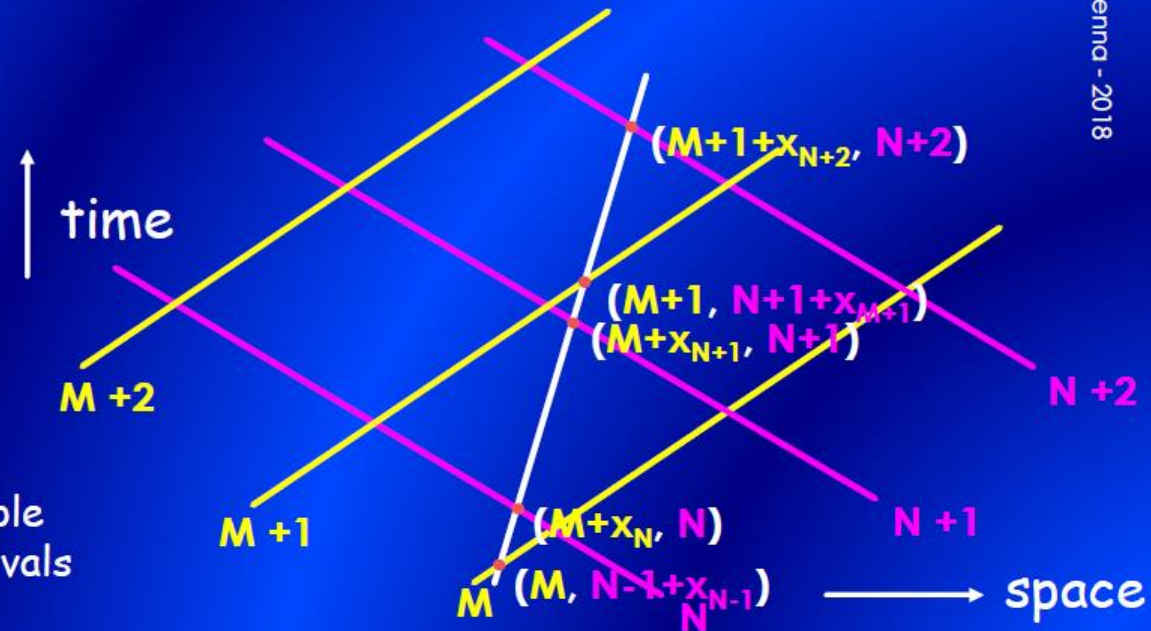
A linear algorithm

i.e. a practical way to evaluate the fractional part x

When the worldline of the user is straight — or may be thought to be approximately straight — the knowledge of the time span between the arrivals of the pulses is sufficient to uniquely localize the reception events, and then the position of the user

Given a sequence of eight arrivals, simple linear relations between the time intervals and the x's hold

time

space

$M+2$

$M+1$

M

N

$N+1$

$N+2$

$(M+1+x_{N+2}, N+2)$

$(M+1, N+1+x_{M+1})$

$(M+x_{N+1}, N+1)$

$(M+x_N, N)$

$(M, N-1+x_{N-1})$

Solving the corresponding system of linear equations leads to the complete definition of the positions in spacetime of the first four reception events

With a moving sequence of events, it is then possible to fully reconstruct the whole worldline of the receiver

A linear algorithm

The arrival times of the signals in the sequence will correspond to the following space-time positions:

$r_1 = (n_1 T)^a X_a + [(n_1 + x_1)T]^b X_b + [(n_1 + x_1)T]^c X_c + [(n_1 + x_1)T]^d X_d$

We choose the first event as coinciding with the crossing of a hypersurface belonging to the a-family, so that xa1 = 0

$r_2 = [(n_2 + x_2)T]^a X_a + (n_2 T)^b X_b + [(n_2 + x_2)T]^c X_c + [(n_2 + x_2)T]^d X_d$

$r_3 = [(n_3 + x_3)T]^a X_a + [(n_3 + x_3)T]^b X_b + (n_3 T)^c X_c + [(n_3 + x_3)T]^d X_d$

The second event will be at the next crossing of a b-hypersurface, the third will be at the encounter with the subsequent c-hypersurface, and so on

$r_4 = [(n_4 + x_4)T]^a X_a + [(n_4 + x_4)T]^b X_b + [(n_4 + x_4)T]^c X_c + (n_4 T)^d X_d$

$r_5 = [(n_1 + 1)T]^a X_a + \cdots$

$r_6 = \cdots$
$r_7 = \cdots$
$r_8 = \cdots$

$$r_{ij} = r_j - r_i = \left(X_{aj} - X_{ai} \right) \chi^a = \Delta X_{aij} \chi^a$$

$$\frac{\tau_{ij}}{\tau_{jk}} = \frac{\Delta X_{1ij}}{\Delta X_{1jk}} = \frac{\Delta X_{2ij}}{\Delta X_{2jk}} = \frac{\Delta X_{3ij}}{\Delta X_{3jk}} = \frac{\Delta X_{4ij}}{\Delta X_{4jk}}$$

At least 8 events (two series of four)

Coordinates in the null frame

We may easily count the n's but have no direct means to measure the x's.

However if we suppose that the acceleration of the receiver is small enough to allow for the identification of the world line with a straight line — in a couple of periods of the emitters — and if we carry on board the receiver a clock, we are able to measure the proper time intervals between the i-th and j-th arrival events, τ_{ij}

With all this, trivial geometric considerations lead to the values of our interest:

$$x_{a1} = 0, \; x_{b1} = 1 - \frac{\tau_{12}}{\tau_{26}}, \; x_{c1} = 1 - \frac{\tau_{13}}{\tau_{37}}, \; x_{d1} = 1 - \frac{\tau_{14}}{\tau_{48}}$$

$$x_{a2} = \frac{\tau_{12}}{\tau_{15}}, \; x_{b2} = 1, \; x_{c2} = 1 - \frac{\tau_{13}}{\tau_{37}} + \frac{\tau_{12}}{\tau_{37}}, \; x_{d2} = 1 - \frac{\tau_{14}}{\tau_{48}} + \frac{\tau_{12}}{\tau_{48}}$$

....

$$\tau_{ij} = \tau_j - \tau_i$$

Difference of the proper arrival times between the j_{th} and the i_{th} event

Uncertainties in the light coordinates

$$\left|\frac{\delta x}{x}\right| \leq 4\left(\frac{1}{\tau_{i,i+4k}} + \frac{\tau_{i,i+1}}{\tau_{i,i+4k}^2}\right)\delta\tau$$

$\delta\tau$: accuracy of the onboard clock (a few ns)

$$\left|\frac{\delta x}{x}\right| \sim 10^{-9}$$

Conversion from null to practical coordinates

- Straighforward when sources at infinity (pulsars)

- More elaborate when sources are at finite distance

- In any case: very high accuracy when positioning is with respect to a starting point along the space-time trajectory of the receiver

Conclusions

Despite the apparent complexity of the mathematics, we have discussed a very simple method for the use of emitters on earth for localization purposes

The local measurements to be done are just time measurements that can be obtained with great accuracy: the basic formulae are plain linear relations

The effects of acceleration, either from gravitational or non-gravitational origin, appear at the second order and again calculations are very simple

Double aim of the application of the RPS to G4S:

a) To offer an additional approach to the orbit determination

b) To test the RPS in inverse configuration, in view of other applications

H2020-ESA-038

GNSS Evolutions Experimental Payloads and Science Activities – Call for Ideas

Statement of Work

9.1 Optical payload for ranging and communications (including QKD experiments)

Experimental Payload:	Optical payloads for ranging and communications	TRL:	2-4
Description:			

Inter-Satellite Links for GNSS have been carefully assessed during the last years having large potential in terms of a number of features including improved navigation system performance at user level (inter-satellite ranging used for Orbit Determination and Time Synchronisation process), enhanced mission, monitoring and control data dissemination, among others.

Optical technology for Ranging and Communications may have a number of possible advantages over RF solutions including: data rate, volume and accommodation (TBC), security, full-duplex communications; while other aspects may remain a challenge (pointing and acquisition time, reliability, cost).

Optical ISL payloads may also enable the possibility to perform quantum communication experiments. This could be, for instance, a possible technology demonstration of Quantum Key Distribution (QKD) between two nodes (two spacecrafts or one spacecraft and one ground station).

Potential benefits to operational system:

Use for ranging on Orbit Determination and Time Synchronisation process.
Use for control / mission communicaions.
Use for quantum communication experiments such as Quantum Key Distribution (for expected increased of security robustness for key distribution).

9.2 Radiation Monitoring Unit

Experimental Payload:	Radiation Monitoring Unit	TRL:	6-9
Description:			

Radiation monitors have been embarked on Galileo satellites since Giove-A. Two FOC satellites incorporate Environmental Monitoring Units (EMU) with the main purpose to characterise the radiation environment in MEO. It is recommended, first of all, to ensure access to the scientific data associated to these units. In addition, it is recommended that at least one additional Galileo satellite incorporates an equivalent unit for measuring radiation, allowing, in turn, a minimum of one equipped satellite per plane.

In MEO radiation environment, main threat comes from relativistic electrons, ionising and non-ionising dose and internal charging. Electrons and protons are trapped in two radiation belts, Galileo orbit goes near and above the outer belt peak. Other radiation effects may occur due to protons during Solar Particle Events and Cosmic Rays (heavy ions)

Purpose of the instrument is the sampling and collection of radiation environment data including electron and proton fluxes, heavy ions, total ionising dose.

Benefit of the mission are brought to:
- monitoring the radiation environment is essential for forecasting and analysing the effect of ionizing particles on Galileo satellites. This is relevant for correlation of events with radiation. Moreover, the data will be essential for the design and operations of the orbit raising phase, if applicable, considering the current knowledge of radiation environment over the whole in MEO.
- Radiation data, if provided externally to Space Situational Awareness service, may be of relevance to space weather services, research institutes, Space Agencies, satellite operators and space insurance companies.

Potential benefits to operational system:

Monitoring and Control for susceptibility to radiation effects. Better understanding of MEO radiation environment.
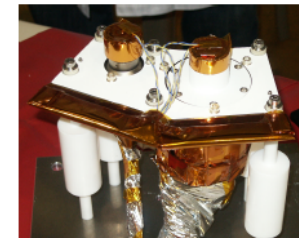
9.3 Plasma Monitoring Unit

Experimental Payload:	Plasma Monitoring Unit	TRL:	4-5
Description:			

Galileo orbit is ideal for observing outer radiation belt dynamics since it crosses almost whole of outer radiation belt. It also allows to observe outer magnetosphere features, such as plasma as observable. Plasma environment in MEO includes low-energy plasma particles (protons and electrons) and causes surface charging on spacecraft. The plasma dynamic behaviour is very different from the radiation belts, therefore requiring a different detector.

This experiment would allow a better-understanding of magnetosphere and its interaction with low-energy plasma and it could contribute to Space Weather Monitoring and Space Situational Awareness.
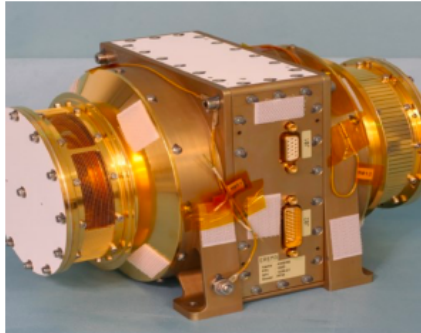
Benefit of the mission are brought to:
- Space weather services, research institutes and Space Agencies. For gathering data and improving knowledge about space weather events and the solar-magnetosphere interactions. It is worth to mention here the European efforts to provide a Space Situational Awareness service (SSA programme from ESA) including Space Weather services, similar to those currently offered by NOAA. These instruments embarked on Galileo satellites could contribute to such services.
- Satellites operators: the data on space weather nowcasting (and eventually forecasting) will be used for evaluating satellite anomalies due to charging depending on satellites orbits.
- Satellite industry: the evaluation of the space weather events in terms of particles involved their energy and the time dynamic support the satellites manufacturer in the design of new technologies and COTS.
- Space insurance companies: space insurance companies will exploit space weather data to accurately estimate the risk associated to a specific mission in terms of likelihood of a disruptive event and its impact.

Potential benefits to operational system:

Monitoring and Control for spacecraft surface charging and post-anomaly data. Better understanding of MEO environment with respect to EMC requirements, and its associated Space Weather.
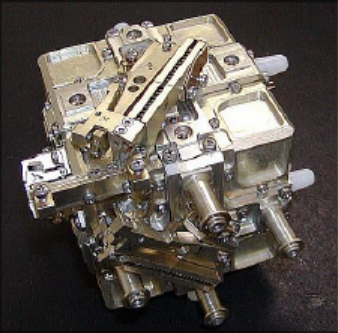
9.4   Other Space Weather instruments

Experimental Payload:	Other Space Weather instrument (magnetometer, photometer)	TRL:	3-4
Description:			
In addition to radiation and plasma monitors, other instruments may be further considered for supporting Space Weather monitoring consisting of the following: • a magnetometer, for measuring in-situ Earth's magnetic field; • photometers to measure incoming X-ray, ultraviolet, visible, near-infrared, and total solar radiation, for solar flare assessment, direct measurement of solar radiation pressure on satellite, analysis of Earth atmosphere under eclipse for better understanding of Solar Flux and photo ionisation.			
Potential benefits to operational system:			
Monitoring and Control for susceptibility of Platform/Navigation Payload to magnetic field and radiation			

9.5 Advanced Laser Retro Reflector

Experimental Payload:	Advanced Laser Retro Reflector (Passive or Active)	TRL:	3-5

Description:

The LRR is a payload which allows the determination of the position and time (in case of active payload) by exploiting a global network of Laser Ranging Stations which very precisely measure the ranging from the satellite to the station. All existing Galileo satellites already embark Laser Retro-Reflectors. Novel passive reflectors (circular arrays or hollow cubes) may be considered for improved performance or accommodation.

Alternatively, an Active Laser Retro-Reflector (A-LRR) would allow the possibility to synchronize remote ground atomic clocks over inter-continental distance using standard Satellite Laser Ranging (SLR) techniques, as well as comparing ground clocks to the on-board atomic clocks directly, and may support the accurate independent orbit and clock determination. Such an idea has been demonstrated by SLR ground stations with the T2L2 instrument on board the Jason-2 satellite, and is expected for the ELT (European Laser Timing) instrument of the ACES experiment on board the ISS. Having an optical two-way time transfer on a Galileo satellite is unique because of the possibilities for common view of the satellite on the ground and the combination with a highly stable space atomic clock, providing the possibility of comparing ground clocks in non-common view (inter-continental comparisons) with high accuracy, offering the scientific community (time & frequency, metrology, fundamental physics, and geodesy) two-way range tracking, ground-to-space and ground-to-ground time transfers. Furthermore, two-way time transfers would be free (to the 1st-order) from errors coming from orbit models, which is one of the limitations of current GNSS systems. This would permit a unique characterization of the behaviour of the on-board atomic clocks, with respect to parameters such as temperature, radiation, magnetic field and aging. The availability of A-LRR in a Galileo satellite would be an opportunity to realize on-board co- locations between different space geodesy techniques (GNSS and SLR), in particular, if other scientific instruments such as a VLBI transmitter were co-located. It would allow relativity tests and ultimate time transfer capabilities and comparison between various techniques (e.g. PPP, TWSTFT, T2L2).

Potential benefits to operational system:

Independent M&C monitoring (orbit determination, orbit & clock determination).
Galileo mission as aid for orbit determination, in particular for ground-based ranging (exploiting improvements in existing Galileo satellites incorporating passive LRR).
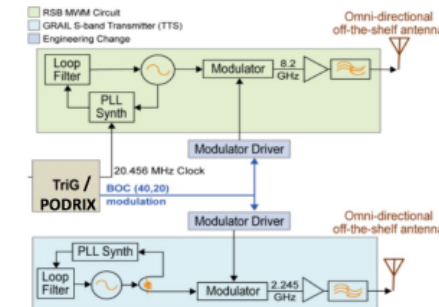Time transfer / synchronization of distant clocks if active LRR is used.

9.6 Accelerometer

Experimental Payload:	Accelerometer	TRL:	3-4

Description:

Considering that solar radiation pressure (SRP) constitutes the most important contribution to the error budget affecting precise orbit modelling, accelerometers able to measure such non-gravitational accelerations are considered of interest, provided that their sensitivity and calibration approach is sound and their envelope is reasonable. They directly measure solar radiation pressure and other non-gravitational perturbations, measurements that may be directly used as perturbing accelerations in orbit determination, assimilated into models or for offline characterisation and model improvement. The critical questions for direct use as accelerations in the orbit integration are related to the level of sensitivity required for obtaining improvements, and the need to calibrate accelerometer biases which may limit the potential benefits. As alternative to ingesting the accelerometer measurements into the orbit integration, they may be used to calibrate parameters of complex satellite models. Numerous studies are currently ongoing in this topic. Accelerometers may, in addition, support for example rapid recovery of precise orbits after manoeuvers and possibly reduce the update rate of satellite ephemerides due to longer orbit predictions.

From a scientific point of view, the higher quality of orbits which could be achieved thanks to such accelerometers would enable a large variety of scientific products related to geodesy and geodynamics (reference frame accuracy and stability, geocentre coordinates, Earth Rotation and Earth Orientation Parameters), atmospheric physics, meteorology and climate (zenith and slant delay and radio occultation observables). This would, in turn, allow recording the "fingerprints" of global change processes as an independent source of high accuracy information for many global change studies, potentially supporting the Global Geodetic Observing System (GGOS) side by side with Copernicus.

Potential benefits to operational system:

ODTS estimation and prediction either as direct measure of SRP or by assimilating the data into improved SRP models.
Monitoring of micro-vibrations for post-anomaly assessment (TBC)
Support to electric orbit raising attitude control (TBC)

9.7   VLBI Transmitter

Experimental Payload:	VLBI Transmitter	TRL:	3-4

Description:

The idea of embarking low power spectral density wideband transmitters on Galileo satellites optimized for Very Long Baseline Interferometry (VLBI) is relevant to obtain and maintain accurate and long-term stable reference frames, both on Earth and in space. This has been recognised in 2015 by the United Nations by adopting a resolution on the Global Geodetic Reference Frame. It can only be established and maintained by an international observational network often referred to as the Geodetic Global Observing System (GGOS). The goals of GGOS are a position accuracy of 1 mm and a velocity (rate) uncertainty of 0.1 mm/year. A key element in this process is to have a co-location of the different space geodetic techniques at fundamental sites on the ground, as well as on satellites in space. Therefore, a VLBI beacon on-board GNSS satellites offers a unique opportunity for high-precision tying of two of the major space geodetic techniques and ideally complements the already existing tie with SLR Retro-Reflectors. Three out of four space geodetic techniques would thus be co-located on Galileo satellites.

Numerous open questions related to the frequency coverage, required transmitted power spectral density, signal polarization, number of satellites with a transmitter, and if there were a sufficient number of telescopes available worldwide, remain to be addressed. In conclusion, the geodetic community has recently discussed several different satellite missions in order to improve the global geodetic reference frame(s). The possibility of including white noise transmitters on next Galileo generation satellites is a very innovative and promising idea that deserves to be considered and studied further for implementation, given the open questions specified.

The VLBI transmitter Unit will broadcast very low power spectral density wideband signals in the VLBI band (3-14 GHz). An initial design and building blocks exist from E-GRASP mission proposal.

Potential benefits to operational system:

Through the broadcast of very low wideband VLBI-like noise signals for ground VLBI observations it would allow to improve ties between Galileo Terrestrial Reference Frame and VLBI Inertial Reference Frame (improved data from GRSP) and may support independent orbit determination.

A few examples from past studies are presented below:

Programme:	GSP	Title	Galileo gravitational Redshift Experiment with eccentric sATellites (GREAT)
Summary:			

Immediately after the recovery of Galileo Satellites 5 & 6 (which due to a mishap of a Fregat Soyuz Upper stage were placed in an eccentric orbit), ESA and the scientific community suggested that they could provide extraordinary means to test Einstein's general relativity gravitational redshift, a way of testing Einstein's local position invariance. Following the recommendations of GSAC, two parallel studies were launched with SYRTE/Paris Observatory and ZARM/University of Bremen in 2015. The so-called GREAT project (Galileo gravitational Redshift Experiment with eccentric sATellites) aimed at measuring the gravitational redshift predicted by Einstein General Relativity Theory with the highest possible accuracy.

The two parallel teams presented consolidated results and their methodology, after having assessed accumulated data for over 1000 days. Both team confirmed, in an independent way, the gravitational redshifts with accuracies better than any previous results. This represents the first reported improvement on one of the longest standing results in experimental gravitation, the Gravity Probe A (GP-A) hydrogen maser rocket experiment back in 1976, and a major scientific achievement. During this first quarter of 2018, some of the orbit systematic errors have been further reduced thanks to some refinements on the orbit modelling algorithms performed by the ESOC navigation office. The new estimates are confirmed to be several times better than the GP-A reference. Final results have recently been published in Physical Review Letters.
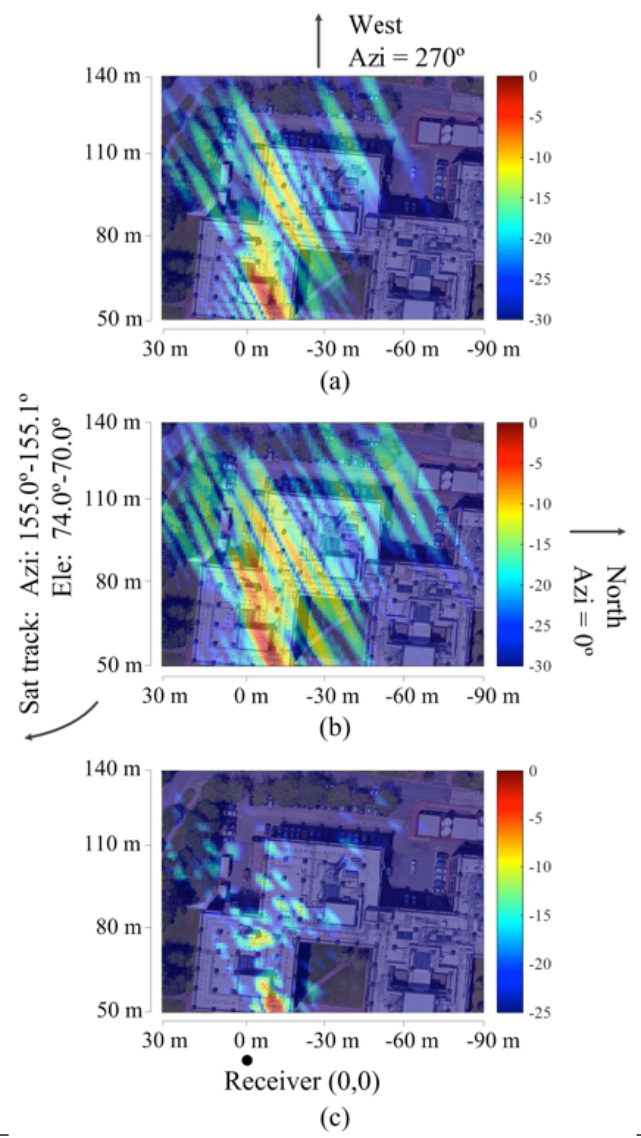
Programme	EGEP ID89.04	Title	Galileo AltBOC signal exploitation for Synthetic Aperture Radar imaging (BSAR)

Summary:

The activity targets the development of a bi-static Synthetic Aperture Radar system to exploit GNSS signals (and in particular the aggregate Galileo AltBOC E5 signal) and hence produce high-resolution images of Earth passively. A navigation satellite is used as the transmitter, while the receiver is on or near the surface of the Earth. The system can provide imagery by exploiting the relative motion between the transmitter and/or the receiver relevant to an observation area. In this manner, an effective ("synthetic") antenna aperture can be generated at the signal processing level to drastically improve spatial resolution in the azimuth direction. The range resolution is dominate by the signal bandwidth.

The signal processing algorithms were implemented into the Ifen SX3 software receiver and a field experiment was performed. The activity has demonstrated the practical implementation of bi-static SAR with GNSS signals into a software receiver and the fact that spatial resolution can be drastically improved by the use of full E5 channel.

This activity contributes to the exploitation of Galileo signals for scientific uses, in particular remote sensing, such as local land use mapping. In addition, local area monitoring with Galileo is also of interest, for example for persistent infrastructure monitoring.

| Programme:	EGEP ID89.07	Title	Improving Time transfer with Galileo E5 ALTBOC (TIME5)

Summary:

The activity objective is to determine the achievable timing performances the Galileo E5 ALTBOC for time synchronization and time transfer, for both real-time and post-processing applications. The advantage of a single-frequency analysis is to have uncertainties reduced.

The performances of the E5 AltBOC signal for time transfer could not be sufficiently quantified due to the limited data set, however initial results indicate that for synchronization in single-frequency, E1 should be preferred to E5 AltBOC because of the uncertainties on the iono corrections; their impact is larger than the noise difference between E1 and E5. For frequency steering however, the use of E5AltBOC improves significantly the short term (< 10 min) stability of the solutions with respect to the use of E1. Furthermore E5 AltBOC could bring more advantages if it can be more precisely corrected for the ionospheric delays than what is currently available.

An additional output of the project was that E5 AltBOC can be used for timing applications only if an absolute BGD for (E1,E5 AltBOC) is made available to the users. More generally, for accurate synchronization based on Galileo single-frequency measurements, it is important to put absolute BGDs at the disposal of the users.

Finally, The SW to produce the CGGTTS time transfer standard for Galileo has been finalized and distributed to the timing community so that Galileo data can now be introduced in the computation of TAI (International Atomic Time).

The activity contributes to the scientific and general timing exploitation of Galileo signals.
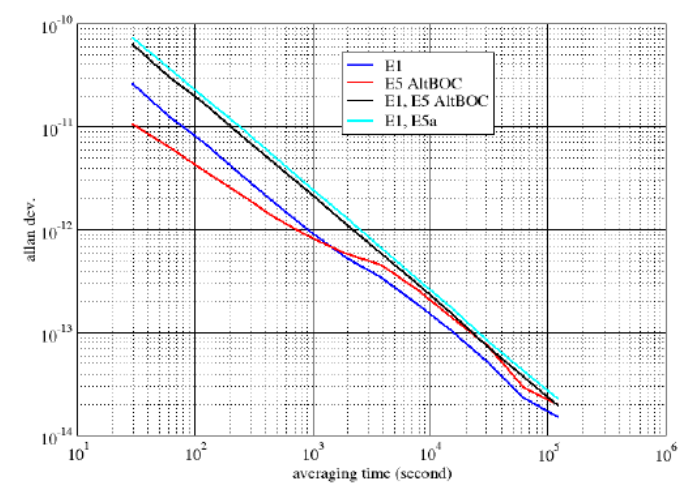
ALLAN DEVIATION OF THE LINK BRUSSELS-TURIN WITH EITHER GALILEO SINGLE-FREQUENCY ANALYSIS (E1 OR E5 ALTBOC) OR DUAL-FREQUENCY ANALYSIS (E1 WITH EITHER E5A, OR E5 ALTBOC). THE MGEX IGS PRODUCTS ARE USED FOR SATELLITE CLOCK AND ORBITS, AND THE IGS IONEX MAPS ARE USED FOR THE IONOSPHERIC CORRECTIONS OF SINGLE-FREQUENCY SOLUTIONS.

| Programme:	EGEP ID89.21	Title	Integrity of Ionospheric Models (INTIMOD)

Summary:

GNSS measurements are affected by ionospheric delays caused by the signal's propagation through the ionosphere. As these delays can severely degrade receiver position determinations, a model to correct for this ionospheric error is necessary. To this end, GPS broadcasts the coefficients of the Klobuchar model. The residual errors that remain after Klobuchar's ionospheric corrections are applied are modelled themselves in SBAS Minimal Operational Standards [RTCA MOPS] which can be used to compute integrity related parameters such as the horizontal protection level. In 2005, this model was validated for the aviation requirements used for the en-route and non-precision approach phases of flight. Galileo uses the NeQuick-G model, which is a three-dimensional and time-dependent ionospheric model based on a single input parameter called the effective ionization level (Az) which captures the solar activity information to feed the model.

The objective of the activity is twofold: first to establish an overbounding residual error model of the Galileo single-frequency ionospheric correction algorithm for safety-of-life applications; second, to analyse the interoperability of Galileo and GPS ionospheric correction models for single-frequency multi-constellation receivers.

A number of case studies have been analysed: one case based on worst-observed sample using nominal data and analysis of all collected (as-broadcast) data, one case considering severe underestimation during storms, one case based on the probability of severely overestimated corrections during quiet ionospheric conditions. The study resulted in the conclusion that due to the independency of the actual corrections, the model from RTCA MOPS works equally well for NeQuick-G and Klobuchar and therefore the model can also be applied to the NeQuick-G corrections.

The additional investigation into the interoperability of the GPS and Galileo ionosphere models indicates that the performance of the NeQuick-G model is better than that of the Klobuchar model for ionospheric on quiet condition days. For disturbed conditions, Klobuchar showed slightly better performance, however the results are not conclusive due to the fact that the NeQuick model is based on observations of a relatively small number of ranging measurements, as at the time this research was done, Galileo was not yet fully deployed.
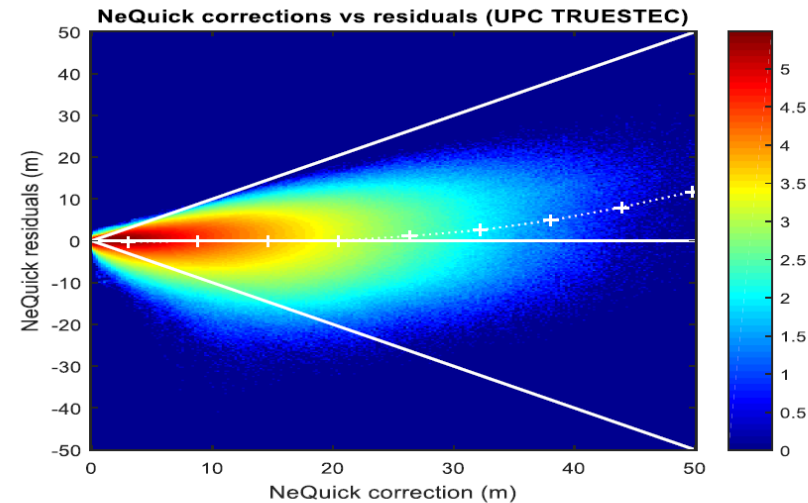
NEQUICK G CORRECTION VERSUS RESIDUAL ERROR FOR ALL OBSERVATIONS IN WORLDWIDE SET OF STATIONS DURING 2014

Programme	EGEP ID103	Title	Accurate calibration of multi-system/multi-frequency GNSS receiver chains (AKAL)

Summary:

Absolute delay calibration of GNSS receivers has been gaining interest inside the timing community due to the low uncertainty level that can be achieved, and to the need of having a reference calibrated receiver to perform relative calibrations, especially in a multi-GNSS context.

In this project, enhanced techniques for the absolute calibration of receiver chains as used in timing reference stations were developed and different results of the calibration and validation of two absolutely calibrated receiver chains were performed with novel methods, which include the influence of multipath effects in different receivers, the observation on the dispersions of the satellite dependent biases, most probably due to the chip-shapes and how they compare between Galileo and GPS signals.

The elements of the GNSS chain (antenna, receiver and cable) are each calibrated individually and with careful considerations regarding the uncertainty level assigned to them. All the elements are calibrated in a multi-frequency and multi-system environment, considering all frequencies of GPS and Galileo, and legacy frequencies of GLONASS.

The absolute GNSS antenna calibration have been historically done in small and so-called "portable" anechoic chambers, that could give a good approximation of the group delay of the antenna for signals at elevation 90 degrees, but cannot be used if an analysis versus azimuth and elevation is required. During this work we extract absolute delays of the GNSS antenna, using the Antenna Laboratories at ESA/ESTEC.

Additionally to using large anechoic chambers, which helps reducing the uncertainty of the measurements, we developed a novel calibration technique considering a physical reference point of the antenna. This allows for ultra-precise determination of the distance between the two antennae and produce a very low uncertainty related to scenario characterization, not having to rely on phase center calculations. We also present the proper transformation between the used reference point and the phase center of the GNSS antenna, to comply with CGGTTS standard computation procedure.

The receiver chain calibrations were then validated in several on-site experiments, using the commonly known common-clock setup. This initial validation, performed at the ESTEC site, was performed to assess the uncertainty of the calibration when operating in a real environment. After initial analysis of the results, the receivers were also installed in a common antenna setup, to mitigate the effects of the multipath coming in the antenna.

Having two fully calibrated stations, for multiple GNSS signals, allows for the comparison between the receivers, as well as for analysis of the stability of the group delays of each receiver model. One possible application would be the identification of the impact of multipath effects on one or both receiver chains.

GNSS ANTENNA GROUP DELAY CHARACTERIZATION VERSUS AZIMUTH AND ELEVATION, INSIDE ANECHOIC CHAMBER.